Aus der Medizinischen Klinik und Poliklinik IV
Klinikum der Ludwig-Maximilian-Universität München

The effects of triple blockade of the mineralocorticoid receptor, the renin-angiotensin system, and sodium glucose transporter 2 on kidney lifespan in mice with Alport nephropathy. A preclinical double-blinded randomized controlled trial.

Dissertation
zum Erwerb des Doktorgrades der Medizin
an der Medizinischen Fakultät der
Ludwig-Maximilians-Universität München

vorgelegt von
Zhihui Zhu
Aus Dezhou, China
2023

Mit Genehmigung der Medizinischen Fakultät der
Ludwig-Maximilians-Universität zu München

Erster Gutachter:	Prof. Dr. med. Hans-Joachim Anders
Zweiter Gutachter:	Prof. Dr. Bärbel Lange-Sperandio
Dritter Gutachter:	Prof. Dr. Peter Weyrich
ggf. weitere Gutachter:	
Mitbetreuung durch den promovierten Mitarbeiter:	Prof. Dr. med. Volker Vielhauer
Dekan:	Prof. Dr. med. Thomas Gudermann
Tag der mündlichen Prüfung:	23.08.2023

Zusammenfassung

Die Hemmung des Renin-Angiotensin-Systems (RAS), des Sodium-Glucose-Transporters (SGLT) 2 und des Mineralocorticoid-Rezeptors (MR) haben alle in großen klinischen Studien bei diabetisch bedingter chronischer Nierenerkrankung (CKD) renoprotektive Effekte gezeigt. Darüber hinaus hat sich auch die Kombination aus RAS- und SGLT2-Hemmung bei nicht-diabetischer CKD als renoprotektiv erwiesen. Basierend auf diesen Ergebnissen wurde vermutet, dass die Kombination aus RAS-, SGLT2- und MR-Hemmung bei nicht-diabetischer CKD noch wirksamer sein könnte.

Um diese Vermutung zu überprüfen, wurde eine präklinische randomisierte Kontrollstudie bei Col4a3-defizienten Mäusen mit spontaner und progressiver CKD (Registrierungs-ID: PCTE0000266) durchgeführt. Die Behandlungen bestanden aus Lebensmittelzusätzen bei geschätzten Dosen von 10 mg/kg Ramipril, 30 mg/kg Empagliflozin und 10 mg/kg Finerenone, die von 6 bis 14 Wochen alter ausgegeben wurden. Das primäre Studienendpunkt war die Gesamtlebensdauer bis zum Auftreten von Uraämie. Als sekundäre Endpunkte wurden Marker der Nieren-Exkretionsfunktion (GFR, Proteinurie) sowie histomorphologische Parameter der Niere bei einer Untergruppe von Tieren untersucht. Weitere Analysen wurden durchgeführt, um die Auswirkungen der Behandlungen auf die Histologie, Genexpression und andere Mechanismen zu bewerten.

Zum Zeitpunkt der Zufallsauswahl zeigten die *Col4a3*-/- Mäuse Anzeichen einer Nierenerkrankung, einschließlich Albuminurie, erhöhter Kreatininspiegel, Glomerulosklerose, tubulärer Atrophie und interstitieller Fibrose. Die Gesamtlebensdauer betrug 63,7 ± 10,0 Tage (Vehikel), 77,3 ± 5,3 Tage (Ramipril), 80,3 ± 11,0 Tage (Ramipril + Empagliflozin) und 103,1 ± 20,3 Tage (Triple-Therapie). Die Histopathologie, die Genexpressionsanalyse und die RNA-Sequenzierungsanalyse deuteten alle auf eine potente antisklerotische, entzündungshemmende und antifibrotische Wirkung der Triple-Kombination hin.

Zusammenfassend verlängerte die zusätzliche Gabe von Finerenon zur Kombination aus RAS- und SGLT2-Inhibition das urämie-freie Lebensalter der Mäuse, auch wenn es in einem fortgeschrittenen Stadium der Alport-Nephropathie begonnen wurde. Die Ergebnisse deuten darauf hin, dass die Kombination aus RAS-, SGLT2- und MR-Inhibition eine potente Behandlungsstrategie sein könnte, um das urämie-freie Lebensalter bei Patienten mit einer CKD im Zusammenhang mit Alport-Syndrom und möglicherweise auch anderen Nierenerkrankungen zu verlängern.

Summary

The inhibition of the renin-angiotensin system (RAS), the sodium-glucose transporter (SGLT) 2, and the mineralocorticoid receptor (MR) have all shown protective effects on the kidneys in large clinical trials of diabetes-related chronic kidney disease (CKD). Additionally, the combination of RAS and SGLT2 inhibition has also been found to be renoprotective in non-diabetic CKD. Based on these findings, it was hypothesized that the combination of RAS, SGLT2, and MR inhibition would be even more effective in non-diabetic CKD.

To test this hypothesis, a preclinical randomized controlled trial was conducted in *Col4a3*-deficient mice with spontaneous and progressive CKD (registry ID: PCTE0000266). The treatments consisted of food admixes at estimated exposure doses of 10 mg/kg ramipril, 30 mg/kg empagliflozin, and 10 mg/kg finerenone, given from 6-14 weeks of age. The primary endpoint of the study was the total lifespan up to uremic death. The secondary endpoint was makers of kidney excretory function (GFR, Proteinuria) and histomorphological parameters of the kidney in a subgroup of animals. Further analysis was performed to assess the effects of the treatments on histology, gene expression, and other mechanisms.

At the time of randomization, the *Col4a3*-/- mice showed signs of kidney disease including albuminuria, elevated creatinine levels, glomerulosclerosis, tubular atrophy, and interstitial fibrosis. Total lifespan was 63.7 ± 10.0 days (vehicle), 77.3 ± 5.3 days (ramipril), 80.3 ± 11.0 days (ramipril+empagliflozin), and 103.1 ± 20.3 days (triple therapy), respectively. The histopathology, gene expression analysis, and RNA sequencing analysis all indicated a potent anti-sclerotic, anti-inflammatory, and anti-fibrotic effect of the triple combination.

In conclusion, the addition of finerenone to the combination of RAS and SGLT2 inhibition prolonged the uremia-free lifespan of the mice even when started at an advanced stage of Alport nephropathy. The results suggest that the combination of RAS, SGLT2, and MR inhibition could be a potent treatment strategy for prolonging the uremia-free lifespan in patients with CKD related to Alport syndrome and potentially other progressive kidney disorders.

1. Introduction

1.1 Chronic kidney disease

Chronic kidney disease (CKD) is a significant worldwide public health issue as it poses a substantial risk of cardiovascular complications and mortality. Additionally, CKD frequently progresses to kidney failure, necessitating kidney replacement treatment. [1-3]. Globally, more than 850 million individuals are affected by kidney disease, and an estimated 5.3-10.5 million of them require kidney replacement therapy. [4, 5]. In Germany, around 95,000 CKD patients require dialysis, costing approximately 40,000€ per person per year [6]. The progression of CKD is influenced by several factors, including: a) reduced number of nephrons at birth or prior nephron loss, b) ongoing presence of the underlying disease, c) metabolic and hemodynamic overload of remaining nephrons, and d) aggravating factors such as obesity, diabetes, and high salt and protein-rich diets [7-9].

1.1.1 Definition of CKD

CKD is characterized by long-term structural and functional impairment of the kidneys caused by various factors [10]. According to the Kidney Disease: Improving Global Outcomes (KDIGO) 2012 clinical practice guideline, CKD is defined as abnormalities in kidney structure or function that have an impact on health, present for over three months [11]. The KDIGO 2012 criteria for CKD include a reduction of glomerular filtration rate (GFR) to less than 60 ml/min per 1.73 m^2 or the presence of markers of kidney damage such as albuminuria, abnormalities in urinary sediment, electrolyte imbalances and tubular disorders, abnormalities detected by histology, structural abnormalities seen on imaging, and a history of kidney transplantation for at least 3 months [11].

1.1.2 Staging of CKD

CKD staging is used to determine the stage of CKD in patients, so as to identify appropriate prevention and treatment goals and take appropriate measures. According to KDIGO 2012, CKD is classified based on the cause, GFR, and albuminuria category (CGA) [12, 13]. Table 1 shows the GFR categories. In CKD stage G1, GFR is normal or slightly elevated, above 90 ml/min per 1.73 m^2. At this point, kidneys are in a sub-healthy state. In G2, GFR has decreased from above 90 ml/min per 1.73 m^2 in G1 to 60-89 ml/min per 1.73 m^2, indicating that CKD is becoming more serious. As CKD progresses from G2 to G3, the kidneys are moderately abnormal, with GFR levels of 45-59 ml/min per 1.73 m^2 for G3a and 30-44 ml/min per 1.73

m^2 for G3b. In G4, CKD has severely reduced GFR to 15-29 ml/min per 1.73 m^2. G5, which is kidney failure, has a GFR level below 15 ml/min per 1.73 m^2.

Table 1.1: GFR categories in CKD

GFR category	GFR (ml/min/1.73 m^2)	Terms
G1	≥90	Normal or high
G2	60-89	Mildly decreased
G3a	45-59	Mildly to moderately decreased
G3b	30-44	Moderately to severely decreased
G4	15-29	Severely decreased
G5	< 15	Kidney failure

CKD: chronic kidney disease; GFR: glomerular filtration rate.

1.1.3 Risk stratification of CKD

According to KDIGO 2012, factors influencing poor prognosis in CKD include: the underlying cause of CKD, the GFR category, the albuminuria category, and other risk factors [11]. To aid in determining the risk level of CKD patients, the guidelines also provide a system of classification, which divides the risk into four grades as depicted in figure 1.1. This system helps in identifying the appropriate prevention and treatment goals and in taking appropriate measures for patients with different levels of risk.

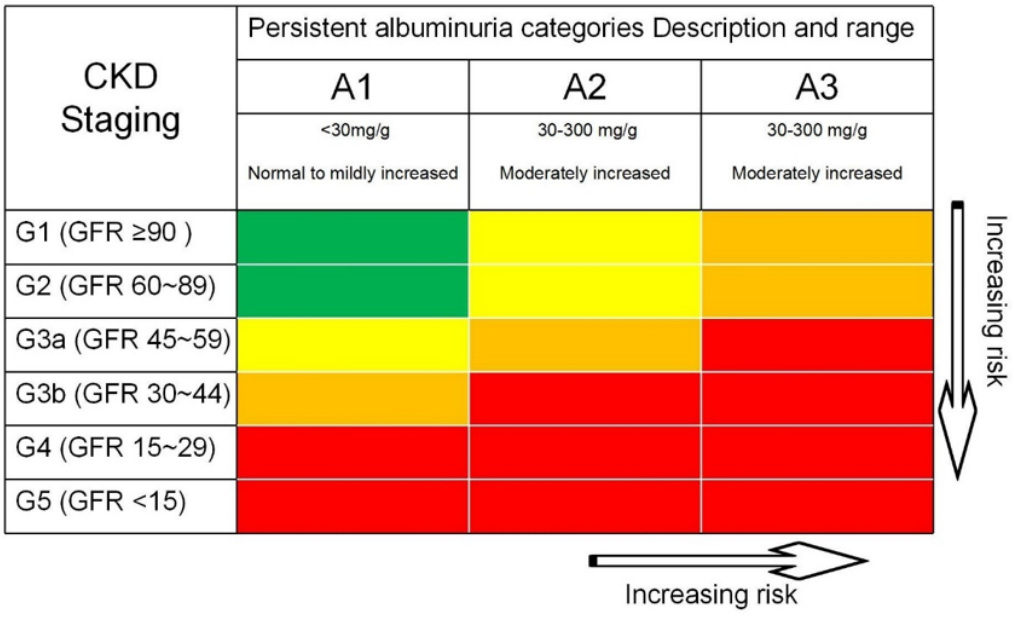

Figure 1.1 The KDIGO categorization of CKD prognosis is determined by GFR and urine albumin excretion levels. The risk of CKD progression is indicated by the background color, with green denoting low risk, yellow for medium risk, orange for high risk, and red for very high risk. GFR (ml/min/1.73m^2)

1.2 Alport syndrome

1.2.1 Definition of Alport syndrome

Alport syndrome is a monogenic disorder affecting around 1 in 5,000 to 53,000 children. It is characterized by the progressive scaring and atrophy of the glomeruli, the filtering compartment of the nephrons of the kidney and by abnormalities of the inner ear and eyes [14, 15]. The disorder was first identified by Cecil A. Alport in a British family in 1927 [16].

This disorder is caused by an inherited defect in type IV collagen, which is a main component of the glomerular basement membrane (GBM) [17]. These mutations result in abnormal collagen structure in organs, which manifests as hereditary glomerular diseases, including hematuria, proteinuria, and gradual deterioration in kidney function, often accompanied by hearing loss as well as ocular abnormalities [18]. Alport syndrome can be inherited through three ways: as an X-linked disorder, autosomal recessive disorder, or autosomal dominant disorder. [19].

1.2.2 Pathogenic mechanism of Alport syndrome

Variants in the genes COL4An (n=3, 4, 5) that encode for the α3, α4 and α5 chains of type IV collagen cause the disease [20, 21]. Table 1.2 give a brief overview. Inheritance patterns are typically X-linked (80%-85%), autosomal recessive (12%~15%), or autosomal dominant (5%~8%). The vast majority of instances of X-linked heritance entail a genetic mutation within the COL4A5 gene, which is situated on the X chromosome at locus Xq22 [22-24]. The chief underlying factor for the inheritance of autosomal recessive and dominant traits is the presence of genetic mutations in the COL4A3 or COL4A4 gene located on chromosome 22q35-37. These genes code for the α3 and α4 chains of type IV collagen [25-27].

Table 1.2 Causative genes of Alport syndrome

Gene	Col4A3	Col4A4	Col4A5
Location	chr2:228029281-228179508 **(2q36.3)**	chr2:227867427-228029275 **(2q36.3)**	chrX:107683019-107940775 **(Xq22.3)**
Number of exons	52	48	51
encoded protein	IV collagen α3 chain	IV collagen α4 chain	IV collagen α5 chain
Inheritance	AD/AR	AD/AR	XD
Incidence	12%~15%	5%~8%	80%~85%

AD: autosomal dominant; AR: autosomal recessive; XD: X-linked dominant.

Various kinds of mutations, such as deletions of small fragments, insertions, missense mutations, nonsense mutations, and splice site mutations, can occur throughout the gene. Large fragment recombination or deletion of the entire gene can also occur [28, 29]. Additionally, there is a subtype of Alport syndrome with this inheritance pattern, that results from mutations in the COL4A5 and COL4A6. However, there have been no reported cases of Alport syndrome resulting from a single COL4A6 gene mutation [30, 31].

The gene responsible for autosomal recessive Alport syndrome is either COL4A3 or COL4A4 [32]. The most severe cases of Alport syndrome are attributed to homozygous and compound heterozygous mutations, but it is not yet confirmed if double gene mutations exist. Most reported mutations are small and include synonymous, missense, splice site, and nonsense mutations [33, 34].

The clinical manifestations of Alport Syndrome vary depending on the mutation type and the particular gene that is impacted [35]. Deletions in the COL4A5 gene and severe splice variants result in kidney impairment and hearing loss. Missense mutations can cause either juvenile-onset or adult-onset hearing loss with or without kidney involvement. Deletion of the 5' end of the COL4A5 gene and the adjacent 5' end of the COL4A6 gene may cause esophageal and genital leiomyomas [22, 30, 36, 37]. Alport syndrome, which is inherited in an autosomal recessive pattern, is caused by mutations that affect both copies of either the COL4A3 or COL4A4 gene, referred to as homozygous or compound heterozygous mutations, and heterozygous mutations may lead to benign familial hematuria disorders such as familial thin basement membrane disease [38, 39].

1.2.3 Kidney injury in Alport syndrome

The glomerular filtration barrier, which is essential for kidney function, consists of three components: the GBM, the endothelium, and the podocytes [40]. Figure 1.2 showed the partial glomerular capillary, Bowman's capsule, and proximal tubule in healthy and Alport syndrome situations. During healthy kidney development, mature α3α4α5 collagen type IV heterotrimers replace the immature α1α1α2 type [41]. In individuals suffering from Alport syndrome, however, mutations in the genes responsible for producing α3(IV), α4(IV), or α5(IV) chains result in a GBM structure that consists mainly of immature α1α1α2 collagen IV. Despite being capable of temporarily maintaining the integrity of the GBM structure and delaying the onset of the disease, this mechanism eventually leads to kidney dysfunction via multiple pathways as a result of prolonged exposure over time [40].

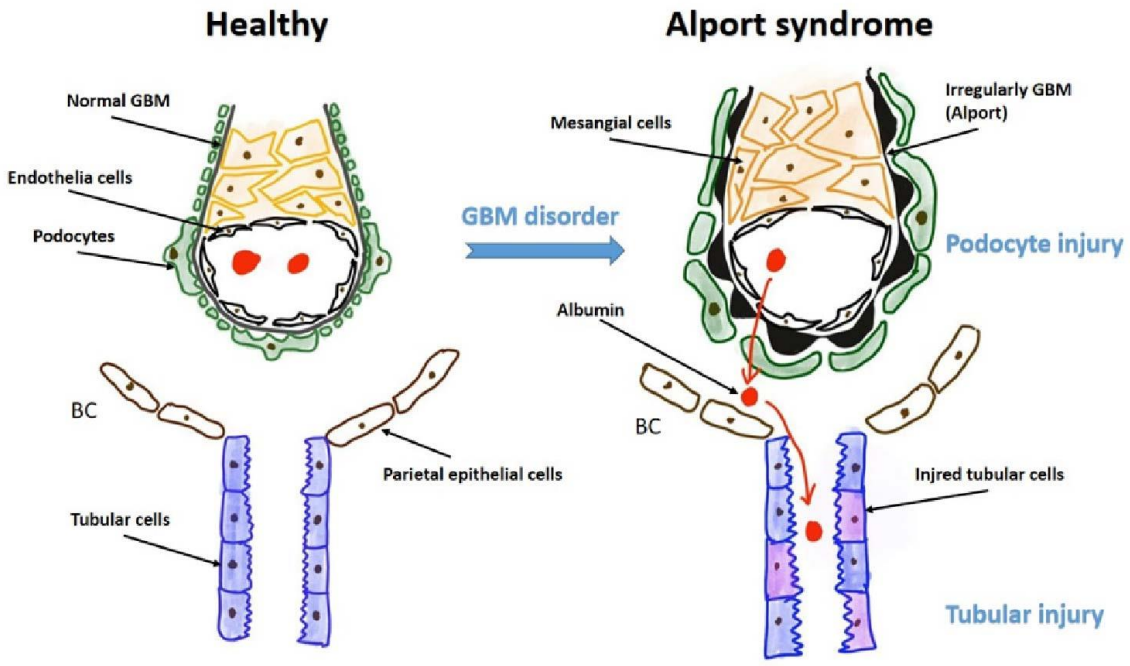

Figure 1.2 Schematic of a partial glomerular capillary, Bowman's capsule (BC), and proximal tubule in healthy and Alport syndrome situations.

The podocytes are intricately linked to the protein network in the GBM and the slit diaphragm, ensuring the stability of both the glomerular cells and the surrounding extracellular structures [42]. However, mutations in collagen can cause altered signaling pathways, resulting in increased expression of factors that promote inflammation and fibrosis, such as TGF-beta, MMP2, MMP3, MMP9, CTGF, and chemokines, ultimately contributing to kidney injury [41, 43].

Compared to the mature α3α4α5 collagen type IV heterotrimers, the α1α1α2 heterotrimers present in Alport syndrome patients have fewer interchain disulfide crosslinks, making them less stable [40, 43]. The heightened instability of the GBM can make it more vulnerable to degradation by proteases such as matrix metalloproteinases (MMPs). [40]. Additionally, patients with Alport syndrome display elevated elasticity in the GBM, which enhances the biomechanical tension on mesangial cells and podocytes, disrupting the receptors' interaction and signaling between podocytes and GBM proteins. [43]. With ongoing nephron loss, glomerular pressure continues to increase, further exacerbating the biomechanical strain on the glomerular cells [42]. This high level of biomechanical strain on podocytes in Alport syndrome patients exacerbates glomerular injury [42].

The progression of Alport syndrome to CKD and kidney failure involves a continuous activation of renin-angiotensin system (RAS). This involves an upregulation of the canonical axis (ACE/Ang II/AT1 receptor) and a downregulation of the alternative axis (ACE2/Ang (1-7)/Mas receptor) [44, 45]. The

elevated levels of Ang II result in increased glomerular pressure, which contributes to proteinuria and the production of chemokines and reactive oxygen species [44]. At the same time, the reduction of Ang-(1-7) and ACE2 levels exacerbates pro-fibrotic and pro-inflammatory states [45, 46]. However, studies have shown that administering Ang-(1-7) and ACE2 to Alport syndrome mice can produce renoprotective effects. These effects include the inhibition of TGF-beta and IL-6 expression, as well as a reduction in COL1A1 mRNA expression and an accumulation of extracellular matrix proteins [45]. As a result, angiotensin-converting enzyme inhibitors (ACEi) are the preferred medications for delaying the deterioration of kidney function in individuals with Alport syndrome.

The normal replacement of α1β1γ1 and α2β1γ1 laminins by α5β2γ1 heterotrimers during kidney development does not occur. Instead, α1β1γ1 and α2β1γ1 laminins are abnormally deposited in the GBM [40, 41]. This abnormal deposition of laminins leads to altered signaling in adjacent receptors, hindering normal polymerization and signaling of α5β2γ1 laminin and integrin α3β1 [40, 44]. This in turn leads to further damage such as proteinuria, degradation of the GBM, loss of foot processes, activation of kappa B (NF-κB) and heightened pro-inflammatory responses [41, 44]. The result is worsening of glomerulosclerosis, nephron loss, and glomerular hypertension.

Ultimately, the pathophysiological mechanisms of Alport syndrome lead to glomerular degeneration, progressive CKD and kidney failure early in life [41, 47]. Figure 1.3 shows the physiopathology in kidney of Alport syndrome.

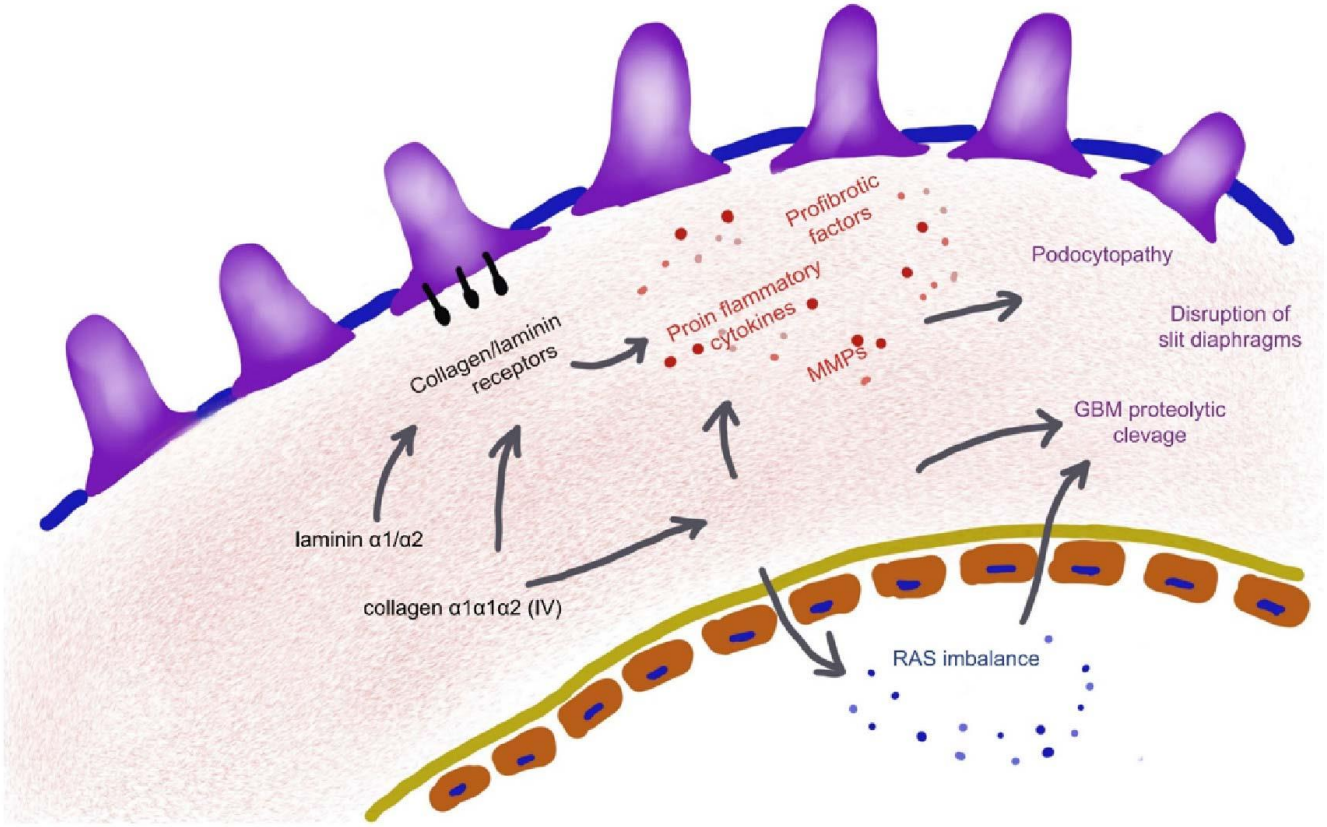

Figure 1.3 Pathophysiology in Alport syndrome kidneys. The lack of α3α4α5(IV) collagen in Alport syndrome leads to increased production of α1α1α2(IV) in the GBM. This immature collagen interacts with podocyte receptors and triggers proinflammatory cytokine, profibrotic factor, and MMP overexpression. The α1α1α2(IV) collagen also has weaker interchain disulfide bonds, making the GBM more elastic and unstable, increasing susceptibility to proteolytic degradation and RAS imbalance. The abnormal deposition of laminins α1β1γ1 and α2β1γ1 in the GBM further exacerbates the disease by interacting with adjacent receptors. This leads to podocytopathy, slit diaphragm disruption, and GBM proteolytic cleavage.

1.2.4 Conventional treatments for Alport syndrome

Studies indicate that controlling proteinuria, combating fibrosis, and other treatments can slow the progression of Alport syndrome and delay kidney failure [48]. Since there is no cure for Alport syndrome, e.g., by gene therapy, standard of care for Alport syndrome patients involves using drugs to control RAS activation and proteinuria to decelerate the progression of Alport syndrome towards kidney failure. [18]. Figure 1.4 illustrates the clinical presentation of Alport syndrome and the potential impact of treatment.

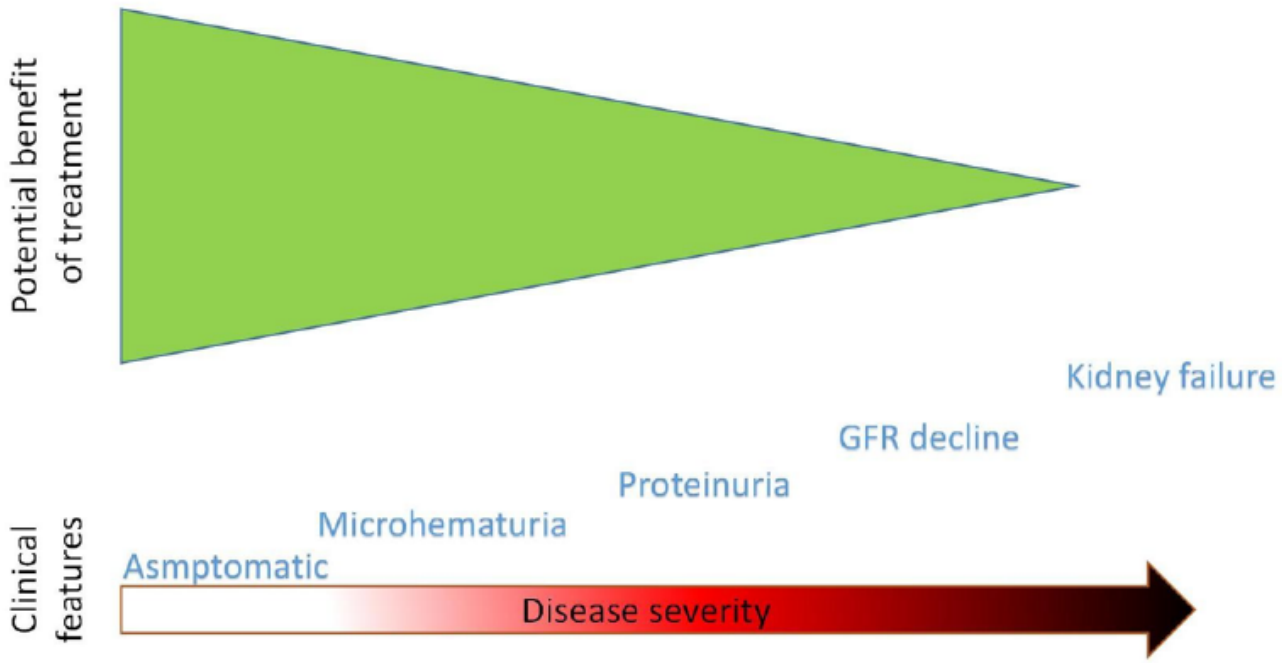

Figure 1.4 Clinical features of Alport syndrome and the potential efficacy of treatment options. The effectiveness of treatment varies based on the stage of the disease, with decreasing potential impact as the severity of the disease increases.

The International Alport Syndrome Expert Group's 2013 diagnosis and treatment guidelines classify treatment drugs into first-line (e.g. ACE inhibitors such as ramipril and enalapril) and second-line (Angiotensin Receptor Blockers and aldosterone receptor antagonists) categories [48]. The recommended ACEI dosage for those under 18 is listed in table 1.3. The recommended dosages for ARBs and aldosterone receptor antagonists for individuals under 18 are listed in Table 1.4. For patients aged 10 to 20, the recommended spironolactone dose is 25 mg/day and should be reduced for those under 10 [48]. Long-term use of ACEis or ARBs can cause a decrease in serum aldosterone levels initially, but levels later rise above baseline, referred to as "aldosterone escape" [49, 50]. This can result in persistent proteinuria in children taking ACE inhibitors, hence spironolactone can be utilized as a second-line treatment, either as a monotherapy or in conjunction with ARBs [51].

Despite any treatment efforts, Alport syndrome will eventually result in kidney failure, which requires the implementation of kidney replacement therapy [52]. This includes dialysis techniques including hemodialysis, peritoneal dialysis and kidney transplantation [53].

Table 1.3 First-line therapy of Alport syndrome

Agent	Dose
Ramipril	Starting dose of 1 to 2 mg/m^2/day; increase by 1 to 2 mg/m^2/day every 3 months until target Urine protein to creatinine ratio or adverse effect is attained; maximum dose 6 mg/m^2/day
Enalapril	2 × Ramipril dose (2 to 4 mg/m^2/day)
Lisinopril	4 × Ramipril dose (4 to 8 mg/m^2/day)
Cilazapril	1 × Ramipril dose (1 to 2 mg/m^2/day)
Trandolapril	0.5 × Ramipril dose (0.5 to 1 mg/m^2/day)

Table 1.4 Second-line therapy of Alport syndrome

Agent	Dose
Losartan	12.5 mg/m^2/day; double dose every 3 month until target Urine protein to creatinine ratio or adverse effect is attained; maximum dose 50 mg/m^2/day
Candesartan	0.2 × Losartan dose (6.25 mg/m^2/day)
Irbesartan	3 × Losartan dose (37.5 mg/m^2/day)
Telmisartan	0.8 × Losartan dose (10 mg/m^2/day)
Valsartan	1.5 × Losartan dose (18.75 mg/m^2/day)
Epresartan	12 × Losartan dose (150 mg/m^2/day)

1.3 From monotherapy to combination therapy for CKD

1.3.1 RAS inhibition therapies ACEI and ARB

The main objective in CKD treatment is to block the RAS activity. [54]. To effectively reduce proteinuria, decelerate the advancement of CKD, and mitigate the likelihood of cardiovascular disease, the blockade of RAS using either an ACEI or an ARB is considered the cornerstone therapy [55]. Several well-conducted clinical trials have demonstrated that blokinging RAS is an effective way to protect the kidneys [56-58]. The main clinical trials studying the blockade of RAS are detailed in table 1.5, which highlights the significance of RAS inhibition in the management of CKD.

Circulating RAS remained active even during treatment with only ACEI or ARB, leading to expectations that enhanced RAS blockade would better protect the kidneys [59]. In theory, inhibiting multiple steps in the RAS system would enhance the inhibition effect and maximize nephroprotection [60]. Studies have demonstrated that the combined treatment of ACEI and ARB is more efficient in decreasing proteinuria than monotherapy [61]. However, some studies have demonstrated conflicting results. The ONTARGET/TRANSCEND trials demonstrated that telmisartan (80 mg per 24h) was as effective as ramipril (10 mg per 24h) and associated with less angioedema among individuals who have vascular disease or diabetes with a high-risk profile. However, combining both medications resulted in more negative effects without any additional advantages. [62]. Another trial from the ONTARGET study showed that telmisartan

(80 mg/day) had similar effects on major kidney outcomes as ramipril (10mg/day) in individuals who are 55 years old or above and have confirmed atherosclerotic vascular disease or diabetes accompanied by damage to end-organs. The combined therapy reduced proteinuria compared to monotherapy, but overall worsened major kidney outcomes [63]. The VA NEPHRON-D trial studied the dual therapy of ACEI and ARB in individuals with diabetes and proteinuria, but some individuals in dual-drug treatment showed significant hyperkalemia and acute decline of kidney function, which led to the trial being terminated prematurely [64]. Thus, the renal protective benefits of combining RAS blockers are not evident in individuals with hyperalbuminuria and kidney insufficiency, raising significant questions about its efficacy and safety [59]. Overall, these independent large clinical trials did not endorse using combined RAS blockade as a means of preventing CKD progression.

Soon, it became evident that RAS inhibitors had a limited capacity in curbing the progression of CKD across a range of diseases. This realization was driven by the understanding RAS activation contributes the shared pathomechanism of excessive hemodynamic stress on the remaining functional nephrons in CKD. [1, 65, 66]. Monotherapy with RAS inhibitors showed only limited renoprotection, making RAS blockade more of a secondary treatment when addressing the underlying causes of CKD [67]. Combination therapies have been shown to be more effective than monotherapy for diseases with complex pathophysiologies, such as hypertension, autoimmune and tumor diseases, organ transplants, and platelet inhibition after coronary surgery [68-72]. It is reasonable to assume that the same could be expected for progressive CKD due to its varying and complicated causes [1, 2, 9]. This is especially pertinent for older individuals, as the pathogenesis of CKD in this demographic often involves multiple factors.

Table 1.5 The main clinical trials studying RAS blockade

Clinical Trials	Study agents	Numbers of patients	Participant	Follow-up time	Primary outcomes	Results
REIN [57]	Ramipril vs. placebo	590	Non-diabetic CKD	31 months	Change in GFR, Time to ESKD, Time to overt proteinuria	52% decreased risk of overt proteinuria (p = 0.005). 56% decreased risk of ESKD (p = 0.01). No difference in rate of GFR decline
IDNT [73]	Irbesartan vs. amlodipine vs. placebo	1,715	DM nephropathy	2.6 years	SCr doubling, ESKD or Death	Risk reduction 20% vs. placebo (p = 0.02), 23% vs. amlodipine (p = 0.006)
RENAAL [56]	Losartan vs. placebo	1,513	DM nephropathy	3.4 years	SCr doubling, ESKD, or Death	Risk reduction 16% (2–28%), p = 0.02
IRMA-2 [74]	Irbesartan vs. placebo	590	Type 2 DM and Hypertension	2 years	Onset of overt albuminuria	Irbesartan 300 mg HR = 0.30 (0.14-0.61)
AASK [75]	Ramipril vs. Metoprolol vs. Amlodipine	1,094	Hypertensive kidney disease	4.1 years	50% GFR reduction, ESKD, or death	R v M= Risk reduction 22% (1–38%, p = 0.04)
ONTARGET [62]	Ramipril + Telmisartan vs. monotherapy	25,620	Type 2 DM with end-organ damage or atherosclerotic vascular disease	56 months	SCr doubling, ESKD, or death	HR = 1.09 [1.01–1.18]
VA-NEPHRON [76]	Lisinopril + Losartan vs. monotherapy	1,448	DM nephropathy	2.2 years*	GFR decline, ESKD, or death	HR = 0.88 [0.70–1.12]
ALTITUDE [77]	Aliskiren + ACEi or ARB vs. monotherapy	8,561	Type 2 DM with CKD or CVD	32.9 months*	SCr doubling, ESKD, or death	HR = 1.03 [0.87–1.23]
PRONED [78]	Lisinopril + Irbesartan vs. monotherapy	133	DM nephropathy	32 months	>50% increase in baseline SCr, ESKD, or death	HR = 0.96 [0.44–2.05] vs. lisinopril HR = 0.90 [0.39–2.02] vs. irbesartan
ALLHAT [79]	Lisinopril vs. Amlodipine vs. Chlorthalidone	5,545	Hypertensive kidney disease	8.8 years	ESKD	HR = 0.91 [0.73–1.14] vs. Chlorthalidone

CKD, Chronic kidney disease; DM, Diabetes mellitus; SCr, Serum Creatinine; GFR, Glomerular filtration rate; ESKD, End-stage kidney disease; CVD, Cardiovascular disease; ACEi, Angiotensin-converting enzyme inhibitor; ARB, Angiotensin receptor blocker; HR, Hazard ratio (95% confidence interval). *Terminate early due to increased adverse events.

1.3.2 SGLT2 inhibitors and dual RAS/SGLT2 inhibition

Sodium-glucose cotransporter 2 (SGLT2) inhibitors are drugs utilized to manage type 2 diabetes (T2DM) by regulating the sodium-glucose transport proteins in the nephron [80, 81]. They mainly work by inhibiting kidney glucose reabsorption for improved glycemic control and have shown to provide cardiovascular benefits for T2DM patients [82, 83]. In 2022, the American Diabetes Association (ADA) designated SGLT2 inhibitors as the first line of drug therapy for T2DM in its standards of care for diabetes. This treatment is often combined with metformin and is particularly indicated for individuals who have CKD and cardiovascular disease [84]. During the last ten years, SGLT2 inhibitors showed remarkable effectiveness in preventing progression of CKD beyond what is achieved by RAS inhibition [85, 86]. This is likely due to their ability to significantly reduce the metabolic workload on the remaining nephrons by hindering the reuptake of sodium and glucose in the proximal tubule [87, 88]. Table 1.6 showed the summary of kidney outcomes in clinical studies with SGLT2 inhibitors. The precise mechanism underlying the kidney-protective effect of SGLT2 inhibitors is currently a topic of debate. However, there are a few potential explanations that have been proposed. One such mechanism involves the improvement of glomerular hemodynamics. Diabetes leads to a compromise of tubuloglomerular feedback through the activation of SGLT2, which results in the afferent arteriole to dilate, the efferent arteriole to indirectly constrict,, and an increase in filtration pressure and GFR. [89, 90]. SGLT2 inhibitors reverse these effects and this way reduce hyperfiltration and proteinuria. The same mechanism reduces the workload on the cells of the proximal tubules by decreasing their metabolic stress due to less glucose and sodium reabsorption per cell. This reduction in activity leads to a decrease in both the oxygen and energy demand [91, 92]. Besides, influenced by proteinuria and elevated glucose levels, inflammatory mediators, fibrotic mediators, and reactive oxygen species are triggered in tubular cells. So, another mechanistic is that SGLT2 inhibitors could act by reducing inflammatory response and kidney fibrosis [93, 94].

Table 1.6 Kidney outcomes in clinical trials with SGLT2 inhibitors.

Clinical Trials	SGLT2i	Numbers of patients	Participant	Follow-up time	Kidney outcomes	Kidney Results
EMPA-REG [95]	Empagliflozin	7,020	Type 2 Diabetes	3.1 years	Incident or worsening nephropathy and incident albuminuria.	Scr doubling, GFR<45 ml/min, dialysis, RR- death 0.54 [0.40–0.75]
CANVAS [96]	Canagliflozin	10,142	Type 2 Diabetes	188.2 weeks	Progression of albuminuria, kidney-replacement therapy, RR-death,	Albuminuria progression 0.73 [0.67–0.79] ≥40% GFR decrease, ESKD, or RR-death 0.60 [0.47–0.77]
DECLARE-TIMI [97]	Dapagliflozin	17,160	Type 2 Diabetes	4.2 years	The rate of change in GFR, ESKD, death from kidney or cardiovascular causes	Risk reduction 16% (2–28%), p = 0.02
CREDENCE [98]	Canagliflozin	4,401	Diabetic Nephropathy	2.62 years	ESKD, a doubling of the SCr level, or death from kidney or cardiovascular causes	SCr doubling, ESKD, or RR-death 0.66 [0.53–0.81]
CVD-REAL3 [99]	Different kinds of gliflozins*	35,561	Type 2 Diabetes	14.9 months	The rate of change in GFR	>50% GFR decrease or ESKD 0.49 [0.35–0.67]
DAPA-CKD [100]	Dapagliflozin	4,304	Proteinuric nephropathy (diabetic and non-diabetic nephropathy)	2.4 years	Decline in GFR least 50%, ESKD, death from kidney or cardiovascular causes	>50% GFR decrease, ESKD, RR- death 0.56. [0.45–0.68]

CKD, Chronic kidney disease; SCr, Serum Creatinine; GFR, Glomerular filtration rate; ESKD, End-stage kidney disease; RR-death, kidney related death.

*Several kinds of glifozins (Dapagliflozin 58%; Empagliflozin 34%; Canagliflozin 6%; Pragliflozin; Tofogliflozin 2%; Luseogliflozin).

A study conducted in 2016 found that a combined RAS/SGLT2 blockade had strong effects that protect the kidney in individuals with CKD and T2DM [95]. A RAS/SGLT2 blockade has up to 57% effect size in preventing gradual decline in kidney function in individuals with non-diabetic glomerulopathies, which is higher than diagnosis-specific therapies [101]. Like heart failure, dual RAS/SGLT2 inhibition can preserve kidney function by reducing workload. SGLT2 and RAS inhibitors act at different parts of the kidney, but have synergistic effects when combined, as shown in figures 1.5 and 1.6 for T2DM. Theoretically, their protection of kidney function should be synergistic due to complementary mechanisms [102].

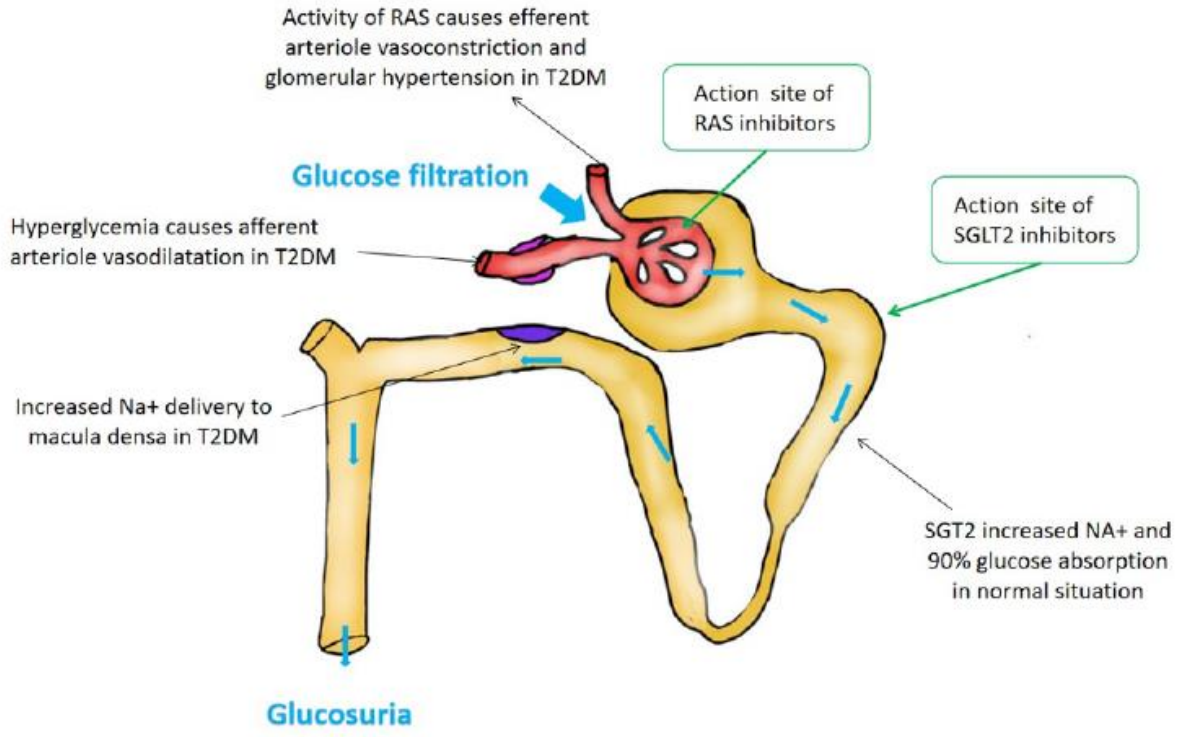

Figure 1.5 The sites of action of SGLT2 and RAS inhibitors and synergistic mechanisms of their combination therapy in T2DM. RAS: renin-angiotensin system; T2DM: type 2 diabetes mellitus; SGLT2: sodium-glucose co-transporter 2.

Studies have showed that simultaneous using SGLT2 inhibitors as well as ACEI/ARB inhibitors in diabetic Dahl salt-sensitive rats has a higher impact in protecting the kidneys compared to using either drug alone. This combination therapy was more effective in preserving kidney function [103, 104]. A phase III clinical trial revealed a 33.2% decrease in albuminuria and systolic blood pressure in individuals with diabetic kidney disease (DKD) when combining ACEI/ARB with dapagliflozin. Results demonstrated that the decline of albuminuria was largely separate from the glucose-lowering effect of dapagliflozin, and instead, several other factors contributed to the proteinuria decrease [105]. Additionally, the SGLT2 inhibitor treatment group experienced a decrease in serum uric acid and normal serum potassium levels during the double-blind treatment period [106-108]. It's noteworthy that the slightly reduced eGFR

observed at the start with SGLT2 inhibitors fully recovered after discontinuation, indicating that the functional nephrons were not affected [105]. Table 1.7 shows the effect of SGLT2 inhibitors in combination with ACEI/ARBs.

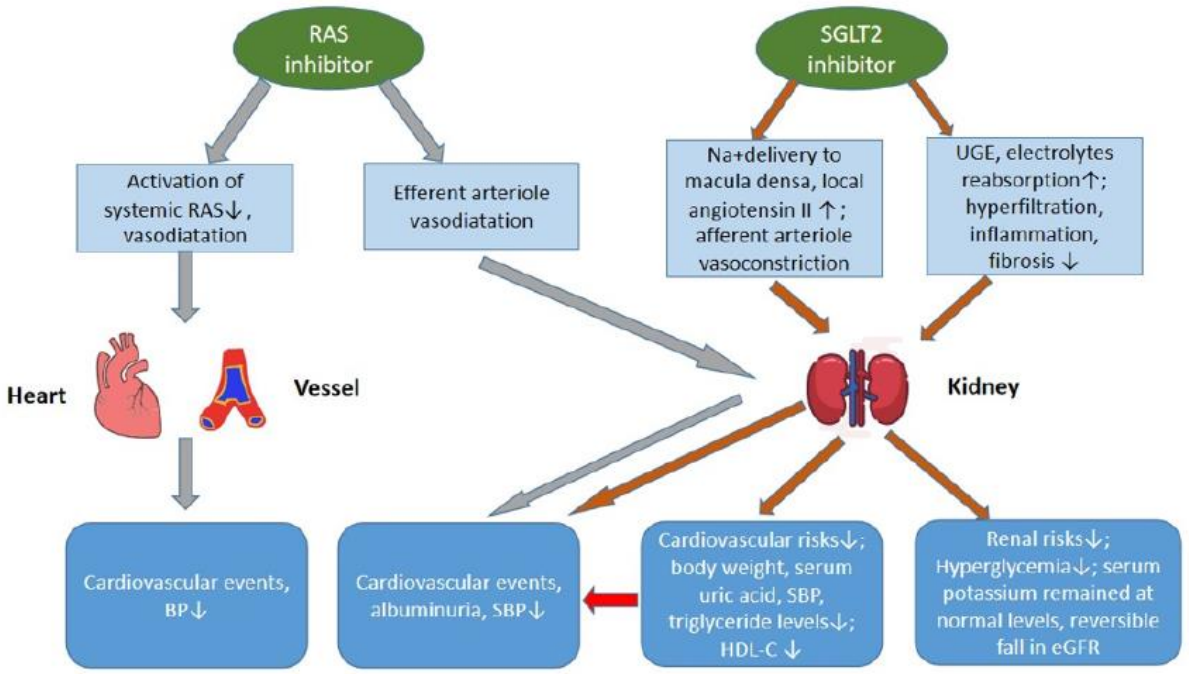

Figure 1.6 Synergistic effects of SGTL2 and RAS inhibitors. RAS: renin-angiotensin system; SGLT2: sodium-glucose co-transporter 2; UGE: urinary glucose excretion; BP: blood pressure; SBP: systolic blood pressure; HDL-C: high density lipoprotein-cholesterol; eGFR: estimated glomerular filtration rate.

Table 1.7 Effect of SGLT2 inhibitors combined with ACEI/ARBs.

Clinical Trials	Intervention	Numbers of patients	Participant	Follow -up time	Difference amongst groups (95% CL)					
					△HbA1c (%)	△FPG (mmol/L)	△eGFR (ml/min/1.73m^2)	△UACR	△Serum uric acid (μmol/L)	△Albumi-nuria
Heerspink [109]	A: DAPA 10mg+ACEI/ARB B: ACEI/ARB+PBO	A: n=167 B: n=189	Type 2 Diabetes	12 weeks	A-B: -0.5% (-0.7, -0.3)	NR	A-B: -2.80 (-5.43, -0.16)	A-B: -23.5% (-37.6, -6.3)	NR	A-B: -33.2% (-45.4, -18.2)
Weber [110]	A: DAPA 10mg+ACEI/ARB B: ACEI/ARB+PBO	A: n=302 B: n=311	Type 2 Diabetes	12 weeks	A-B: -0.49% (-0.59, -0.33)	AB:(−0.69 vs 0.38)	NS	NR	A-B:(−17.84 vs 5.95)	NR
Weber [105]	A: DAPA 10mg+ACEI/ARB B: ACEI/ARB+PBO	A: n=225 B: n=224	Type 2 Diabetes	12 weeks	A-B: -0.61% (-0.76, -0.46)	A-B: -1.2 (-1.7, -0.8)	NS	NS	A-B: -23.67 (-33.7, -13.64)	NR
Sha [106]	A: CANA 300mg +ACEI/ARB+MET B: ACEI/ARB+ PBO+MET	A: n=18 B: n=18	Type 2 Diabetes	12 weeks	A-B: -0.6% (-0.9, -0.3)	A-B: -1.6 (-2.3, -0.9)	A-B: -4.0 (-8.7, -0.7)	NR	NR	NR

Data reported as placebo-adjusted difference (95% CI) or adjusted mean change from baseline of A group vs B group.

SGLT2, Sodium-glucose Cotransporter-2; ACEI/ARBs, angiotensin-converting enzyme inhibitors/angiotensin receptor blockers; 95% CI, 95% confidence interval; HbA1c, glycated haemoglobin; FPG, fasting plasma glucose; eGFR, estimated glomerular filtration rate; UACR, urinary albumin creatinine ratio; DNPA, dapagliflozin; PBO, placebo; NR not reported/retrievable; vs, versus; NS, not-significant; CANA, canagliflozin; MET, metformin.

1.3.3 MR inhibitor and triple RAS/SGLT2/MR blockade

Growing evidence suggests that mineralocorticoid receptor (MR) overactivation plays a crucial role in the onset and advancement of CKD [111-114]. Although MR can positively regulate blood pressure and sodium retention, it has become increasingly clear that its hyperactivation plays a role in inflammation and fibrosis development in kidney as well as cardiac systems [115]. The excessive activation of MR leads to the up-regulation of genes related to inflammation and fibrosis, ultimately causing harm to the organs [116]. As a result, blocking MR is becoming a helpful treatment approach to decelerate CKD progression and decrease mortality ralated to cardiovascular disease. Figure 1.7 depicts the action of MR antagonists as well as their impacts on both tissue and clinical outcomes.

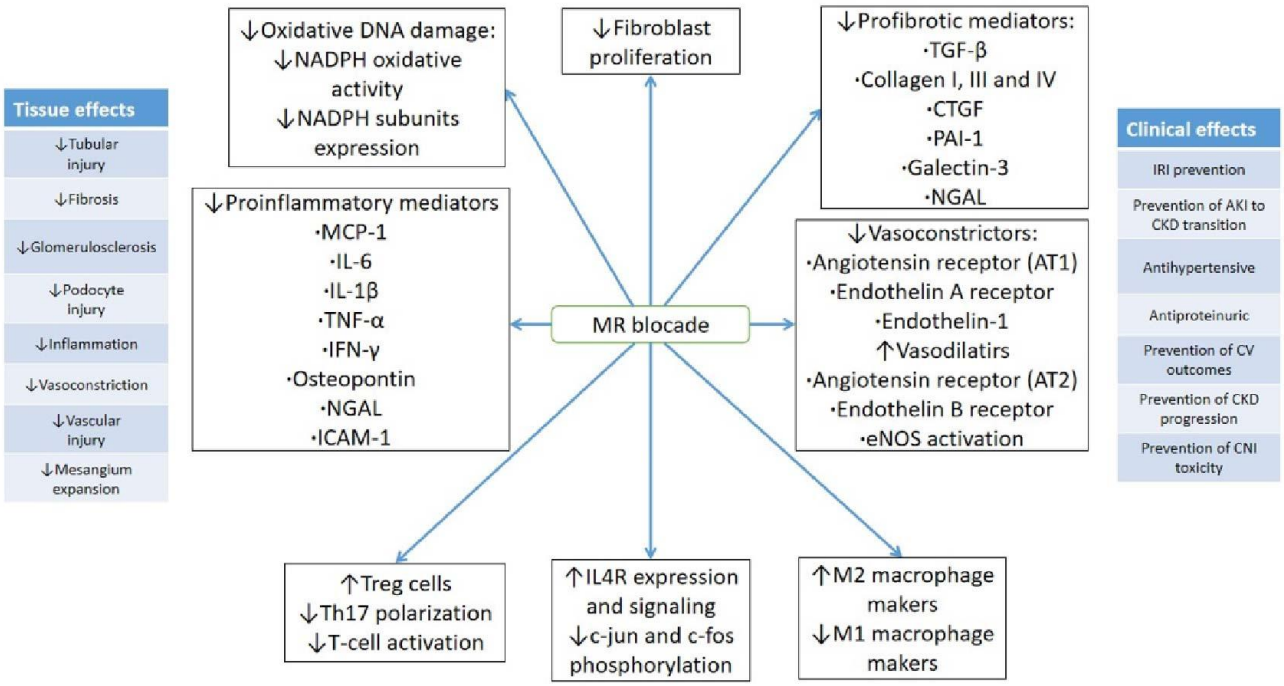

Figure 1.7 The mode of action of MR antagonists and tissue and clinical effects. AKI: acute kidney injury; CKD: chronic kidney disease; CNI: connective tissue growth factor; CV: cardiovascular; eNOS: endothelial nitric oxide synthase; ICAM: intercellular protein; MR: mineralocorticoid receptor; NADPH: nicotinamide adenine dinucleotide phosphate; NGAL: neutrophil gelatinase-associated lipocalin; PAL: plasminogen activator inhibitor; TGF: transforming growth factor; TH17: T helper 17; TNF: tumor necrosis factor.

In the late 1950s, MR antagonists were developed and tested for therapeutic effectiveness. The U.S. Food and Drug Administration (FDA) approved the oral steroid MRA spironolactone in 1960 to manage edema and hypertension [117]. However, steroidal MRAs can cause negative effects including hyperkalemia as well as decreased kidney function, especially in patients with severe kidney insufficiency [118]. Additionally, spironolactone may cause side effects like gynecomastia and impotence, leading to

restrictions or contraindications in certain patient populations [119, 120]. The development of non-steroidal MRAs is a significant advancement in cardiokidney disease [117, 121]. To date, two non-steroidal MRAs, esaxerenone and finerenone, have received approval for treating hypertension and type 2 diabetes-related CKD [122, 123].

Finerenone is a powerful drug designed to mitigate the likelihood of various adverse health outcomes in adults who have type 2 diabetes and CKD [124, 125]. It has been specifically formulated to reduce the linkihood of a loss in kidney function, to prevent the onset of kidney failure, to lower the chance of mortality related to heart disease, and to decrease hospitalizations in heart failure [126]. This medication marks a major advancement in treating diabetes-related CKD, providing a comprehensive approach to managing this complex and debilitating condition [127]. It targets MR with high selectivity and potency due to its affinity and bulk as an MR antagonist, changing the receptor's conformation [120, 128]. Finerenone prevents MR cofactor aggregation, altering gene expression [117, 129]. Transcriptome analysis shows that it is more effective than spironolactone in blocking aldosterone-induced transcripts (20% vs 5%) [130]. The main difference between finerenone and MRAs lies in their chemical structure and specificity of action, with finerenone being a non-steroidal compound with more selective receptor binding activity, and MRAs being steroidal compounds with a broader range of receptor binding activity [125, 128]. Figure 1.8 illustrates finerenone's mode of action and pharmacology.

To date, five clinical studies have evaluated effectiveness of finerenone, including three Phase II studies (ARTS, ARTS-DN, and ARTS-HF), and two Phase III trials (FIDELIO-DKD and FIGARO-DKD). [131-135]. The ARTS trial (NCT01345656) was designed to evalute the effectiveness of finerenone in CKD individuals suffering from Heart Failure with Reduced Ejection Fraction (HFrEF). Another Phase IIb trial called ARTS-DN (NCT01874431) targeted individuals with diabetes and elevated albuminuria levels who were undergoing treatment with ACEI or ARB. Another Phase IIb trial called ARTS-HF (NCT01807221) investigated the effectiveness of finerenone in individuals with T2D as well as CKD who were hospitalized in emergency departments with HFrEF. Additionally, the FIDELIO-DKD (NCT02540993) study tested finerenone combined with standard care to placebo, with the aim of evaluating its impact on slowing the CKD progression and improving cardiovascular outcomes in individuals with CKD as well as T2D. Finally, the FIGARO-DKD (NCT02545049) study examined finerenone combined with standard care versus placebo in improving cardiovascular outcomes in CKD patients. Table 1.8 provides a comprehensive summary of all the finerenone clinical trials.

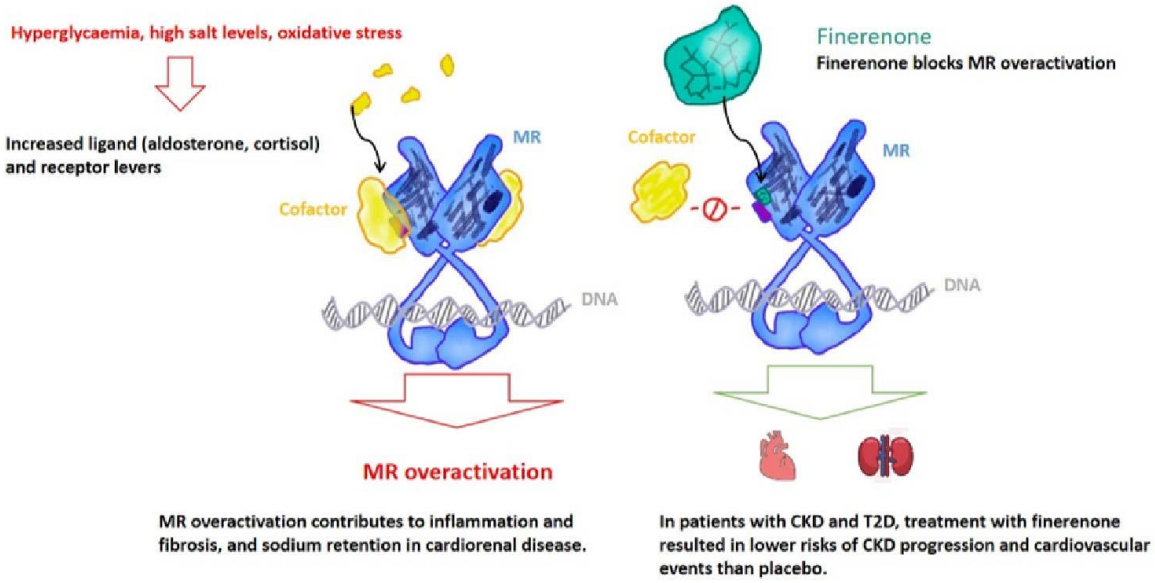

Figure 1.8 Proposed mode of action and pharmacology of finerenone. CKD: chronic kidney disease; MR: mineralocorticoid receptor; TD2: type 2 diabetes.

The FIDELIO study investigated the effectiveness of a dual treatment using RAS inhibitors as well as finerenone in treating type 2 diabetic CKD patients. This combination treatment showed a decreased likelihood of CKD progression compared to RAS inhibitors monotherapy [134]. Importantly, most of these patients had not received any prior treatment with SGLT2 inhibitors. Preclinical studies have supported the potential cardiokidney protective benefits of finerenone together with empagliflozin in a rat model of end-organ damage induced by hypertension [136]. The FIDELITY study found that 6.7% of individuals received treatment with SGLT2 inhibitors, suggesting additive benefits with the combination of MA blockade and SGLT2 inhibitors [137]. Sub-group analysis of the FIDELIO study did provide some positive results for combination therapy of finerenone and SGLT2 inhibitors, but, these results were not derived from another trial and should be interpreted with caution [138, 139]. Currently, there is only one ongoing trial that is assessing the effectiveness of finerenone combined with empagliflozin in CKD and T2D patients [140]. Research has demonstrated that the administration of dual RAS/SGLT2 inhibitors treatment can forestall the deterioration of kidney function, leading to the question of whether a triple inhibitor of the RAS, SGLT2, and MR would still have additive effects in prolonging kidney lifespan in CKD patients. Some post-hoc analyses of major trials or small single-center studies have provided positive signals in this regard, but these were underpowered and based on surrogate markers such as proteinuria [140]. A investigation was carried out to evaluate the effectiveness of dapagliflozin and eplerenone as individual and in combination among CKD patients [141]. The results showed that combining dapagliflozin with eplerenone led to a noteworthy

decrease in the urinary albumin creatinine (UACR) and did not correlate with each other [141]. A well-powered randomized controlled trial (RCT) with relevant clinical endpoints is still needed to provide definitive answers in this area.

Table 1.8 Summary of finerenone clinical trials.

Clinical Trials	Intervention	Numbers of patients	Participant	Follow up time	Primary outcomes	Key Results
ARTS [132]	Finerenone (2.5, 5, or 10 mg QD, or 5 mg BID). Placebo.	392	HFrEF and mild or moderate CKD	28 days	Change in serum potassium	Mean increases in serum potassium: significantly smaller with finerenone (all doses) vs. spironolactone. A similar or greater decrease in BNP, NT-proBNP, and albuminuria with finerenone (5 and 10 mg/day) than with spironolactone (25 or 50 mg/day).
ARTS-DN [131]	Finerenone (1.25-20 mg/day). Placebo.	823	CKD and T2D receiving RAS inhibitors	90 days	Change in UACR	Reduction in UACR: dose dependent at the 4 highest doses of finerenone vs. placebo; 38% UACR reduction with finerenone 20 mg/ day ($p < 0.001$). Hyperkalemia leading to discontinuation: not observed in the placebo and finerenone 10 mg/ day groups; incidences in the finerenone 7.5-20 mg/day groups were low (1.7%–3.2%).
ARTS-HF [133]	Finerenone (2.5-15 mg/day). Placebo.	1066	HFrEF and T2D and/or CKD	90 days	Proportion of patients with >30% decline in NT-proBNP	Proportion of patients with>30% decline in NT-proBNP: similar with finerenone vs. eplerenone. Composite clinical endpoint of all-cause death, CV hospitalizations, or emergency presentation for worsening HF (prespecified exploratory endpoint): occurred numerically less frequently with finerenone vs. Eplerenone.
FIDELIO-DKD [134]	Finerenone (10–20 mg/day). Placebo	5734	CKD and T2D receiving RAS inhibitors	2.6 years	Time to kidney failure, sustained decrease of ≥40% in eGFR or death from kidney causes	Primary outcome: significantly less with finerenone vs. placebo ($p = 0.001$). Secondary outcome: significantly less with finerenone vs. placebo ($p= 0.03$). Frequency of AEs: similar with finerenone vs. placebo. Hyperkalemia leading to discontinuation: higher with finerenone than with placebo (2.3% vs. 0.9%).
FIGARO-DKD [135]	Finerenone (10–20 mg/day). Placebo	7437	CKD and T2D receiving RAS inhibitors	3.4 years	Composite of time to CV death, nonfatal MI, nonfatal stroke, or hospitalization for HF	Primary outcome: significantly less with finerenone vs. placebo ($p = 0.03$); benefit was driven primarily by a lower incidence of hospitalization due to HFc. Secondary outcome: similar with finerenone vs. placebo. Frequency of AEs: overall similar with finerenone vs. placebo. Hyperkalemia leading to discontinuation: higher with finerenone than with placebo (1.2% vs. 0.4%).

AE: adverse event; BID: twice daily; BNP: B-type natriuretic peptide; CKD: chronic kidney disease; CV: cardiovascular; eGFR: estimated glomerular filtration rate; HF: heart failure; HFrEF: heart failure with reduced ejection fraction; MI: myocardial infarction; NT-proBNP: N-terminal pro-B-type natriuretic peptide; QD: once daily; RAS: renin-angiotensin system; T2D: type 2 diabetes; UACR: urinary albumin-to-creatinine ratio.

1.4 Preclinical randomized controlled trials.

In drug development, preclinical studies are performed prior to clinical trials to gather important data on feasibility, drug safety, and iterative testing. This stage typically involves testing in laboratory animals [142]. However, the scientific community faces a "replication crisis" or "translational roadblock," as data reproducibility has become a major challenge in recent decades across various research fields [143].

The translation of drug efficacy from small rodents to human clinical trials is often unsuccessful, indicating a significant gap in the process of transitioning from preclinical validation to human RCTs [142, 144]. This gap is not fully understood or easily solved, as showed in Figure 1.9. Unlike human RCTs, which have strict study designs that include calculated sample sizes, randomized double-blind methods, clear inclusion and exclusion criteria, and robust endpoints, preclinical research is carried out at a single center and carried out by novice researchers who may be influenced by the findings and without independent data quality control [145]. In human clinical trials, deaths or withdrawals of patients and data missing and imputation are carefully documented and reported, but this level of detail is usually lacking in animal studies. This absence of data can significantly influence the results of the animal study [146]. In addition, researchers are often unblended during biosample or data processing that can further skew the results of animal experiments. If scientists selectively choose data, such as by not reporting outliers or extreme values, the resulting differences between groups may be artificially amplified [147, 148]. Therefore, minimizing all sources of bias can aid in closing the divide between animal and human studies to ensure validity and reliability of results in drug development and to make more reliable predictions on the potential outcome of a respective human RCT.

Preclinical RCTs (pRCTs) are a novel method for making more accurate predictions about the outcomes of future human RCTs (as demonstrated in figure 1.9) [145]. pRCTs address these limitations and attempt to minimize biases due to unblinded personnel, inadequate sample sizes, low statistical confidence, and low protocol validity [145]. To improve the validity, pRCTs incorporate elements from clinical RCTs, including registered protocols, blinded study designs, randomization, strict inclusion and exclusion criteria, data analysis by independent research centers, and rigorous testing and data reporting [144, 149]. Unlike single-center preclinical studies, which are often exploratory in nature, pRCTs seek to generate definite and reliable results [149]. pRCTs integrate components from both preclinical as well as clinical research designs to enhance the validation and prediction of clinical drug effects [144]. Thus, pRCTs hold promise for bridging the disparity between preclinical validation and human RCTs.

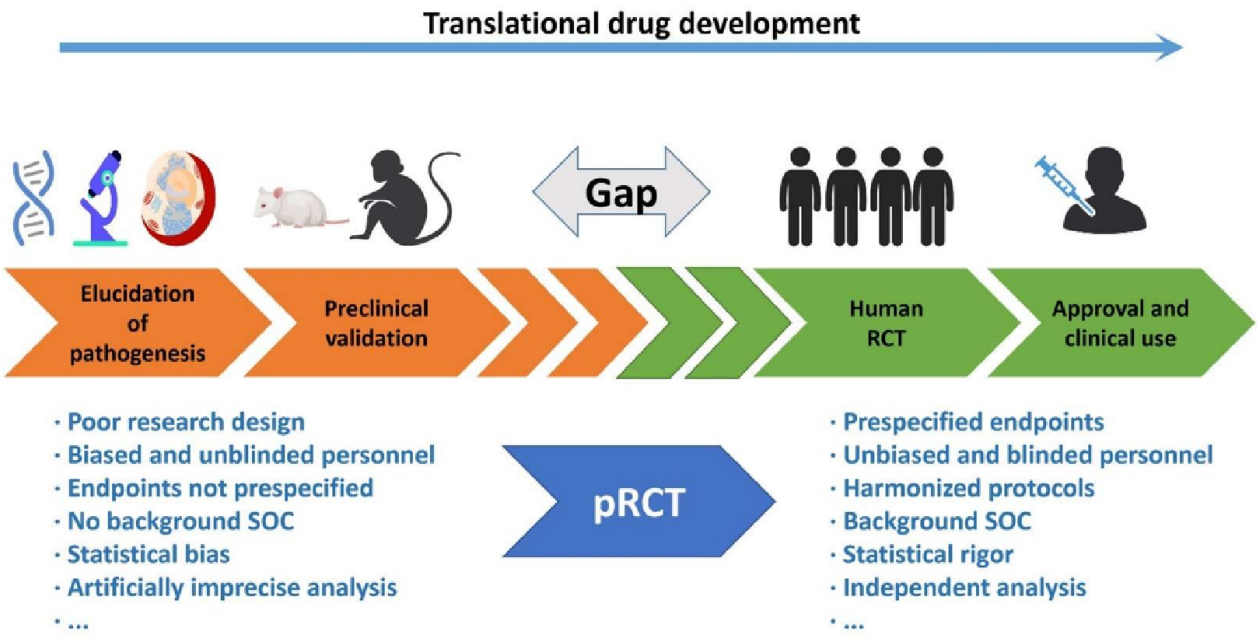

Figure 1.9 Preclinical randomized controlled trials (pRCTs) as a link in the translational drug development. RCT: Randomized controlled trials; SOC: standard-of-care. pRCT: preclinical randomized controlled trials.

For example, Lei et al. conducted a pioneering multi-center pRCT in the field of nephrology, aiming to assess the effectiveness of baricitinib therapy for systemic lupus erythematosus (SLE) and lupus nephritis [150]. The result of this trial predicted poor effects size for baricitinib in heterogeneous populations. Nevertheless, two clinical RCTs (SLE-BRAVE-1 and SLE-BRAVE-2) were performed tsting baricitinib in SLE patients. However, consistent with the prediction made with the pRCT, these trials showed poor efficacy of baricitinib, resulting in the sponsor discontinuing the drug development program [151]. Therefore, we hypothesize that a properly executed pRCT can provide reliable predictions regarding the clinical efficacy of drug interventions for CKD.

2. Research hypotheses

CKD is a global health concern because CKD drastically accelerates cardiovascular aging, implies secondary immunodeficiency, and can progress to kidney failure, which is inevitably fatal, unless access to kidney replacement therapy is available and affordable. Until recently, inhibitors of the RAS had been the only class of renoprotective drugs, and by today remain so for paediatric CKD patients. RAS inhibition started at CKD stage G1 or G2 can have profound effects on kidney lifespan, e.g., among pediatric patients who suffer from Alport syndrome. However, RAS inhibition capacity to prolong kidney lifespan is limited when started at CKD stage G3 or more, which encompasses the vast majority of CKD in adults, where CKD is diagnosed at later stages in most cases. Meanwhile, inhibitors of the sodium-glucose transporter SGLT-2 have demonstrated renoprotective effectiveness on top of RAS inhibition in patients who have diabetic and non-diabetic CKD stage G2-4 and A1-3. Hence, dual RAS/SGLT2 inhibition has emerged as the latest standard of care for optimizing the lifespan of kindeys in CKD. The non-steroidal mineralocorticoid receptor antagonist (MRA) finerenone has demonstrated antiproteinuric effects and attenuation of GFR decline among diabetic individuals who have CKD stage G3 A2-3 and its molecular mechanism-of-action could be complementary to RAS and SGLT2 inhibitors but whether triple RAS/SGLT2/MR inhibition has additive effects over dual RAS/SGLT2 inhibition is currently unknown.

Thus, we hypothesized that the triple combination of ramipril (RASi), empagliflozin (SGLT2i), and finerenone (MRA) significantly prolongs kidney lifespan over dual RAS/SGLT2 inhibition.

3. Materials

3.1 Animal studies

Animal narcosis, injectables, sacrifice

BD Microlance™ Stainless Steel Needles	Becton Dickinson, NJ, USA
BD Plastipak™ Syringes	Becton Dickinson, NJ, USA
Reverter	CP-Pharma, Burgdorf, Germany
Operation table	Medax, Germany
Isoflurane-Forene	Abbott, Wiesbaden, Germany
Vaporizer for Forene (100 Series)	Smiths Medical PM, Norwell, America
Surgical/forceps	Medicon, Tuttlingen, Germany
Anatomical/forceps	Medicon, Tuttlingen, Germany
Scalpel	Pfm medical ag, Cologne, Germany
Scissors (Surgical)	Medicon, Tuttlingen, Germany
Clip/Applying/Forceps	Medicon, Tuttlingen, Germany

Animal diet

Animal diets were purchased from Ssniff Spezialdiäten GmbH and stored at 4 °C. Food admixed with drugs and control diet was provided during the 6th to 14th week of the mouse's life, and standard diet was provided at other times. The ingredients of the diet were as follows:

Standard diet

Ingredient	Quantity
Crude protein	22.0 %
Crude fat	4.5 %
Crude fiber	3.9 %
Raw ash	6.7 %
Calcium	1.0 %
Phosphorus	0.7 %
Vitamin A	25000 U/kg
Vitamin D_3	1500 U/kg
Vitamin E	125 mg/kg
Iron (II) sulphate monohydrate	100 mg/kg
Zinc sulfate monohydrate	50 mg/kg
Manganese (II) sulphate monohydrate	30 mg/kg
Copper (II) sulfate pentahydrate	5 mg/kg
Sodium selenite	0.1 mg/kg
Calcium iodate Anhydrate	2.0 mg/kg

Control diet (Color Yellow)

Ingredient	Quantity
Crude protein	19.0 %
Crude fat	3.3 %
Crude fiber	4.9 %
Crude ash	6.4 %
Starch	36.5 %
Sugar	4.7 %
Vitamin A	25000 U/kg
Vitamin D_3	1500 U/kg
Vitamin E	125 mg/kg
Vitamin K_3	20 mg/kg
Iron (II) sulphate monohydrate	100 mg/kg
Zinc sulfate monohydrate	50 mg/kg
Manganese (II) sulphate monohydrate	30 mg/kg
Copper (II) sulfate pentahydrate	5 mg/kg
Sodium selenite	0.1 mg/kg
Calcium iodate Anhydrate	2.0 mg/kg

Ramipril diet (Color Green)

Ingredient	Quantity
Crude protein	19.0 %
Crude fat	3.3 %
Crude fiber	4.9 %
Crude ash	6.4 %
Starch	36.5 %
Sugar	4.7 %
Vitamin A	25000 U/kg
Vitamin D_3	1500 U/kg
Vitamin E	125 mg/kg
Vitamin K_3	20 mg/kg
Iron (II) sulphate monohydrate	100 mg/kg
Zinc sulfate monohydrate	50 mg/kg
Manganese (II) sulphate monohydrate	30 mg/kg
Copper (II) sulfate pentahydrate	5 mg/kg
Sodium selenite	0.1 mg/kg
Calcium iodate Anhydrate	2.0 mg/kg
Ramipril	50 mg/kg

Ramipril+Empagliflozin diet (Color Red)

Ingredient	Quantity
Crude protein	19.0 %
Crude fat	3.3 %
Crude fiber	4.9 %
Crude ash	6.4 %
Starch	36.5 %
Sugar	4.7 %
Vitamin A	25000 U/kg
Vitamin D_3	1500 U/kg
Vitamin E	125 mg/kg
Vitamin K_3	20 mg/kg
Iron (II) sulphate monohydrate	100 mg/kg
Zinc sulfate monohydrate	50 mg/kg
Manganese (II) sulphate monohydrate	30 mg/kg
Copper (II) sulfate pentahydrate	5 mg/kg
Sodium selenite	0.1 mg/kg
Calcium iodate Anhydrate	2.0 mg/kg
Ramipril	50 mg/kg
Empagliflozin	150 mg/kg

Ramipril+Empagliflozin+Finerenone diet (Color Blue)

Ingredient	Quantity
Crude protein	19.0 %
Crude fat	3.3 %
Crude fiber	4.9 %
Crude ash	6.4 %
Starch	36.5 %
Sugar	4.7 %
Vitamin A	25000 U/kg
Vitamin D_3	1500 U/kg
Vitamin E	125 mg/kg
Vitamin K_3	20 mg/kg
Iron (II) sulphate monohydrate	100 mg/kg
Zinc sulfate monohydrate	50 mg/kg
Manganese (II) sulphate monohydrate	30 mg/kg
Copper (II) sulfate pentahydrate	5 mg/kg
Sodium selenite	0.1 mg/kg
Calcium iodate Anhydrate	2.0 mg/kg

Ramipril	50 mg/kg
Empagliflozin	150 mg/kg
Finerenone	50 mg/kg

Ramipril overview

Article Name	Ramipril, CAS [87333-19-5]
Biozol Catalog Number	APE-B2208
Supplier Catalog Number	B2208
Manufacture	ApexBio
Category	Biochemikalien
Molecular Weight	416,51
Formula	C23H32N205

Empagliflozin overview

Article Name	Empagliflozin, CAS [864070-44-0]
Biozol Catalog Number	MCE-HY-15409
Supplier Catalog Number	HY-15409
Manufacture	MedchemExpress
Category	Biochemikalien
Molecular Weight	450,91
Formula	C23H27ClO7

Finerenone overview

Article Name	Finerenone, CAS [1050477-31-0]
Biozol Catalog Number	BYT-ORB746434
Supplier Catalog Number	orb746434
Manufacture	Biorbyt
Category	Biochemikalien
Molecular Weight	378,42
Formula	C21H22N4O3

3.2 Glomerular filtration rate measurement

NIC-Kidney device	Medibeacon, Germany
Double-sided adhesive patch	Lohmann, Neuwied, Germany
FITC-sinistrin	Medibeacon, Germany
Rechargeable miniaturized battery	Medibeacon, Germany
Sterile compress	Verbandmittel Danz, Germany

Medical adhesive tape	BSN Medical GmbH, Germany
Razor blades	Gillette, USA

3.3 Urine and blood measurement

Mouse Albumin ELISA Quantitation	Set Bethyl Laboratories, TX, USA
Creatinine FS	Diasys, Holzheim, Germany
Urea FS	DiaSys, Holzheim, Germany
God FS	DiaSys, Holzheim, Germany
96 well MicroWell™ MaxiSorp™ plate	Thermo Fisher, MA, USA
Nunc™ MicroWell™ 96-Well Microplates	Thermo Fisher, MA, USA
Bovine serum albumin fraction v	Roche, Mannheim, Germany
Tris	Carl Roth, Karlsruhe, Germany
Sodium chloride	Merck, Darmstadt,Germany
Tween 20	Sigma-Aldrich, Munich, Germany
Sodium carbonate	Merck, Darmstadt, Germany
Sodium bicarbonate	Merck, Darmstadt, Germany
TMB Substrate Reagent	Set BD Biosciences, NJ, USA
Sulfuric acid	Sigma-Aldrich, Munich, Germany
pH meter	WTW, Weilheim, Deutschland
Tecan GENios™ Microplate Reader	Tecan, Germany

3.4 Serum tests

Mouse Albumin ELISA Kit	Bethyl Laboratories, Montgomery, USA
BUN kit	DiaSys, Holzheim, Germany
Creatinine kit	DiaSys, Holzheim, Germany

3.5 RNA isolation, cDNA conversion, real-time qPCR

RNA isolation

2-Mercaptoethanol	Sigma-Aldrich, Munich, Germany
DNase and RNase free water	Thermo Fisher, MA, USA
96% Ethanol	Merck, Darmstadt,Germany
RNase AWAY® spray	Sigma-Aldrich, Munich, Germany
RNAlater™ Stabilization Solution	Ambion, MA, USA
PureLink™ RNA Mini Kit	Ambion, Darmstadt, Germany
RNase-Free DNase Set	Qiagen, Hilden, Germany
Homogenizer Ultra-Turrax® T25	IKA GmbH, Staufen, Germany

cDNA conversion

NanoDrop™ Spectrophotometer	Biotechnologie, Erlangen, Germany
5x First Strand-Puffer	Invitrogen, Karlsruhe, Germany
Acrylamid	Ambion, Darmstadt, Germany
Dithiothreitol	Invitrogen, Karlsruhe, Germany
dNTP Set	GE Healthcare, Munich, Germany
Hexanucleotid-Mix	Roche, Mannheim, Germany
RNAsin	Promega, Mannheim, Germany
SuperScript II Reverse Transcriptase	Invitrogen, Karlsruhe, Germany
Thermomixer 5436	Eppendorf, Hamburg, Germany

Real-time qPCR

SYBR green I	Sigma-Aldrich, Munich, Germany
PCR Optimizer	Biomol, Hamburg, Germany
MgCl2 25mM	Thermo Fisher, MA, USA
Bovine Serum Albumin PCR grade	Thermo Fisher, MA, USA
PCR-Primer	Metabion, Martinsried,Germany
Taq-Polymerase	New England BioLabs, Ipswich, USA
10X Taq Buffer	New England BioLabs, Ipswich, USA
Lightcycler 480 PCR plate with 96 wells	Sarstedt, Germany
Optical lid strip for 96-well plates	Sarstedt, Germany
LightCycler 480 Multiwell-Plate 96	Roche, Mannheim, Germany
LightCycler 480 Instrument	Roche, Mannheim, Germany

3.6 Bulk RNA-sequencing

Oligo (dT)-attached magnetic beads	Cytiva, Massachusetts, USA
Agilent Technologies 2100 bioanalyzer	BGI, Shenzhen, China
DNBSEQ (G400) Sequencer	BGI, Shenzhen, China

3.7 Antibodies and reagents used for histological assessment

Antibodies used in histology

Anti-mouse WT1 antibody, Clone (WT1/857 + 6F-H2)	Novusbio, Wiesbaden, Germany
Biotin anti-mouse IgG1 antibody	Biolegend, San Diego, USA
Rabbit anti-mouse αSMA antibody	Dako, Hamburg, Germany
Biotin Rat Anti-Mouse IgG2a	BD Biosciences, New Jersey, USA
HRP linked Anti-Goat secondary Ab	Dianova, Hamburg, Germany
HRP linked Anti-Rabbit secondary Ab	Cell signaling, Danvers, MA

F4/80 Antibody (CI-A3-1)	Novusbio, Wiesbaden, Germany
Rabbit anti Rat IgG (H+L)	Vector Laboratories, California, USA

Reagents used in histology

DAB substrate chromogen system	DakoCytomation, Glostrup, Denmark
Avidin-Biotin Complex Kits	Vector Laboratories, USA
Antigen unmasking solution	Vector Laboratories, USA
Avidin	Vector Laboratories, USA
Biotin	Vector Laboratories, USA
DAB Peroxidase Substrate Kit	Vector Laboratories, USA
Nuclear Fast Red solution	Sigma-Aldrich, Munich, Germany
Ammonium persulfate (APS)	Bio-Rad, CA, USA
Disodium tetraborate	Merck, Darmstadt, Germany
Antifade Mounting Medium with DAPI	Vector Laboratories, CA, USA
Picro-Sirius red solution	Sigma-Aldrich, Munich, Germany
Eosin	Merck, Germany
Fixation solution	Acquascience, Uckfield, UK
Formaldehyde	Merck, Germany
Hydrogen peroxide	Merck, Germany
Methanol	Merck, Germany
Paraffin	Merck, Germany
Periodic acid	Carl Roth, Germany
Schiff Reagent	Sigma-Aldrich, Munich, Germany
Nitric acid	Merck, Darmstadt, Germany
Silver nitrate	Carl Roth, Germany
Thiosemicarbazide	Sigma-Aldrich, Munich, Germany
Xylene	Merck, Germany

3.8 Miscellaneous

Falcon 15/50 ml	Greiner BioOne, Germany
Reaction tubes, 1.5/2.0 ml	Paul Boettger, Germany
Safe lock tubes, 1.5/2.0 ml (PCR)	Eppendorf, Germany
Cryovial, 2.0 ml	Alpha Laboratories, UK
Refill pipette tips	Greiner Bio-One, Germany
Serological Pipette, 5/10/25/50 ml	Greiner Bio-One, Germany
EpT.I.P.S. refill pipette tips(PCR)	Eppendorf, Germany
PBS	PAN-Biotech, Germany
Tissue culture dish, 100 mm	TPP, Trasadingen, Switzerland
Analytic Balance	BP110 S Sartorius, Göttingen, Germany

Mettler PJ 3000 Mettler-Toledo	Greifensee, Switzerland
Heraeus, Minifuge T	VWR, Darmstadt, Germany
Heraeus, Biofuge primo	Kendro Laboratory, Germany
Heraeus, Sepatech Biofuge A	Heraeus Sepatech, Munich, Germany
Leica DC 300F	Leica Microsystems, Cambridge, UK
Olympus BX50	Olympus Microscopy, Hamburg,Germany
Microtome HM 340E	Microm, Heidelberg, Germany
Thermomixer 5436	Eppendorf, Hamburg, Germany
Vortex Genie 2™	Bender Hobein, Zurich, Switzerland
Water bath HI 1210	Leica Microsystems, Bensheim,Germany
Easypet® pipette controller	Eppendorf, Germany
Pipetman® pipette	Gilson, Middleton, WI, USA
Research Pro electronic pipettor	Eppendorf, Germany
Multi-channel pipettor, 30-300 µl	Eppendorf, Germany
ELISA/reader	Tecan, Crailsheim, Germany
Rotilabo®-Mikropistill	Carl Roth GmbH, Karlsruhe, G
Centrifuge-5418	Eppendorf, Hamburg, G
Centrifuge-Megafuge (1.0R)	Heraeus Sepatech, Osterode, G

4. Methods

4.1 Animals

4.1.1 Ethical statement

In accordance with the European equivalent of the NIH's Guide for the Care and Use of Laboratory Animals (directive 2010/63/EU), the local government authorities approved all experimental procedures (approval code Gz. ROB-55.2-2532.Vet_02-20-223).

4.1.2 Experimental animals

Col4a3-/- (*Col4a3*^{tm1Dec}) mice with 129X1/SvJ background were obtained from Prof. Oliver Gross's lab at the University of Goettingen, Germany. Exon 5 of the *Col4a3* gene was disrupted using a vector containing the neo-resistance gene. A 129/SvJ-derived ES cell line purchased from Genome Systems was used. These mice were bred with 129X1/SvJ inbred mice for at least one generation. This strain also carries genetic contributions from 129S1/SvImJ. Table 4.1 shows the targeted allele detail of *Col4a3*^{tm1Dec} gene. This is a "no-touch" mouse model of progressive CKD, consistent with the characteristics of human Alport syndrome.

4.1.3 Housing and husbandry

The mice are raised in a specific-pathogen-free environment, housed together with enrichment, and kept under the 12-hour light-dark rhythm. The room temperature was kept at 22 ± 4 °C, and humidity was kept between 50-70%, with facility's air conditioner being responsible for regulating these conditions. Mice are bred in groups of 2-3 in cages with air filters on the top. Mice have ready access to autoclaved water and standard or specific chow from Ssniff company. Throughout the study, mice were provided with materials for nesting and sticks for teeth grinding, as well as houses made of red plastic. Mice's cages are changed three times a week.

Table 4.1 Targeted allele detail of *Col4a3*^{tm1Dec}

Summary			Mutation	Origin		Mutation Description
Symbol	MGI ID	Gene	Parent Cell Line	Strain of Origin	Allele Type	Mutation
Col4a3^{tm1Dec}	1857432	*Col4a3* Location: Chr1:82564642-82699780 bp, + strand Genetic Position: Chr1, 42.32 cM	Not specified (ES Cell)	129X1/SvJ	Targeted (knockout)	Insertion Mutation details: A neomycin selection cassette was inserted into exon 5. Northern blot analysis on RNA derived from the kidney of homozygous mice demonstrated that no detectable transcript is produced from this allele. Immunohistochemistry experiments on kidney sections from homozygous mice confirmed that no detectable protein was made.

4.1.4 Genotyping

Ear punches from mice were used for the genotyping. In brief:

Lysate

1. Sample plus 150 ul Direct PCR reagent.
2. Add 1ul of Proteinase K.
3. Calculate for one more sample due to foam.
4. Put in the machine for 3 h 45 min 55 ℃ and 800rpm.
5. Heat up to 85 ℃ after 3 h 45 mins for 45 min to inactive Proteinase K.

PCR

Mastermix with the following:

	Stock Conc.	Run 1×
total		25.0 µl
H_2O		14.3 µl
PCR Buffer	1.25 mM	2.5 µl
dNTP’s	10 mM	4 µl
Taq	5 U/µl	1 µl
Primer 1	10 µM	1 µl
Primer 2	10 µM	1 µl

Primer 3	10 µM	0.5 µl
DNA		1 µl

Primer sequences

Primer 1: olMR0642: 5'-CCT GCT AAT ATA GGG TTC GAG A-3'

Primer 2: olMR0643: 5'-CCA GGC TTA AAG GGA AAT CC-3'

Primer 3: olMR1100: 5'-GCT ATC AGG ACA TAG CGT TGG-3'

Gel

Create a 2% agarose gel.

Big chamber: 3 g agarose and 150 ml 0.5%TBE.

Use microwave at maximum power for 3min with a lid on top of the piston glass.

Shake constantly and wait until it has cooled down, then add 7.5 ul of Pegreen.

Pour into the chamber slowly but steadily.

Clean the piston glass and put Pegreen back into the fridge.

Electrophoresis

Add 5 ul dye to the samples.

Put the gel into the electrophoresis pool filled with 0.5% TBE.

Insert 12 ul of the sample into a bag.

If using a ladder, add only 6 ul of it.

Start electrophoresis on 220 V for 30 min.

4.1.5 Glomerular filtration rate (GFR)

We measured mouse GFR at weeks 6, 7, and 10 using FITC-conjugated sinistrin clearance. The method involved attaching a device to the mouse skin to record FITC-sinistrin dynamics clearance from the blood [152]. The plasma half-life of FITC-sinistrin was determined by analyzing the recorded signal. Our measurement process was based on the original method with minor modifications based on prior experience [153]. The measurement process was as follows:

1. After anesthetizing, the hair around the neck of the mice was moistened using ethanol (be careful not to expand the area to cause the mouse body temperature to drop), and then the moistened hair was carefully removed to expose about 1.5 x 1.5 cm of skin surface.

2. Connect the battery to the FITC-sinistrin recording device and fix it on the shaved skin of the mouse with tape after the indicator light flashes steadily.

3. Mice were placed individually in cages with filters at the top. Food and water were forbidden and recorded for 15 minutes to obtain basal data on mice.

4. After re-anesthetizing mice, injecting 150 mg per kg FITC-sinistrin, then returned to their cages for 1.5 hours to record data.

5. Anesthetize the mice and remove the recording device.

6. Weigh the mice.

7. Analyze data using MPD Lab software.

The normal curve for FITC-sinistrin signal is divided into three segments: baseline part before sinistrin injection, rising part after injecting, and decline after that. The plasma half-life (t½) values of sinistrin were obtained using MPD software one-compartment model. Then use the following calculation to calculate GFR (µl/min) [153].

$$\mathrm{GFR(\mu l/min)} = \frac{14616.8[\mu l]}{t½[min]} \times \frac{BW[g]}{100g}$$

4.1.6 Blood, urine, and organ collection and storage

Blood samples were taken upon mouse sacrifice, collected in tubes with 10 µl 0.5M EDTA, then centrifuged 5min using 7500 rpm. After preparation, the resulting plasma was moved to a different tube and kept at -80°C, while urine was obtained via bladder massage and promptly preserved at -20°C.

Mice were euthanized by cervical dislocation. Limbs were fixed with syringe needles and chest/abdomen skin was sprayed with 70% alcohol. The chest cavity was exposed by carefully cutting the skin with tweezers and scissors. The heart was accessed by cutting through the ribcage and lifting it with clamp scissors, then a needle was inserted into left ventricle and right ventricle was cut. The heart was perfused with 10ml EDTA and 20ml cold PBS. Kidneys were harvested and one was cut into 3 transverse pieces, with the center stored in 4% formalin for 1 day followed by 70% ethanol for paraffin, the upper pole stored in RNA-later at -80°C and the lower pole in liquid nitrogen and -80 °C. The other kidney was cut

into 2 sagittal pieces, with one stored in 4% formalin and transferred to 70% ethanol for paraffin and the other stored in liquid nitrogen at -80 °C.

4.2 Preclinical RCT

4.2.1 Study design and schedule

Our study was a preclinical, randomized, double-blind, placebo-controlled trial to assess the effectiveness and safety of combination therapy for slowing CKD progression in adult 129-*Col4A3*^{tm1Dec}-/- mice. Randomization of mice was stratified by induction regimen. The treatment group recieved either a vehicle, ramipril, ramipril-empagliflozin, or ramipril-empagliflozin-finerenone daily via food admixes for 8 weeks. Figure 4.1 illustrates the study design. The primary endpoint was the time to (uremic) death, which is equivalent to (kidney) lifespan. Secondary endpoints included kidney function, proteinuria, and kidney atrophy parameters. Kidney function assessments was done by testing GFR, and serum creatinine (SCr) and blood urea nitrogen (BUN) levels were also tested. Study calendar is in Appendix 1.

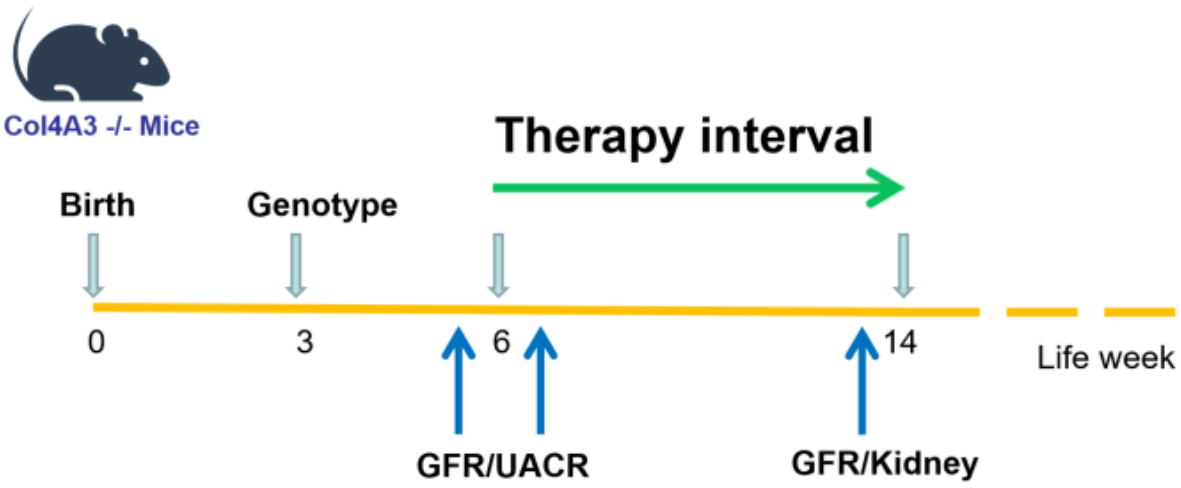

Figure 4.1 pRCT Study flow chart

A safety analysis included animal welfare scoring in all animals and histomorphological analysis of non-kidney tissues in a subset of animals.

This preclinical trial design has been registered on the website of www.preclinicaltrials.eu. (Registration No. PCTE0000266). The registering protocol was published before starting the study and was attached as Appendix 2.

4.2.2 Inclusion criteria

Male and female *Col4A3*^{tm1Dec}-/-mice, six weeks of age.

4.2.3 Exclusion criteria

Mice that fulfilled the exclusion criteria were not included in our study:

1. Score of 4 or ≥ 2 for more than 6 hours during animal welfare surveillance (Appendix 3)
2. Use of any other drugs during study period, such as treatments for skin wounds by a veterinarian
3. Signs of infection
4. Pregnancy
5. Intolerance to ramipril, empagliflozin, and finerenone (anaphylactic reactions).

4.2.4 Intervention

In this study, mice were treated with food admix of either a) vehicle, b) 10 mg/kg ramipril, c) 10 mg/kg ramipril plus 30 mg/kg empagliflozin, or d) 10 mg/kg ramipril plus 30 mg/kg empagliflozin plus 10 mg/kg finerenone. The different types of food preparations were marked by different food colors starting from 6 weeks of age for 8 weeks.

4.2.5 Endpoints

The primary endpoint was the kidney lifespan. As ultimate kidney-related endpoint, we selected the age at uremic death, an equivalent of kidney lifespan in *Col4a3*-/- mice. Animal welfare scoring was performed daily by personnel blinded to treatment groups. Upon reaching a predefined score, animals were sacrificed, and the time point was recorded as the day of uremic death. Tissues and biosamples were harvested to validate kidney failure as the cause of demise. Secondary endpoint was makers of kidney excretory function (GFR, Proteinuria) and histomorphological parameters of the kidney in a subgroup of animals.

4.2.6 Sample size calculation

The main point of comparison in this study was how long the kidneys of the mice in each group were able to survive before reaching a stress score of greater than 2 that persisted for at least 6 hours. To make this comparison, we used the vehicle group as a baseline, which had a minimum survival time of 60 days and an anticipated median survival time of 70 days. They considered a survival time of 85 days to be of

particular clinical significance, and they did not expect any failures to occur before 60 days. The log-rank test was used with a hazard coefficient of 2.5 (85-60) / (70-60). Based on this, we determined that 20 mice per group could be necessary with an α value of 0.05 and a β value of 0.2. We chose to use a two-sided test since the individual therapies being studied could potentially decrease the kidney survival time, which would be a significant finding given that the test substances were already in clinical use.

4.2.7 Randomized and double-blind strategy

"Stratified randomization" was employed for random assignment in clinical trials. Assignments were generated randomly within blocks to maintain treatment balance throughout the trial (refer to figure 4.2). The 'blockrand' package R code can be found in Appendix 4.

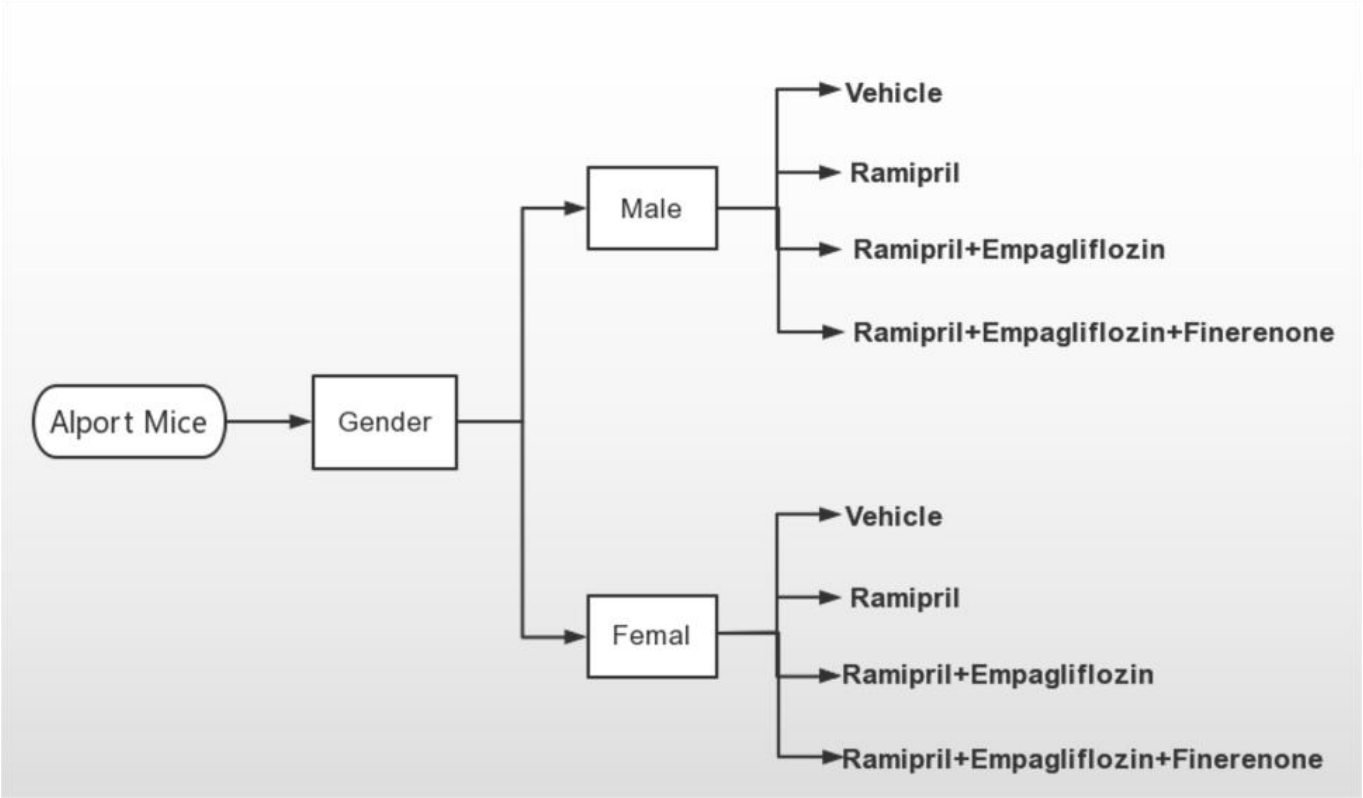

Figure 4.2 Stratified randomization

An impartial third party not involved in the project managed the random card and form, and prepared drug stocks labeled A, B, C, or D, while researchers remain unaware of the ABCD treatment assigned. A random card indicating the treatment type (A, B, C, or D) was provided for each new mouse. Researchers only learned the ABCD treatment after all experiments were completed and results analyzed. The treatment was blocked in the random card before the experiment, and Prof. Anders has verified the uniqueness and

rationality of each card by signing them. Four different colored foods, blocked by color, were requested from Sniff Company and a sealed letter was received and kept in a safe (refer to figure 4.3).

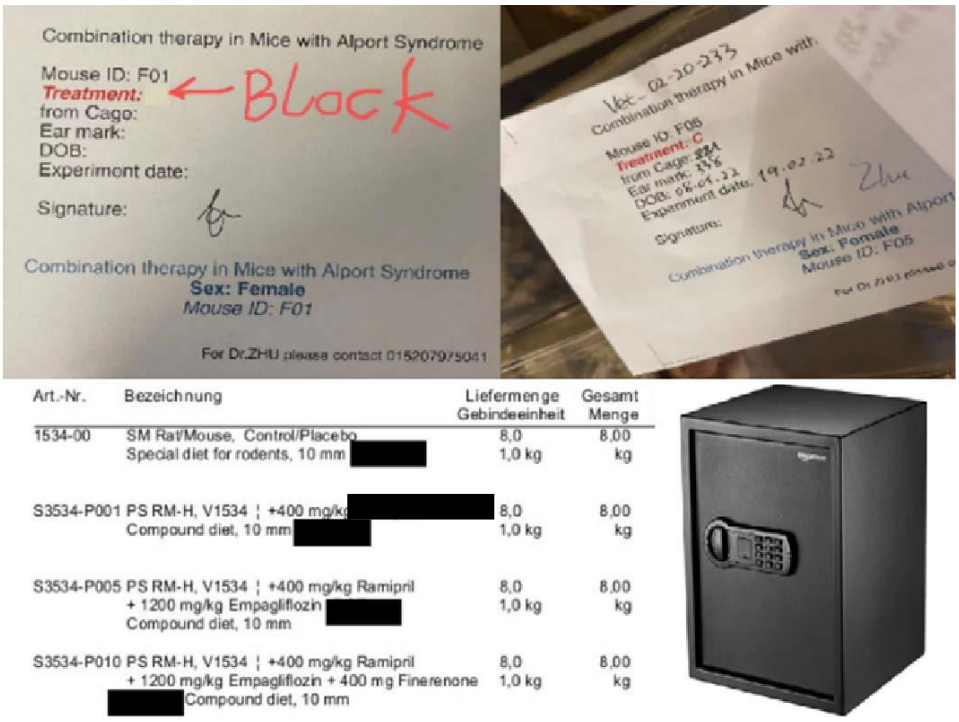

Figure 4.3 Double-blind strategy. A neutral third party who was not part of the project oversaw the random selection of cards and forms, as well as the preparation of drug stocks labeled A, B, C, or D. The researchers were not informed of which ABCD treatment was assigned. The random card indicating the treatment type was blocked until a mouse was involved. Four different colored foods, blocked by color, were requested from Sniff Company and a sealed letter was received and kept in a safe.

4.2.8 Safety endpoints and analysis

Welfare scoring was used for welfare analysis. Sporadic kidney histology done on mice at the end of life confirmed that death was due to kidney failure.

4.2.9 8.5 weeks crossing study

Treatment starting from 6 weeks was continued for 2.5 weeks in six animals per group, and the mice were euthanized when they reached 8.5 weeks for a cross-sectional tissue and biosample analysis.

4.3 Blood and urine measurement

4.3.1 Urine albumin

To determine mouse urine albumin, the Albumin Elisa kit from Bethyl Laboratories was used following the manufacturer's protocol. Steps include:

1. Add 100 µl goat anti-mouse albumin antibody to each well of a 96-well ELISA plate (1 µl antibody in 100 µl coating buffer).

2. Incubate plate for 1 hour RT or overnight at 4 °C.

3. Wash plate 5x with ELISA wash solution (200 µl/well).

4. Add 200 µl/well ELISA blocking solution for 30 min RT.

5. Wash plate 5x.

6. Dilute urine samples and standards.

7. Dilute urine sample: 2 µl in 18 µl dilution solution (1:10).

8. Dilute standards: 2 µl standard in 6.5 ml diluent; 50 µl stock in 950 µl diluent; 500 µl of each dilution 7 times.

9. Transfer 100 µl samples, standards, and blank to plate and incubate 1 hour RT.

10. Wash plate 5x.

11. Add 100 µl goat anti-mouse albumin HRP conjugate (1:100,000 in diluent) per well and incubate 1 hour RT.

12. Wash plate 5x.

13. Add 100 µl TMB substrate and incubate 5-15 min RT in dark.

14. Stop reaction with 100 µl ELISA stop solution (0.18 M H_2SO_4).

15. Read absorbance at 450 nm using ELISA reader and save values.

4.3.2 Plasma and urine creatinine

The Creatinine FS Diasys Kit by the Jaffe method was used to determine creatinine levels in mice plasma and urine. Briefly:

1. Add 10 µl of sample, standard, or blank in duplicate to an ELISA plate.

2. Immediately add the reagent mixture.

3. Measure absorbance at 492 nm at 1, 2, 3, 10, and 20 min intervals until the reaction plateaus. Use ELISA reader and save data.

4. Calculate creatinine levels.

4.3.3 BUN

BUN was determined using Urea FS by enzymatic method. In brief:

1. First, add 2µl Plasma and standards to a 96-well ELISA plate.

2. Mix the reaction reagents and add 200 µl to the plate.

3. Read the absorbance at 360nm using the Elisa reader at the time points of 1, 3, and 15 min.

4. Multiply the urea concentration by 0.467 to obtain the value of urea nitrogen.

4.3.4 Glucose

Urinary glucose was measured using Cayman's Glucose Colormetric Assay Kit (Cayman Chemical, Michigan, USA). Urinary glucose-to-creatinine ratio (UGCR) was calculated as (mg/mg) = urine glucose (mg/dL)/ urine creatinine (mg/dL).

4.4 Immunohistochemistry

Kidney tissue samples were harvested and fixed in 4% formalin for 1 day. The samples were then processed using a tissue processor (Leica) to produce paraffin-embedded blocks. These blocks were subsequently sliced to obtain paraffin sections, which underwent a process of de-paraffinization by being exposed to xylene for three cycles of 5 minutes each. The sections were then rehydrated by immersing them in a range of ethanol solutions, starting with 3 minutes absolute ethanol for 3 cycles, followed by 2 cycles 95% ethanol for 3 minutes, and 3 minutes with 70% ethanol. This was followed by rinsing the sections with PBS for 3 cycles of 5 minutes.

To suppress endogenous peroxidase, tissue sections were treated in a solution consisting of methanol and 3% hydrogen peroxide for a duration of 20 minutes in dark. Subsequently, sections were thoroughly washed with PBS 3 times for 5 min. The process of antigen unmasking was then performed by immersing the tissue sections in an antigen unmask reagent and put them in the microwave for steaming 10 min. To further block endogenous biotin, the sections were further incubated with Avidin (Vector) for 15 minutes, followed by an additional 15 minutes with biotin (Vector). The tissue sections were incubated 12 hours at a temperature of 4℃ with primary antibodies of LTL or THP-1. After that, biotinylated secondary antibodies were applied to the sections for 30 minutes, followed by PBS washing. The sections were then treated with substrate reagent (ABC solution, Vector) for 30 minutes, washed by PBS, rinsed by 5 minutes Tris, and subjected to DAB staining. Methyl-green (Fluka) was used as a counterstain for the sections. Excess stain was removed by washing the sections with 96% alcohol, followed by treatment with xylene. Finally, the sections were mounted with VectaMount (Vector) after drying. Python and OpenCV were utilized for quantifying the THP-1 and LTL, by determining the proportion of THP-1 positive area in the kidney medulla and the proportion fo the LTL positive area in the kidney cortex.

4.4.1 Periodic acid Schiff (PAS staining)

The sections that had been rehydrated were initially treated with 2% periodic acid for 5 minutes, then rinsed with double-distilled water. Subsequently, they were stained with Schiff solution and rinsed with tap water. The sections were counterstained with Hematoxylin solution for 2 minutes and subsequently washed with taq water. After drying, sections were dipped with 90% alcohol and covered with slips. The injury extent of tubular was measured by assessing the corticomedullary junction proportion that demonstrated indications of brush border loss, tubular diatation and cast formation.

Pathological Scoring:

1. Tubulointerstitial fibrosis (Picro-Sirius Red-stained sections): 0 (no lesions), 1 (<25% lesions), 2 (25-50% lesions), 3 (>50% lesions).
2. Glomerulosclerosis and tubular atrophy (PAS-stained sections): 0 (no lesions), 1 (<25% lesions), 2 (25-50% lesions), 3 (>50% lesions).
3. Final Score: Sum of interstitial fibrosis, glomerulosclerosis, and tubular atrophy scores.

4.4.2 Picro-Sirius Red staining

The Weigert's hematoxylin was first used to stain the rehydrated sections for 8 minutes and then washed with double-distilled water. Picro-Sirius Red was applied for 60 minutes, and then rinse the sections with tap water. Following that, the sections were dipped in 90% ethanol and covered with slips after drying. The extent of kidney fibrosis was determined by calculating the percentage of collagen (Red) in the tissue sections using python and OpenCV.

4.4.3 Alpha smooth muscle actin (αSMA staining)

The staining of sections with αSMA (rabbit anti-mouse, 1:500) was followed by the generation of a complete section image using Photoshop, through the merging of a series of low magnitude microscopy images. The merged images were corrected for background using Photoshop, and the software was employed to determine the percentage of SMA-positive nuclei.

4.4.4 WT1 staining

To stain the sections with anti-mouse WT1 antibody (1:200, Santa Cruz Biotechnology), the immunohistochemistry method was utilized. We selected 15-20 glomeruli in the cortex with either a

vascular pole or urinary pole, while disregarding WT-1 positive cells present at the junction between the capsule and tufts. The outcome was expressed as positive cells per glomerulus.

4.4.5 TdT-mediated dUTP-biotin nick end labeling (TUNEL staining)

For the TUNEL staining, TUNEL Assay Kit - FITC (ab66108) was used to identify dead cells in the kidney. Slides were evaluated with a Fluorescence microscope and subsequently photographed. TUNEL-positive cells were assessed using Photoshop software.

4.4.6 F4/80 staining

For the F4/80 staining, sections were stained using the F4/80 antibody (CI-A3-A) via immunohistochemistry (1:100 dilution, Novusbio NB600-404). Slides were scanned with a 200x magnification microscope and analyze using Photoshop. Count the number of F4/80-positive and total pixels per slice and determine the ratio.

4.5 RNA isolation, cDNA synthesis, and real-time qPCR

4.5.1 RNA isolation

Tissue samples were carefully and delicately transferred to a container with 2 milliliters of lysis buffer, which contains 1% 2-mercaptoethanol, using forceps. The samples were always kept on the ice to ensure preservation of the RNA integerity. Samples were homogenized for 20 seconds at a level 5 setting on the Ultra-Turrax machine. Next, the homogenized samples were centrifuged at 6000g for 5 minutes to separate supernatant from pellet. Supernatant was saved and transferred to a new, RNase-free tube. Subsequently, 700 microliters of the supernatant were added to an equal amount of 70% ethanol, and the mixture was thoroughly mixed. The rest of the RNA isolation procedure was carried out by following the Qiagen mRNA extraction kit instructions. The RNA samples were subsequently put in storage at -80℃.

4.5.2 cDNA synthesis

The purified RNA was subjected to a denaturation process by incubating it at 65 °C for 10 min to breakdown the secondary structures of RNA. Reaction was subsequently halted by placing the RNA at 4 ℃. Each sample's RNA was prepared at a final concentration of 2 µg per 22.45 µl of a pre-prepared master mix (table 4.2). Resulting mixture was then kept at 42 °C for 2h followed by 85 °C for 5 minutes to obtain cDNA. The cDNA was stored at -20 °C.

Table 4.2 master mix for RNA reverse transcription

Master mix	Concentration	Volume (µl)
Taq buffer	5x	4.5
DTT	0.1 M	1
dNTPs	25 mM	0.45
Rnasin and ribonuclease inhibitor	40 u/µl	0.5
Acrylamide	15 µg/ml	0.25
Hexanucleotide Mix	10x	0.25
Superscript II	200 u/µl	0.5

4.5.3 Real-time quantitative polymerase chain reaction (RT-qPCR)

The cDNA samples were diluted 1:100 and mixed with SYBR-Green and Taq polymerase (as shown in table 4.3). The master mix was run on a Light Cycler 480 with the following protocol: Pre-incubation at 95 °C for 5 minutes, followed by 40 cycles of Amplification at 95 °C for 15s, 60 °C for 15s, 68 °C for 20s. The melting curve was performed at 95 °C for 5s, 65 °C for 60s. Samples were then cooled to 40 °C for 30s. The cycle threshold values were computed and normalized using the reference gene (18s rRNA) for each sample.

Table 4.3 Master mix for the quantitative real-time PCR

Master mix Volume	Volume (µl)
Mix SybrGreen	10
Taq polymerase (5000 u/ml)	0.16
Forward primer (10 µM)	0.6
Reverse primer (10 µM)	0.6
cDNA	0.2
ddH_2O	8.44
Total	20

4.5.4 Primers

The primer sequences used in the study are displayed in table 4.4.

Table 4.4 Primer sequences

Gene	Forward (5'-3')	Reverse (5'-3')
18s	GCAATTATTCCCCATGAACG	AGGGCCTCACTAAACCATCC
αSMA	CCTTCGTGACTACTGCCGAG	ATAGGTGGTTTCGTGGATGC
Fibronectin	GCCACCATTACTGGTCTGGA	GGTTGGTGATGAAGGGGGTC
TGFβ	CAACCCAGGTCCTTCCTAAA	GGAGAGCCCTGGATACCAAC

E-cadherin	CCCAGAGACTGGTGCCATTT	TGGCAATGGGTGAACCATCA
SMAD4	CAGCCATAGTGAAGGACTGTTGC	CCTACTTCCAGTCCAGGTGGTA
SMAD5	CAGGAGTTTGCTCAGCTTCTGG	ACGTCCTGTCGGTGGTACTCTG
KIM-1	TCAGCTCGGGAATGCACAA	TGGTTGCCTTCCGTGTCTCT
NGAL	ATGTCACCTCCATCCTGG	GCCACTTGCACATTGTAG
IL18	AGAAAGCCGCCTCAAACCTT	TGTCTGATTCCAGGTCTCCATTT
iNOS	AAACCCCTTGTGCTGTTCTCA	GAACATTCTGTGCTGTCCCAG
TNFα	AGCCTCTTCTCATTCCTGCT	TAGACAAGGTACAACCCATC
TIMP2	GCAACAGGCGTTTTGCAATG	AGGTCCTTTGAACATCTTTATCTG
CCL2	CCTGCTGTTCACAGTTGCC	ATTGGGATCATCTTGCTGGT
CXCL1	CCGAAGTCATAGCCACACTCA	CTCCCACACATGTCCTCACC
CXCL2	CCCAGACAGAAGTCATAGCCAC	CTTCCGTTGAGGGACAGCAG
CXCL12	TCAGATTGTTGCACGGCTGA	GTTACAAAGCGCCAGAGCAG
CCR2	GCTGTGTTTGCCTCTCTACCAG	CAAGTAGAGGCAGGATCAGGCT
CCR5	GTCTACTTTCTCTTCTGGACTCC	CCAAGAGTCTCTGTTGCCTGCA
VCAM1	GCTATGAGGATGGAAGACTCTGG	ACTTGTGCAGCCACCTGAGATC
ICAM1	AAACCAGACCCTGGAACTGCAC	GCCTGGCATTTCAGAGTCTGCT
Il1b	TGGACCTTCCAGGATGAGGACA	GTTCATCTCGGAGCCTGTAGTG
IL6	TACCACTTCACAAGTCGGAGGC	CTGCAAGTGCATCATCGTTGTTC
FPR2	GCCTTTTGGCTGGTTCCTGTGT	CAAATGCAGCGGTCCAAGGCAA
CD38	GGTCCAAGTGATGCTCAATGGG	AGCTCCTTCGATGTCGTGCATC
ARG1	GTGAAGAACCCACGGTCTGT	ATCGGCCTTTTCTTCCTTCCC
YM2	GTGACCCTACTGTTAGTGCTGG	GGTACTTCCTGGGTGGCATCAA
IL1a	ACGGCTGAGTTTCAGTGAGACC	CACTCTGGTAGGTGTAAGGTGC
Notch1	GCTGCCTCTTTGATGGCTTCGA	CACATTCGGCACTGTTACAGCC
Notch2	CCACCTGCAATGACTTCATCGG	TCGATGCAGGTGCCTCCATTCT
MAPK8	CGCCTTATGTGGTGACTCGCTA	TCCTGGAAAGAGGATTTTGTGGC
Reg1	AACTGGTTTCTGGAGCGAGG	CGAAGGATGTGCTGGTCTGT
Reg2	ACCTGCAGAACGAAAACCCA	CATCAGGAGGCATGAACCTGT
Reg3	GAACAGTCCCGCCCTGAC	CATCATAGCACACCACTCGC
Reg4	CCTCGTGGGCCCAGCTCCAG	TCCCATGGCTCATTGCCACATTACT
Rank	GGACAACGGAATCAGTGGTC	CCACAGAGATGAAGAGGAGCAG
Nephrin	CTGGGGGACAGTGGATTGAC	GGTCTGTGTCTTCAGGAGCC
Podocin	CTGTGAGTGGCTTCTTGTCCTC	CCTTTGGCTCTTCCAGGAAGCA
Wt1	CTGTACTGGGCACCACAGAG	CCAGCTCAGTGAAATGGACA
Synaptopodin	AGGAGCCCAGGCCTTCTCT	GCCAGGGACCAGCCAGATA
CDK2	TCATGGATGCCTCTGCTCTCAC	TGAAGGACACGGTGAGAATGGC
CDK5	GTACTCCACGTCCATCGACATG	GCCATTGTTCCTCAGTCGGTGT
MYC	TCGCTGCTGTCCTCCGAGTCC	GGTTTGCCTCTTCTCCACAGAC
Mki67	GAGGAGAAACGCCAACCAAGAG	TTTGTCCTCGGTGGCGTTATCC

Col1a1	ACATGTTCAGCTTTGTGGAC	TAGGCCATTGTGTATGCAG
Col3a1	GAGGAATGGGTGGCTATCCG	GCGTCCATCAAAGCCTCTGT
IL1ra	CTGTTGGTGAGGAATGTGGCTG	GGCTCAGGATAACAGGTCTGTC

4.6 RNA-Sequencing

The library construction and sequencing was carried out by Beijing Genomics Institute utilizing the DNBSEQ (G400) platform. The RNA samples wre subjected to 100-base-pair paired-end sequencing. The bioinformatics workflow, which included data filtering, mapped transcript prediction, analysis of differential gene expression and gene ontology, was carried out in accordace with the protocols of hissat2 [154], samtools [155], FeatureCounts [156]/eisaR [157], and clusterProfiler [158].

4.7 Statistical analysis

The data is shown as the mean with SD or as boxplots. Prior to statistical analysis, a normality assessment was performed by comparing the data distribution to the expected normal distribution using a quantile-quantile (Q-Q) plot, and verified by the Shapiro-Wilk test. To test for statistically significant differences in normally distributed data, we utilized ANOVA and performed post hoc Tukey's correction for multiple comparisons. Wilcoxon signed-rank testing or Kruskal-Wallis testing with post hoc Dunn's test correction for multiple comparisons was used to compare non-normally distributed data. Kaplan-Meier curves were utilized to plot survival, and the log-rank test was used to assess differences between groups. Statistical significance was indicated by a p-value less than 0.05. R (Version 3.5.3) was used to perform all statistical analyses.

5. Results

5.1 *Col4a3*-/- mice spontaneously develop CKD progression to fatal kidney failure

To assess CKD progression, additional groups of *Col4a3*+/+ mice were sacrificed at 6 weeks, and *Col4a3*-/- mice were sacrificed at 6 and 9 weeks. BUN and serum creatinine levels, as well as the UACR, were determined as quantitative indicators of kidney function (Figure 5.1).

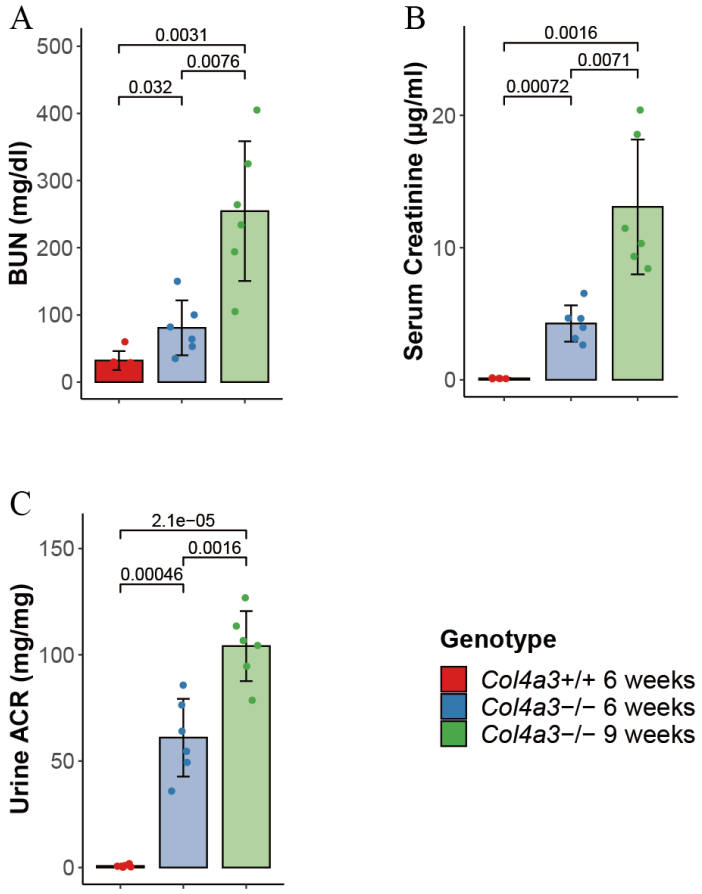

Figure 5.1 Assays for kidney function in *Col4a3*+/+ mice at 6 weeks and *Col4a3*-/- mice at 6 and 9 weeks.
(A) Levels of blood urea nitrogen (BUN). (B) Levels of serum creatinine. (C) Levels of urine albumin-creatinine ratio (UACR). All quantitative data are means ± SD.

At 6 weeks old, *Col4a3*-/- mice displayed significantly higher levels of BUN compared to *Col4a3*+/+ mice. This increase in BUN concentration was further elevated in *Col4a3*-/- mice at 9 weeks (figure 5.1A). The level of serum creatinine, which serves as a marker of kidney function and kidney injury, was also markedly elevated in *Col4a3*-/- mice (figure 5.1B). At 9 weeks of life, *Col4a3*-/- mice showed an additional rise in serum creatinine level. As is commonly seen in humans, elevated urinary protein is a sign of glomerular injury. At 6 weeks of age, *Col4a3*-/- mice exhibited severe proteinuria. The level of UACR in *Col4a3*-/- mice increased at 9 weeks compared to 6 weeks, indicating that the longer the mice live, the more damage to the kidney structure occurred, leading to increased proteinuria (Figure 5.1C).

The indicators of kidney function BUN, serum creatinine, and UACR were significantly increased in *Col4a3*-/- mice at 6 weeks, and then significantly increased at 9 weeks of age. This indicates that *Col4a3*-deficient mice spontaneously develop progressive CKD, and that kidney disease has developed at 6 weeks of age.

Next, we aimed to connect the notable disparities in these biomarkers to differences in kidney histopathology. We examined the *Col4a3*-/- mice at 6 and 9 weeks, when they were close to uremic death and compared the data with those of *Col4a3*+/+ mice. A histological examination using PAS staining on kidney sections of *Col4a3*-/- mice showed the presence of segmental sclerosis and intraglomerular hemorrhage at 6 weeks of age, while these changes were entirely absent in *Col4a3*+/+ mice. Severe glomerular lesions, as well as tubulointerstitial fibrosis, were detected at 9 weeks of age (Figure 5.2).

At an early stage (6 weeks), light microscopy of *Col4a3*-/- mice occasionally revealed sclerotic lesions in the glomerulus, tubular atrophy, and tubulointerstitial fibrosis, while these changes were absent in *Col4a3* +/+ mice. At 9 weeks of age, *Col4a3*-/- mice exhibited fibrotic crescents in the Bowman's space and significant choking of capillary loops due to glomerulosclerosis. In the tubulointerstitial compartment, pronounced tubular atrophy was observed, characterized by detachment of tubular epithelial cells from the basement membrane and prominent collagen deposition in the interstitial space (Figure 5.2A). The results also showed that compared to 6 weeks of age, the glomerulosclerosis score, interstitial fibrosis score, tubular atrophy score, and total damage score were significantly increased in 9-week-old *Col4a3*-/- mice (Figure 5.2B).

Kidney fibrosis is a hallmark of CKD. To evaluate and analyze the presence of kidney fibrosis, we conducted both Picro-Sirius red staining and immunohistochemical staining for α-SMA on *Col4a3*-/- mice at both 6 and 9 weeks of age. The results were then compared to those obtained from *Col4a3*+/+ mice. The data gathered from this analysis are presented in figure 5.3.

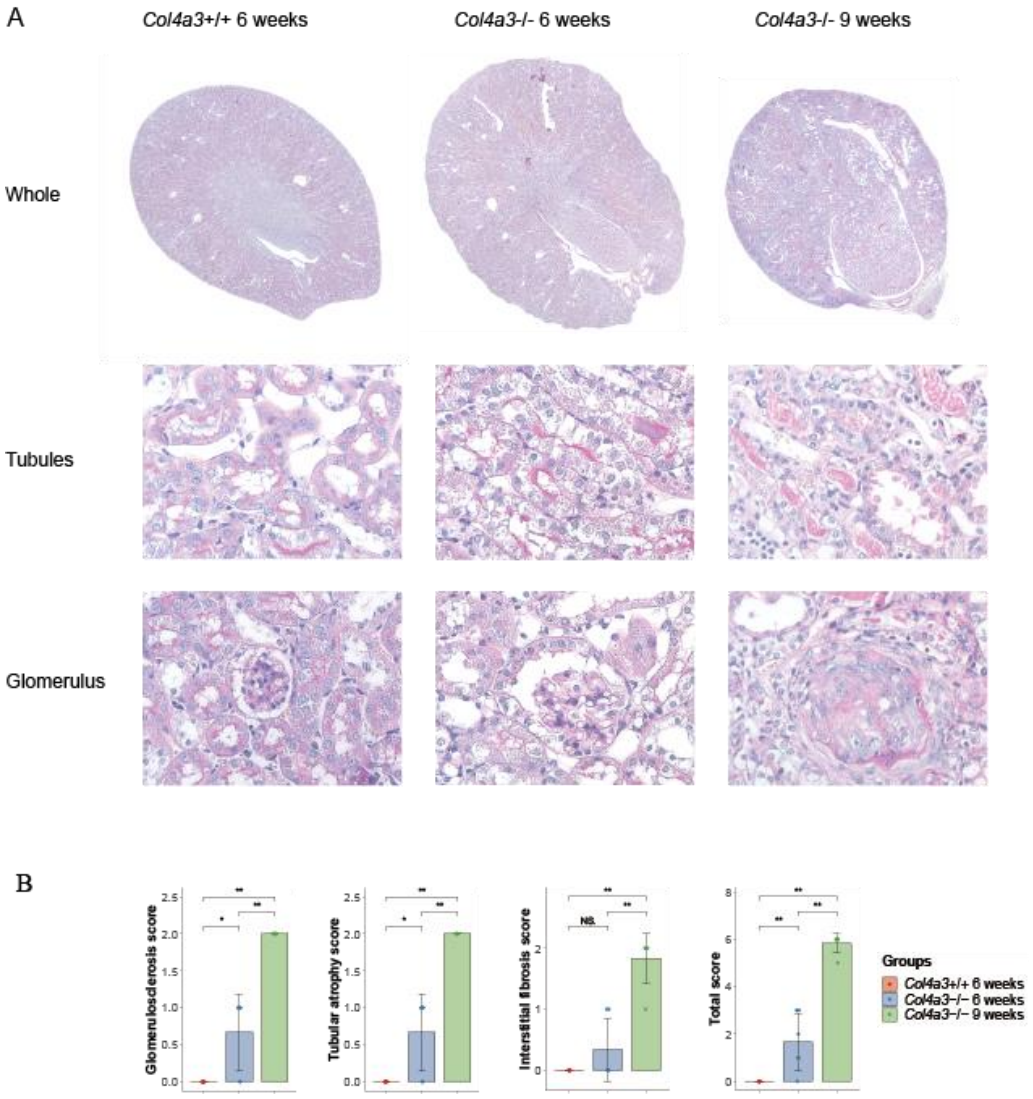

Figure 5.2 Tissue morphology and PAS staining quantitative assessment of scores from *Col4a3*+/+ mice at 6 weeks and *Col4a3* -/- mice at 6 and 9 weeks.

(A) Representative PAS-stained images from the whole kidney, tubules and glomerulus are presented. (B) Kidney sections were independently scored for tubulointerstitial fibrosis, glomerulosclerosis, and tubular atrophy. All quantitative data are means ± SD.*$p < 0.05$, **$p < 0.01$, NS. statistically not significant. Images are shown at the magnification of 200x and 400x.

Our analysis indicate that at 6 weeks, *Col4a3*-/- mice displayed a higher presence of Sirius red positive and αSMA staining positive areas in both the glomeruli and peritubular interstitium when compared to *Col4a3*+/+ mice. This finding indicates that Alport mice developed some degree of kidney fibrosis at this early stage. Further investigation at 9 weeks of age showed typical sclerotic and fibrotic changes in the glomerulus, and the interstitium of *Col4a3*-/- mice, including widespread glomerulosclerosis, periglomerular fibrosis, and interstitial fibrosis. These observations suggest that *Col4a3*-deficient mice experience spontaneous development of kidney fibrosis that worsens over time.

To assess the extent of cell death of kidneys, immunohistochemical TUNEL staining was conducted. The results of this staining can be seen in figure 5.4B. The TUNEL staining showed a rise in the count of

apoptotic cells in *Col4a3*-/- mice compared with *Col4a3*+/+ mice at 6 weeks. At 9 weeks, there was a significant elevation in the count of TUNEL-positive cells, indicating a higher presence of necrotic and apoptotic cells in the kidney tissue of *Col4a3*-/- mice as they age. Thus, the presence of dying kidney cells increases with age in *Col4a3*-/- mice (Figure 5.4D).

In order to examine podocyte loss in the progression of Alport nephropathy, we conducted a WT-1 staining analysis. The analysis involved counting glomerular WT-1-positive cells numbers in a sample of 15-25 cortex glomeruli per kidney section. The results of the analysis were presented in figure 5.4A. Our investigation showed that by the time the mice reached 6 weeks of age, the *Col4a3*-deficient mice had already experienced a decline in the count of WT-1-positive cells per glomerulus compared to the *Col4a3*+/+ mice. Despite the absence of statistical significance ($p = 0.07$), a substantial and significant decline in the count of WT-1-positive cells was observed at 9 weeks of age. This suggests that there was a gradual and persistent loss of podocytes in the *Col4a3*-deficient mice as the disease progressed over time. These findings emphasize the critical role that monitoring the number of podocytes plays in understanding the progression of Alport syndrome and CKD.

Taken together, our results demonstrates that *Col4a3*-deficient mice experience a rapid progression of CKD. The examination of biomarkers of kidney function and histopathology indicated that at just 6 weeks of age, *Col4a3*-/- mice already exhibit significant proteinuria and varying degrees of nephron atrophy and interstitial fibrosis. By 9 weeks of age, the mice are close to death and have experienced further deterioration of their kidney structure. To address this advanced stage of CKD, treatment was initiated at the 6-week time point, when the disease had progressed to the middle and late stages.

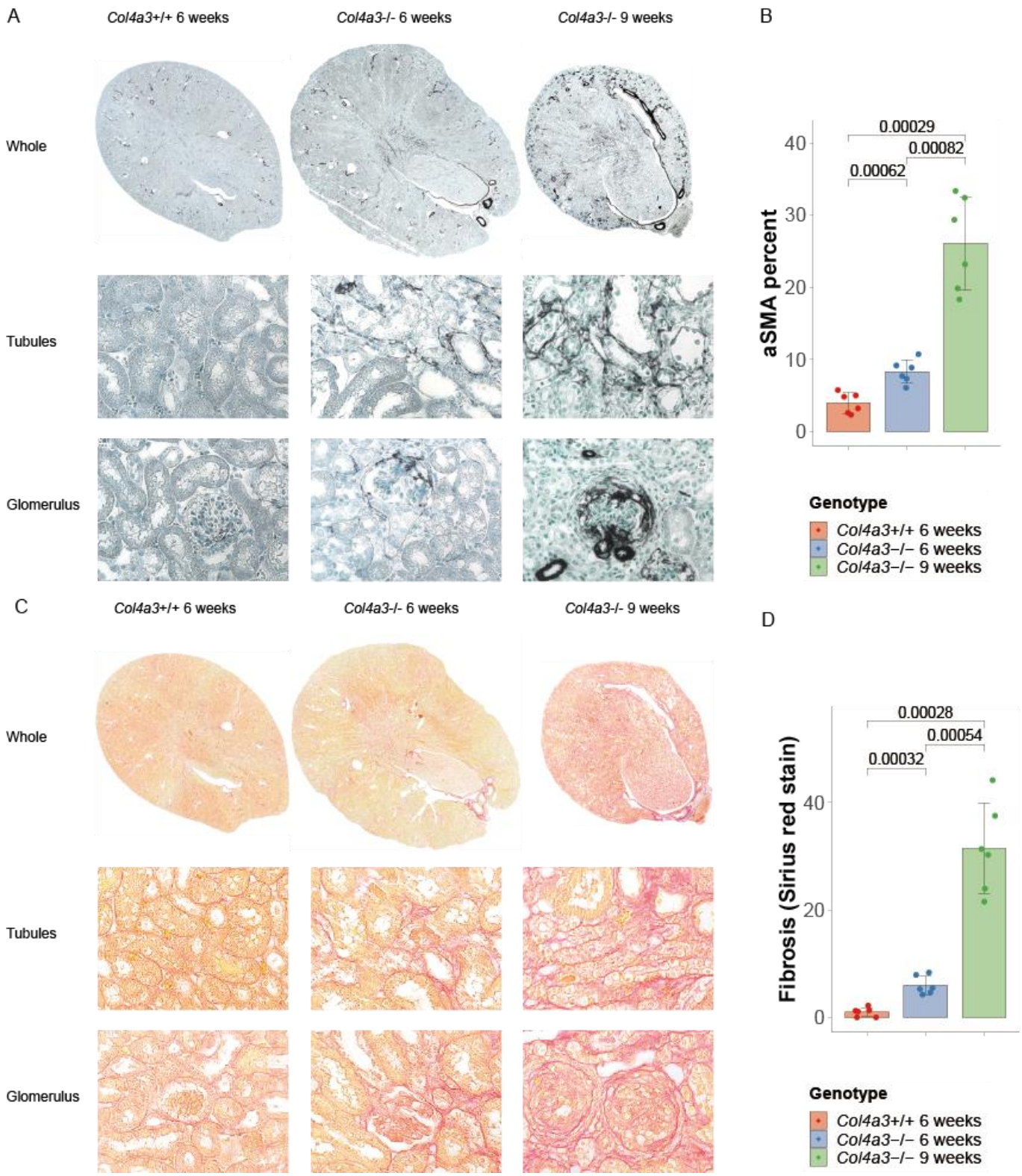

Figure 5.3 Tissue morphology and Sirius red and αSMA staining quantitative assessment of scores from *Col4a*3+/+ mice at 6 weeks and *Col4a3*-/- mice at 6 and 9 weeks.

(A) Representative αSMA-stained images from the whole kidney, tubules and glomerulus are presented. (B) Kidney sections were independently scored for αSMA percent. (C) Representative Sirius red stained images from the whole kidney, tubules and glomerulus are presented. (D) Kidney sections were independently scored for Sirius red percent. All quantitative data are means ± SD. Images are shown at the magnification of 200x and 400x.

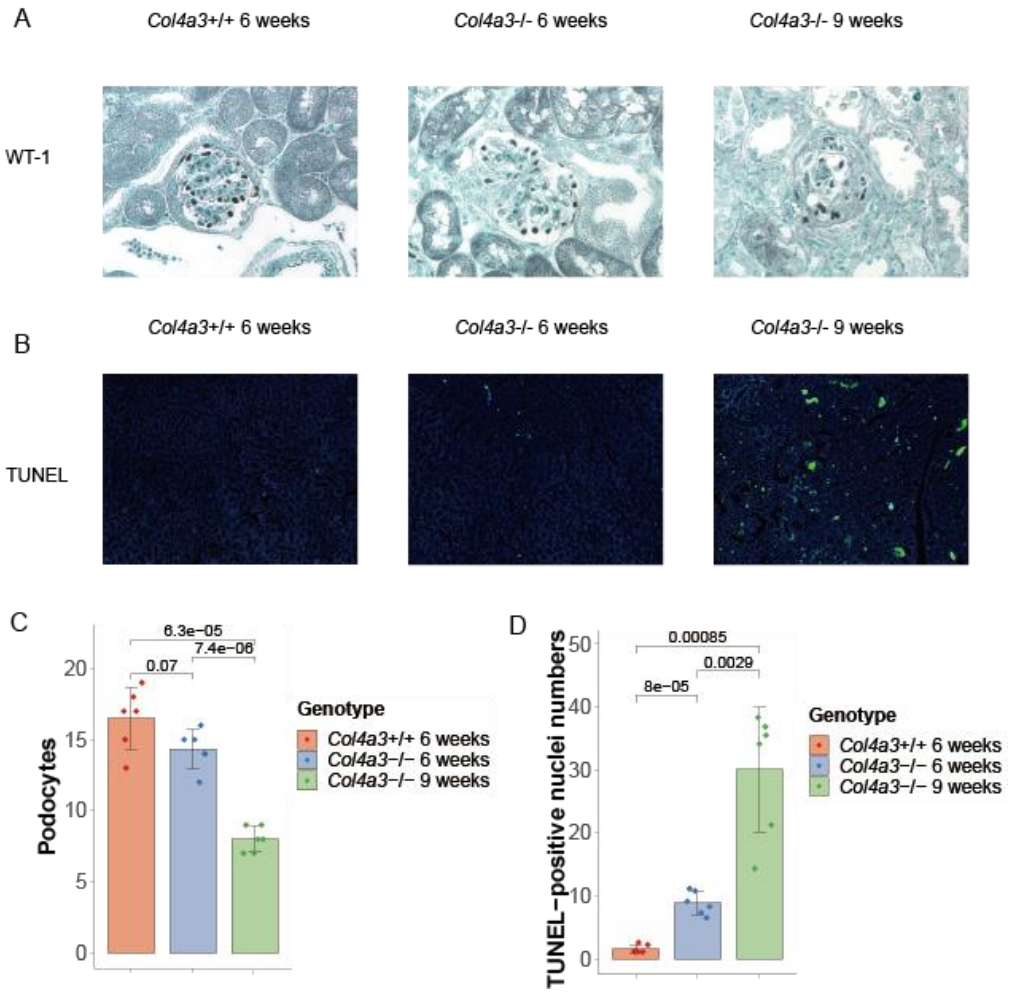

Figure 5.4 Tissue morphology and WT-1 and TUNEL staining quantitative assessment of scores from *Col4a3*+/+ mice at 6 weeks and *Col4a3*-/- mice at 6 and 9 weeks.

(A) Representative WT-1-stained images from the glomerulus are presented. (B) Representative TUNEL stained images from the glomerulus are presented. (C) Kidney sections were independently scored for podocytes numbers. (D) Kidney sections were independently scored for TUNEL-positive nuclei numbers. All quantitative data are means ± SD.

5.2 Characteristics of *Col4a3*-/- mice at the time of randomization

A total of 80 mice with the *Col4a3* gene deletion, all 6 weeks of age, were enrolled in the study between February 2022 and November 2022. We used block randomization to randomly divide the animals into four different groups: a conventional group with 20 mice, a ramipril monotherapy group with 20 mice, a ramipril + empagliflozin dual therapy group with 20 mice, and a ramipril + empagliflozin + finerenone group with 20 mice. The characteristics of these *Col4a3*-/- mice can be found in table 5.1. In each of the four groups, there was an equal 1:1 distribution of male and female mice. The average weight across the four groups was 19.8 g ± 1.7 g, 20.0 g ± 2.7 g, 20.4 g ± 2.5 g, and 20.3 ± 2.3, respectively ($p = 0.76$). Similarly, when looking at the baseline GFR of the mice, the averages across the four groups were well-matched: 185.3 ± 35.7, 180.6 ± 32.1, 187.2 ± 38.5, and 187.6 ± 33.0, respectively ($p = 0.94$). Finally, the average baseline UACR of the mice in the four groups were 51.6 ± 57.7, 55.7 ± 64.5, 51.5 ± 44.2, and 49.4 ± 44.4, respectively ($p = 0.24$). At the start of the study, all mice showed clear signs of Alport nephropathy, as indicated by both urinary abnormalities and a decrease in GFR. However, no significant differences were found among the baseline characteristics across the four groups, suggesting that the random assignment of the mice to each group was successful.

Table 5.1 Baseline characteristics

Characteristics	CKD veh	CKD RASi	CKD RASi/SGLT2i	CKD RASi/SGLT2i /MRA	*p*
N	20	20	20	20	-
Age (week)	6 weeks	6 weeks	6 weeks	6 weeks	-
Female (%)	50%	50%	50%	50%	-
Weight (g)	19.8 ± 1.7	20.0 ± 2.7	20.4 ± 2.5	20.4 ± 2.3	0.76
GFR (µl/min)	185.3 ± 35.7	180.6 ± 32.1	187.3 ± 38.5	187.6 ± 33.0	0.94
UACR (mg/mg)	51.6 ± 57.7	55.7 ± 64.6	51.5 ± 44.3	49.4 ± 44.4	0.24

GFR, glomerular filtration rate; UACR, urine albumin-creatinine ratio; CKD, Chronic kidney disease

5.3 Primary endpoint: overall survival

The primary endpoint of our evaluation was the overall lifespan, which we took as a representation of the kidney lifespan in *Col4a3*-/- mice. Upon analyzing the data, we found that the mean overall survival

for mice receiving vehicle treatment was 63.7 ± 10.0 days. This outcome is in agreement with prior research that has documented the lifespan of this specific mouse strain. [159-161]. The administration of ramipril starting from 6 weeks and continuing for 8 weeks led to a significant increase in the mean lifespan of the mice to 77.3 ± 5.3 days. Further improvement was seen when the mice were treated with dual therapy of ramipril and empagliflozin, resulting in a mean lifespan of 80.3 ± 11.0 days. The most significant effect on mean lifespan was observed when the mice were treated with a triple therapy including finerenone, which increased the mean lifespan to 103.1 ± 20.3 days. The lifespan of the three treatment groups all differed significantly when compared to the vehicle group ($p < 0.001$). Furthermore, a statistically significant distinction in lifespan was observed between the triple treatment group and both the monotherapy and dual therapy groups ($p < 0.001$). Additionally, no statistically significant variation in lifespan was detected between the monotherapy and dual therapy groups ($p = 0.11$). The result suggests that adding finerenone to a dual RAS/SGLT2 inhibition approach can significantly prolong the lifespan of *Col4a3*-/- mice with progressive CKD caused by Alport nephropathy. The survival curves and body weight changes for the four groups can be seen in figure 5.5.

To investigate whether gender has any effect on lifespan, we conducted a subgroup analysis based on gender. The findings demonstrated that there were no significant differences in lifespan between genders in any of the groups, including the vehicle group ($p = 0.49$), the ramipril group ($p = 0.07$), the ramipril + empagliflozin group ($p = 0.68$), and the ramipril + empagliflozin + finerenone group ($p = 0.72$). These effects were independent of sex, as shown in figure 5.6.

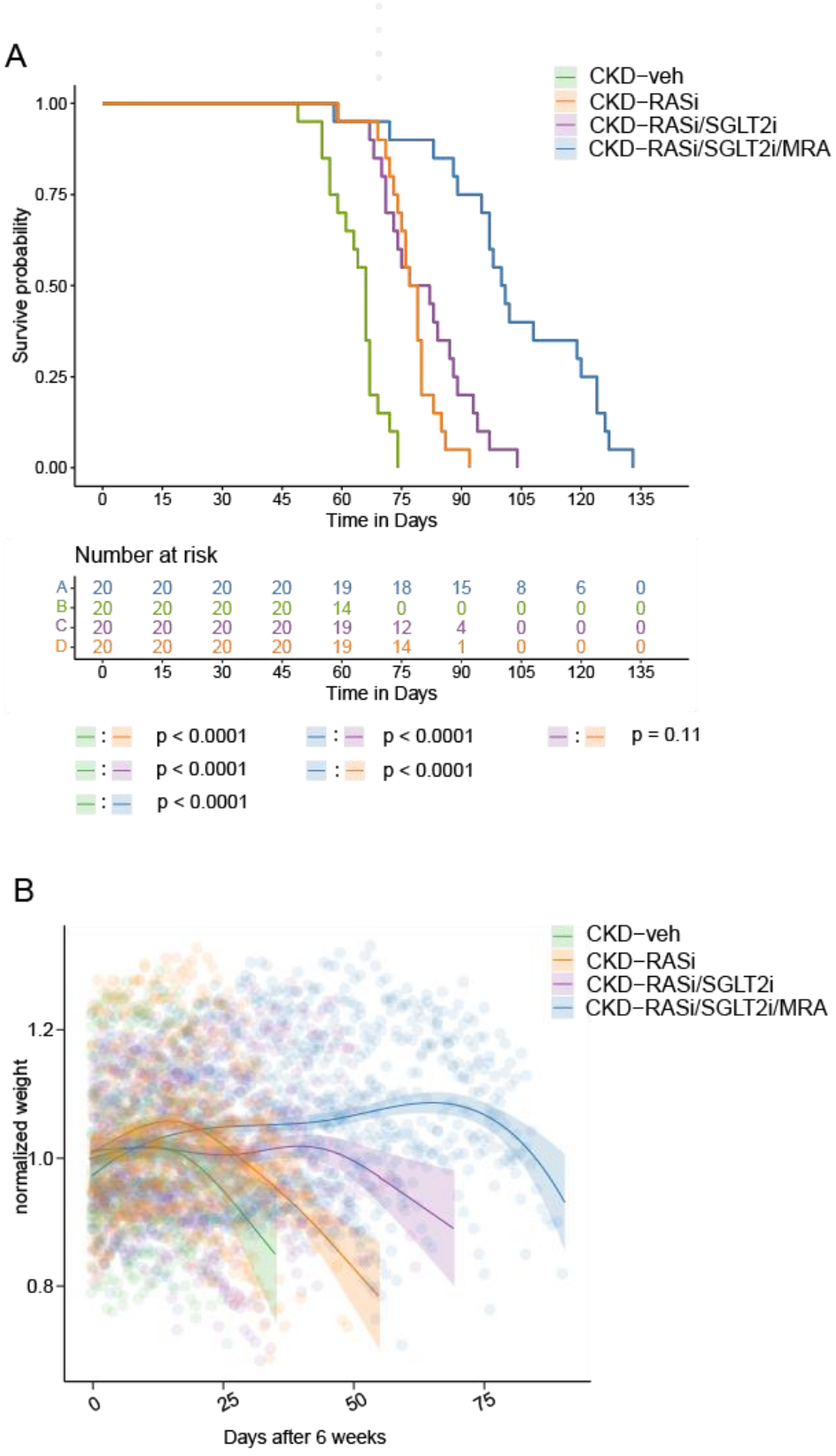

Figure 5.5 Finereone added to a dual RAS/SGLT2 inhibition substantially prolongs lifespan of *Col4a3*-/- mice with progressive CKD due to Alport nephropathy.

(A) Kaplan-Meier graph of survival. (B) Body weight changes after 6 weeks of age (shown as a percentage of initial body weight). All quantitative data are means ± SD.

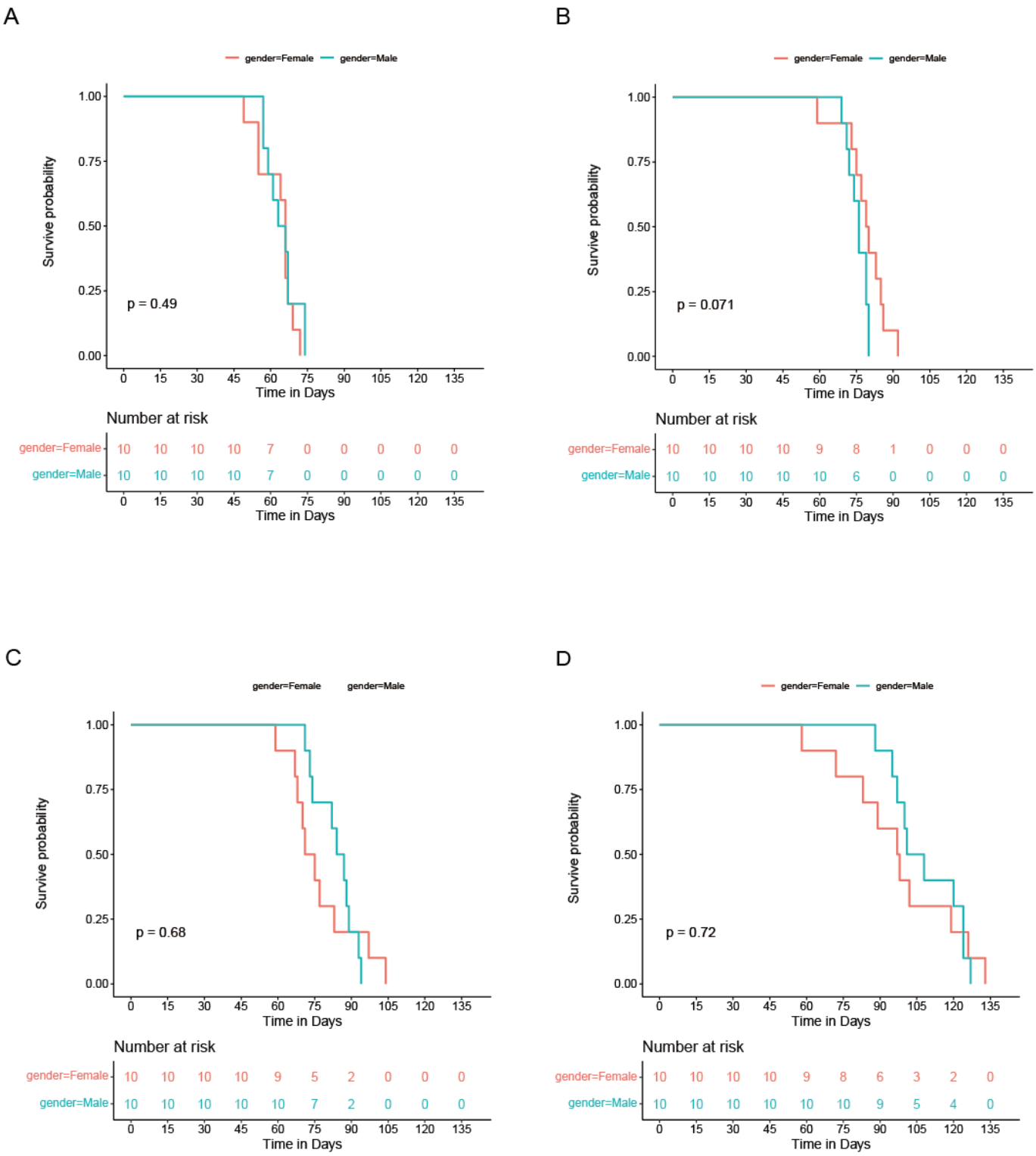

Figure 5.6 Subgroup analysis of lifespan in gender.

(A) Gender differences in vehicle group. (B) Gender differences in RASi group. (C) Gender differences in RASi/SGLT2i group. (D) Gender differences in RASi/SGLT2i/MRA group. All quantitative data are means ± SD.

5.4 Secondary endpoint: GFR slope and other makers of kidney function

Table 5.2 and Figure 5.7 illustrate the findings of the assessment of the impact of various treatments on GFR in Alport mice. The baseline GFR at 6 weeks of age, when the treatment started, did not display any significant differences among all the groups (p = 0.94). However, after one week of treatment, a

significant difference in GFR was observed among the 4 groups ($p = 0.02$). The CKD-veh group showed a decline in GFR from week 6 to 7, while the other treatment groups maintained their GFR, indicating that all treatments played a protective role in kidney function during the short-term treatment of 1 week. By 10 weeks of age, the differences between the groups became even more pronounced, with the result being statistically significant at $p < 0.001$. The CKD-veh group experienced a decline in GFR, with many mice dying before 10 weeks or having a GFR of 0 at 10 weeks of age. On the other hand, the CKD-RASi, CKD-RASi/SGLT2i, and CKD-RASi/SGLT2i/MRA groups showed a retention of about 29%, 30%, and 68% of their GFR from week 6 to week 10, respectively.

Table 2 Evolution of GFR in *Col4a3*-/- mice

Group (n=20)	**GFR (µl/min)**		
	6 weeks	**7 weeks**	**10 weeks**
CKD-veh	180.6 ± 32.1	147.0 ± 62.8	0.0 ± 0.0
CKD-RASi	187.6 ± 33.0	191.5 ± 44.4	54.5 ± 28.4
CKD-RASi/SGLT2i	187.3 ± 38.5	178.6 ± 30.5	55.4 ± 52.7
CKD-RASi/SGLT2i/MRA	185.3 ± 35.7	176.8 ± 39.2	125.4 ± 54.7
p	0.94	0.02	<0.001

GFR, glomerular filtration rate; CKD, Chronic kidney disease.

In comparison to the control group, the treatment groups showed a higher GFR and hence a better preservation of excretory kidney function at week 10. Unlike the control mice that had either passed away prior to or experienced a complete loss of kidney function, the treatment groups, especially the RASi/SGLT2i/MRA triple therapy, demonstrated a remarkable effect in protecting kidney function after 4 weeks of treatment. The results indicate that all three treatments were effective in preserving kidney function, but the RASi/SGLT2i/MRA triple therapy was the most effective among them.

The effect of the three drugs on albuminuria was also evaluated as albuminuria is a critical marker of CKD progression and a predictor of kidney outcome. Figure 5.8 shows the UACR in the CKD-veh, CKD-RASi, CKD-RASi/SGLT2i, CKD-RASi/SGLT2i/MRA groups and a control group at 6 and 8.5 weeks. At 6 weeks, *Col4a3*-/- mice had developed severe proteinuria compared to the control group (Figure 5.8A). All three treatment groups showed an effect in delaying the progression of kidney disease as evidenced by slower increases in UACR at 8.5 weeks of age compared to the CKD-veh group (Figure 5.8B). The

comparison of proteinuria changes from 6 weeks to 8 weeks in each group showed that the proteinuria significantly increased in CKD-veh group (p = 0.006), while it did not show a significant difference in CKD-RASi (p = 0.09), CKD-RASi/SGLT2i (p = 0.20), and CKD-RASi/SGLT2i/MRA (p = 0.93) groups (Figure 5.8C).

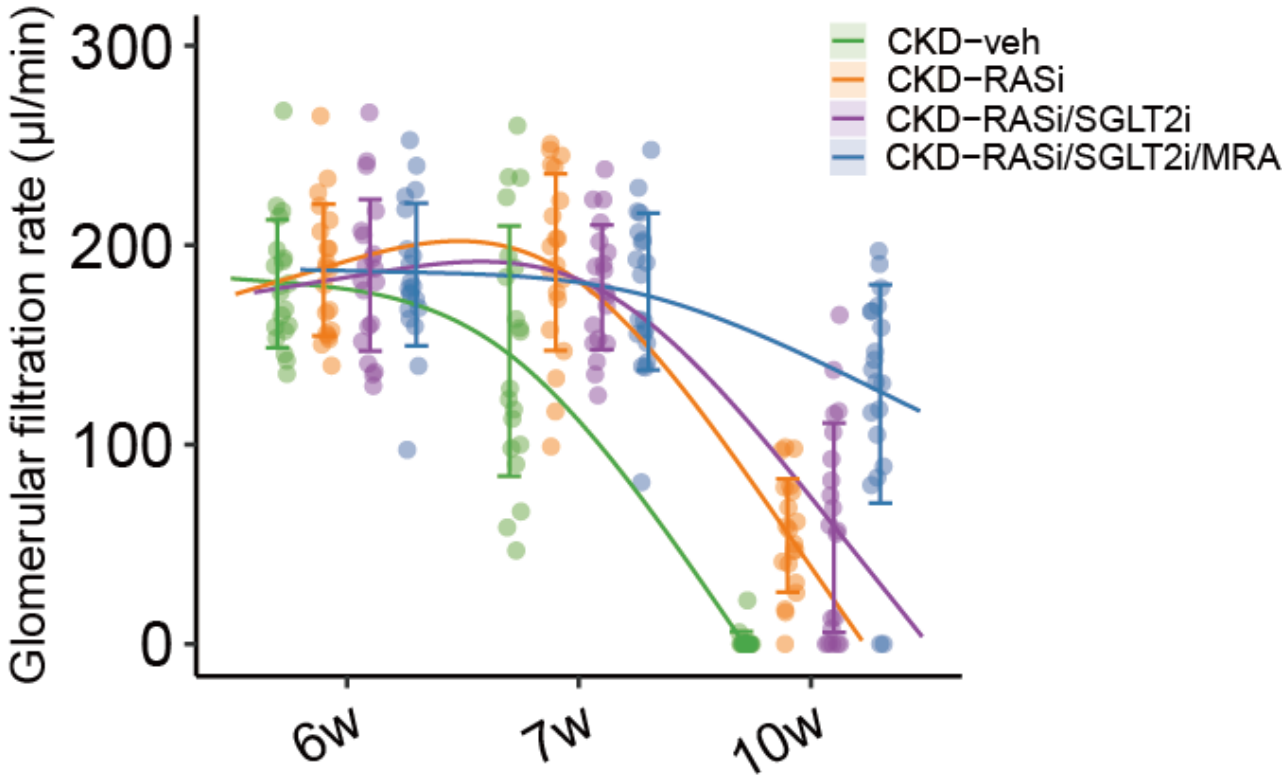

Figure 5.7 Effects of RASi, RASi/SGLT2i, and RASi/SGLT2i/MRA treatments on GFR. GFR was measured at 6, 7, and 10 weeks of age. All quantitative data are means ± SD.

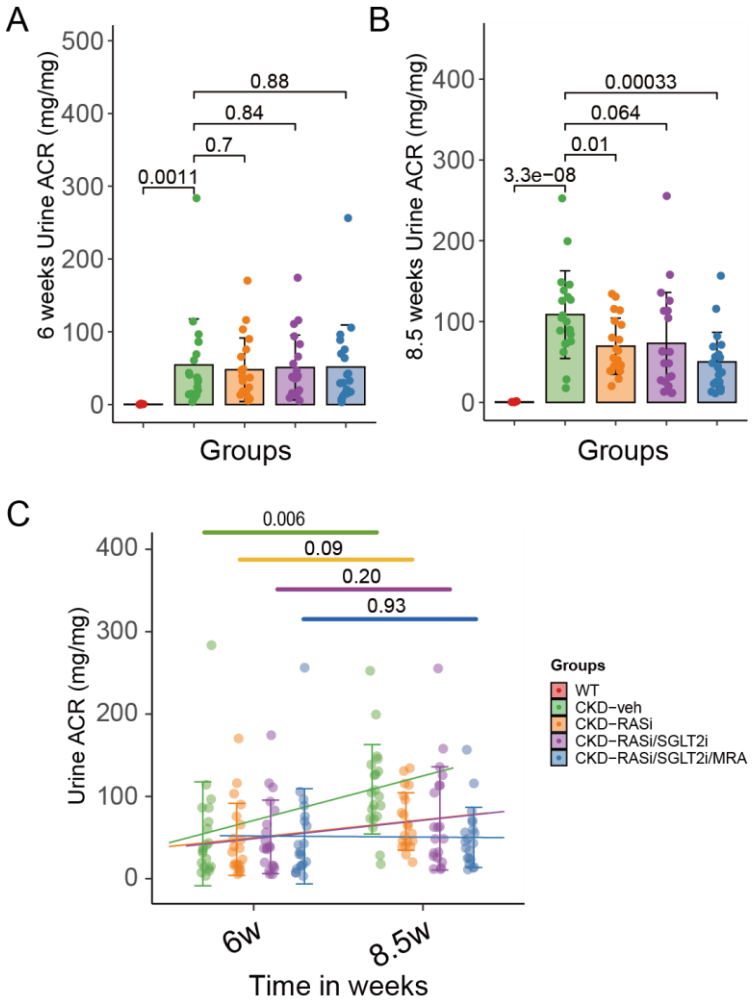

Figure 5.8 Effects of RASi, RASi/SGLT2i, and RASi/SGLT2i/MRA treatments on proteinuria in *Col4a3*-/- mice.
(A) The level of UACR at 6 weeks. (B) The level of UACR at 8.5 weeks. (C) The progression of proteinuria from 6 weeks to 8.5 weeks. All quantitative data are means ± SD.

To comprehend the effect of the various treatments on kidney function, we evaluated other markers of kidney function in *Col4a3*-/- mice at 8.5 weeks, after 2.5 weeks of treatment. The findings demonstrated that BUN level in CKD-RASi/SGLT2i/MRA group was significantly lower when compared with CKD-veh group ($p < 0.05$) (figure 5.9A). Furthermore, the triple therapy combination showed an added effect on serum creatinine levels compared to the CKD-veh, CKD-RASi, and CKD-RASi/SGLT2i groups at 8.5 weeks of age, as demonstrated in figure 5.9B. Furthermore, there were no significant differences observed in the serum levels of potassium and inorganic phosphate across all five groups ($p > 0.05$) (figure 5.10). Despite not reaching statistical significance ($p = 0.07$), we observed a decreasing trend in the potassium level upon adding SGLT2i to RASi treatment. Additionally, the dual and triple combination showed an increase in UGCR when compared with other groups ($p < 0.05$) (figure 5.10). These results suggest that the triple therapy combination has a positive impact on kidney function, as indicated by the improvement in these markers of kidney function. In addition, the absence of hyperkalemia in mice treated with finerenone

is reassuring in terms of potential drug-related toxicity. Also, mice in the groups treated with SGLT2 inhibitors showed a significant increase in urine glucose.

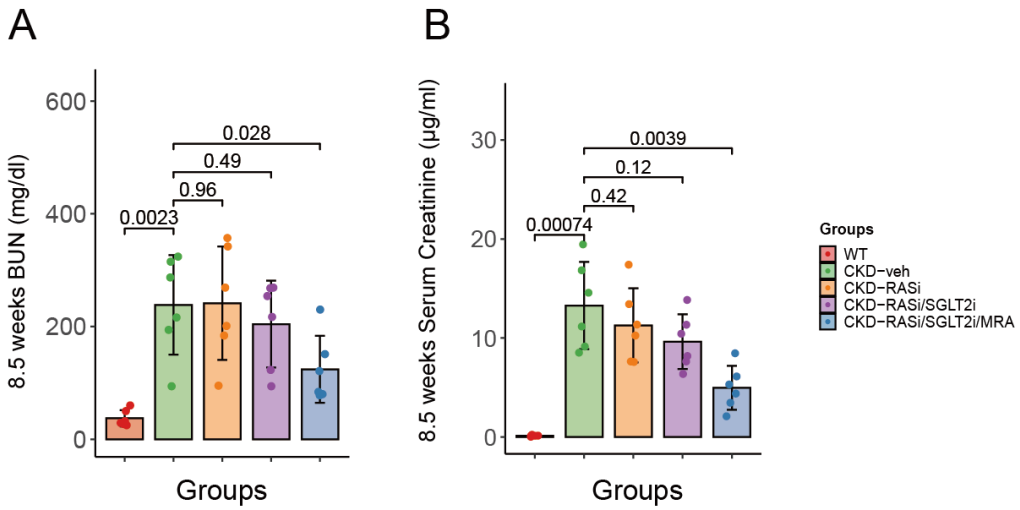

Figure 5.9 Effects of RASi, RASi/SGLT2i, and RASi/SGLT2i/MRA treatments on BUN and Serum Creatinine in *Col4a3*-/- mice.

(A) The level of BUN at 8.5 weeks. (B) The level of Serum Creatinine at 8.5 weeks. All quantitative data are means ± SD.

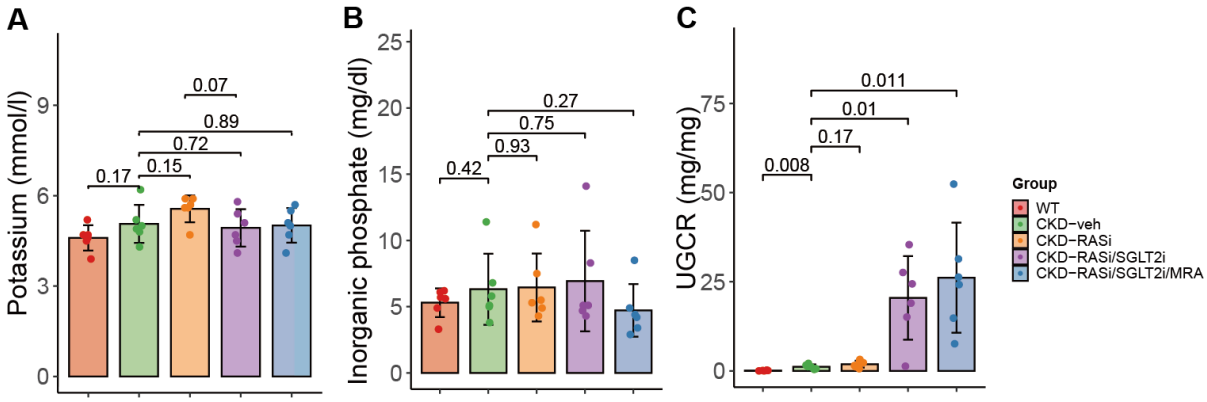

Figure 5.10 Effects of RASi, RASi/SGLT2i, and RASi/SGLT2i/MRA treatments on potassium and inorganic phosphate serum levels and UGCR in *Col4a3*-/- mice.

(A) The serum levels of potassium at 8.5 weeks. (B) The serum level of inorganic phosphate at 8.5 weeks. (C) The UGCR level at 8.5 weeks. All quantitative data are means ± SD.

Together, biomarkers of excretory kidney function suggested that the different lifespan of *Col4a3*-/- mice in the four treatment groups relates to the renoprotective effects of the involved drugs.

5.5 Secondary endpoint: Kidney histology

The results from the treatment effects on the lifespan of *Col4a3*-/- mice and the biomarkers of kidney function suggest the presence of renoprotective effects, potentially impacting kidney injury, tissue remodeling, and atrophy. The triple therapy was particularly effective in preventing kidney atrophy,

bringing it to the level of normal wildtype controls, as depicted in figure 5.11. Further examination of the impact of the treatment was conducted through histological analysis of small subgroups of mice at 8.5 weeks.

Our findings showed that the CKD-RASi/SGLT2i/MRA therapy showed significant renoprotective effects, not only in terms of lifespan of the *Col4a3*-/- mice, but also in terms of biomarkers of kidney function, tissue remodeling, and atrophy. Triple therapy prevented kidney atrophy to the level of wildtype controls, as evidenced by gross kidney morphology (Figure 5.11). Upon further assessment of kidney histology in small subgroups of mice for each treatment at 8.5 weeks of age, the results showed that the CKD-RASi/SGLT2i/MRA therapy was linked to reduced glomerulosclerosis, tubular atrophy, and interstitial fibrosis. The overall damage score was significantly lower in this group compared to the CKD-veh, CKD-RASi, and CKD-RASi/SGLT2i groups ($p < 0.05$) (Figure 5.12). Picro-Sirius Red-stained kidney sections further demonstrated the significant amelioration of interstitial fibrosis in the CKD-RASi/SGLT2i/MRA group compared to the other groups ($p < 0.05$) (Figure 5.13). Additionally, the αSMA labeling in the interstitium was also reduced in the CKD-RASi/SGLT2i/MRA group compared to the other groups ($p < 0.01$) (Figure 5.13).

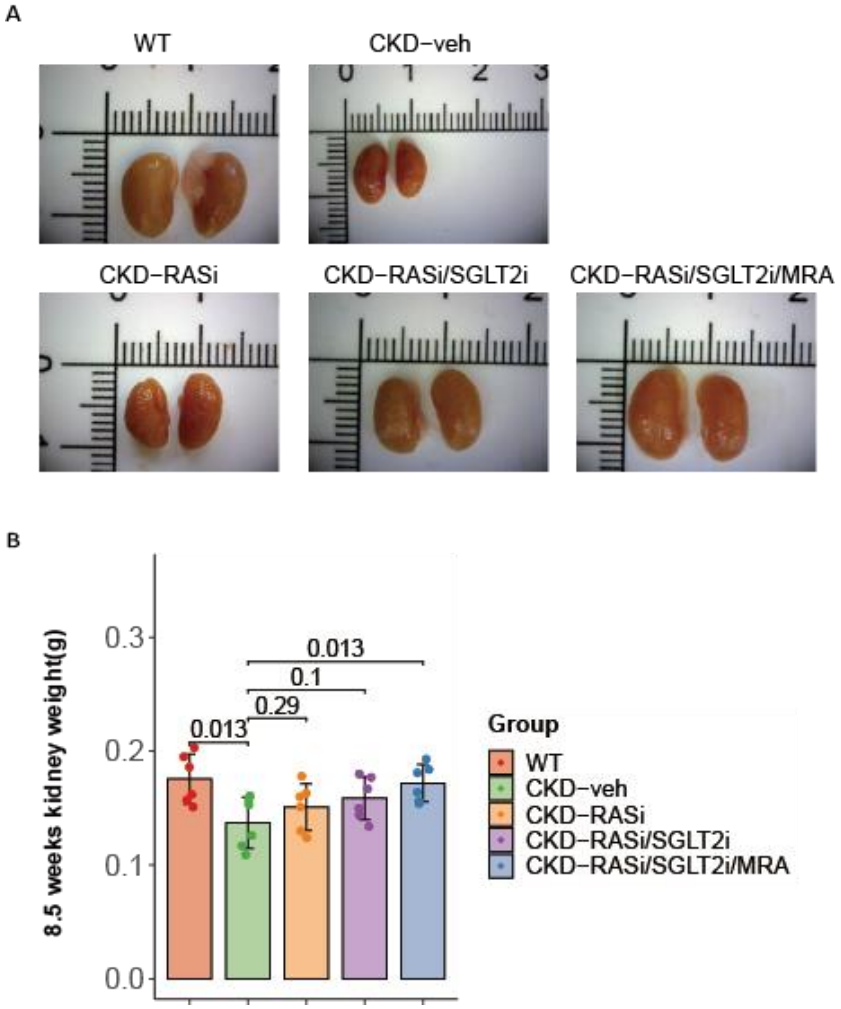

Figure 5.11 Triple therapy prevented kidney atrophy to the level of wildtype controls.

(A) Representative 8.5 weeks kidney images. (B) 8.5 weeks kidney weight. All quantitative data are means ± SD.

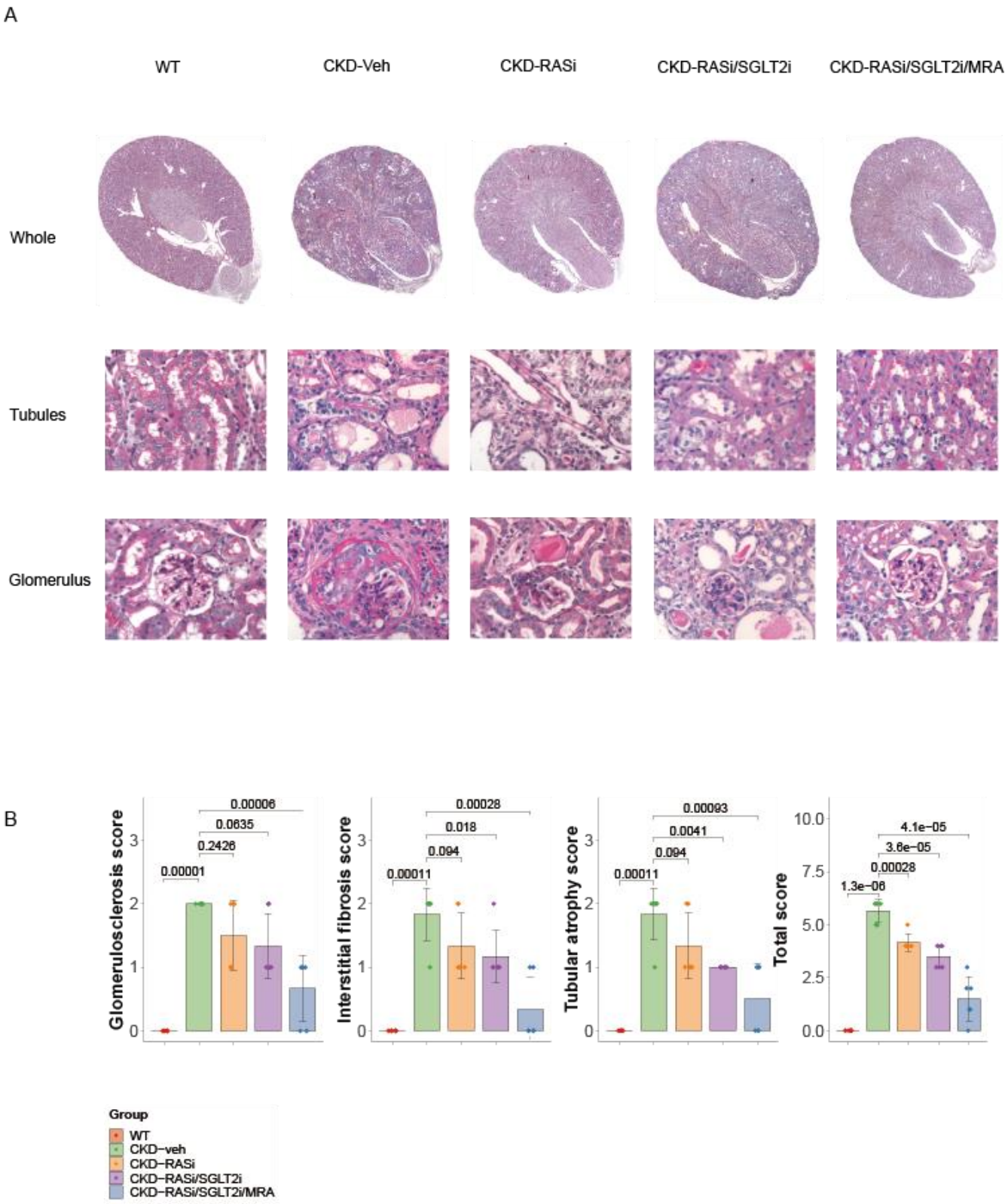

Figure 5.12 Tissue morphology and PAS staining quantitative assessment of scores from *Col4a3*-/- mice in WT, Veh, RASi, RASi/SGLT2i, and RASi/SGLT2i/MRA groups.

(A) Representative PAS-stained images from the whole kidney, tubules and glomerulus are presented. (B) Kidney sections were independently scored for tubulointerstitial fibrosis, glomerulosclerosis and tubular atrophy. All quantitative data are means ± SD. Images are shown at the magnification of 200x and 400x.

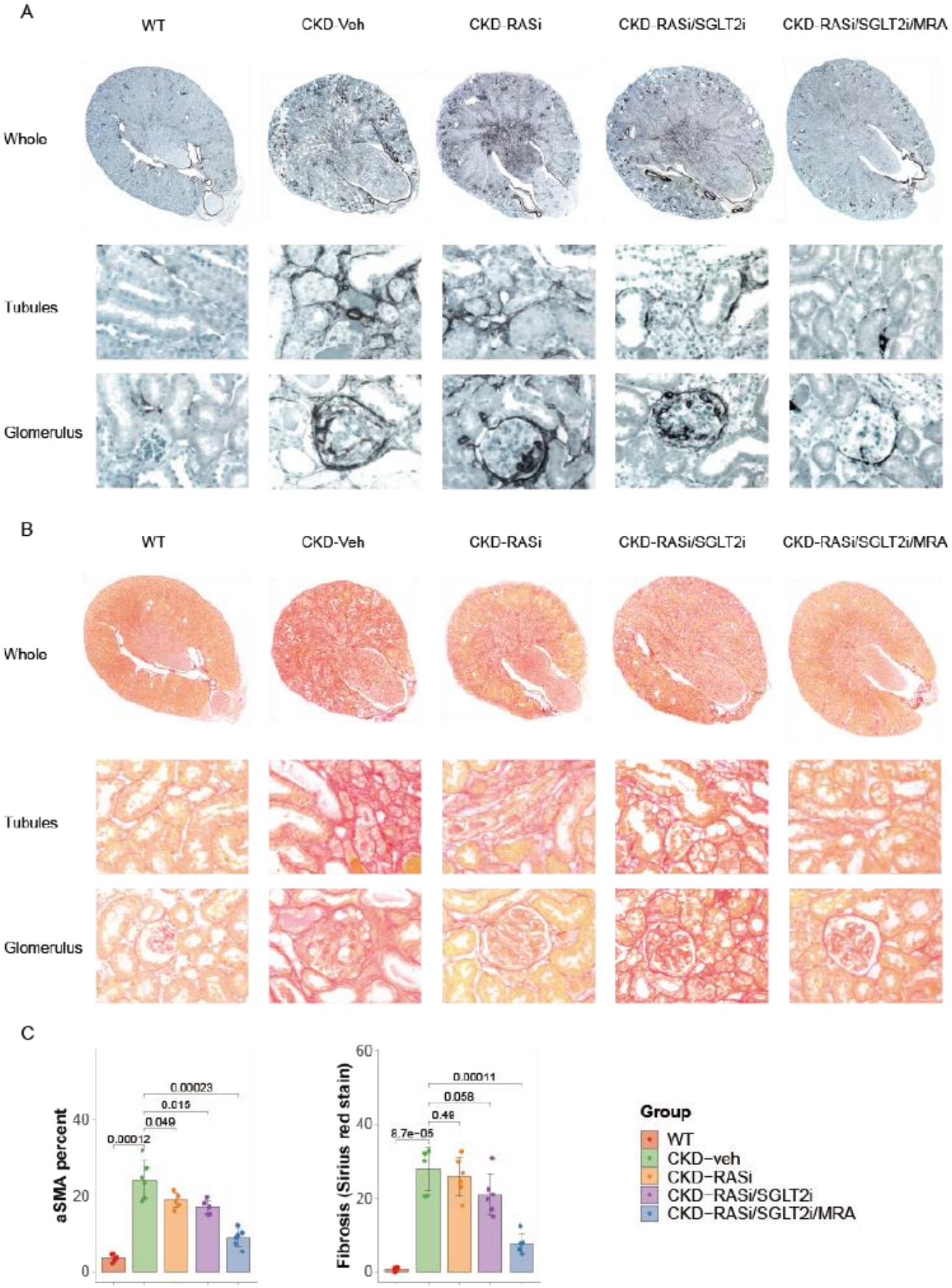

Figure 5.13 Tissue morphology and αSMA and Picro-Sirius red staining quantitative assessment of scores from *Col4a3* -/- mice in WT, Veh, RASi, RASi/SGLT2i, and RASi/SGLT2i/MRA groups.

(A, B) Representative αSMA and Picro-Sirius red stained images from the whole kidney, tubules and glomerulus. (C) Kidney sections were independently scored for αSMA positive percent and Picro-Sirius red positive percent. All quantitative data are means ± SD. Images are shown at the magnification of 200x and 400x.

F4/80 staining was employed to examine of the inflammatory response. The outcome indicated a considerable rise in inflammation in CKD-veh group compared with WT group ($p < 0.01$). Furthermore, the CKD-RASi/SGLT2i/MRA group exhibited a significant reduction in inflammation compared to the CKD-veh group ($p < 0.01$). This information can be observed in figure 5.14A and D.

Podocyte loss is a critical aspect of both Alport syndrome and CKD progression. To assess changes in podocyte numbers, we quantified WT-1 staining on kidney tissue samples. The results showed a significant reduction in the count of WT-1 positive cells per glomerulus in CKD-veh group compared to WT group ($p < 0.01$). Interestingly, the number of WT-1 positive cells per glomerulus in CKD-RASi/SGLT2i/MRA group was found to be greater than the number in CKD-veh, CKD-RASi, and CKD-RASi/SGLT2i groups ($p < 0.05$). This information is presented in figure 5.14B and D.

The TUNEL staining technique, which is indicated in green, revealed a higher number of apoptotic cells in CKD-veh group compared with WT group ($p < 0.01$). Furthermore, the analysis showed a decrease in the extent of cell death in the CKD-RASi/SGLT2i/MRA group when compared to the CKD-veh, CKD-RASi, and CKD-RASi/SGLT2i groups ($p < 0.01$). This information is presented in figure 14 C and D.

The results obtained from a cross-sectional automated tissue analysis after 2.5 weeks of treatment indicate that the varying lifespan of *Col4a3*-/- mice in four groups can be attributed to renoprotective benefits of the drugs administered. By combining finerenone with dual RAS/SGLT2 inhibition, a remarkable antifibrotic effect was achieved and the progression of inflammation, tubular atrophy, and podocyte loss was prevented. The findings further demonstrate the significance of this combination in achieving the desired renoprotective outcomes.

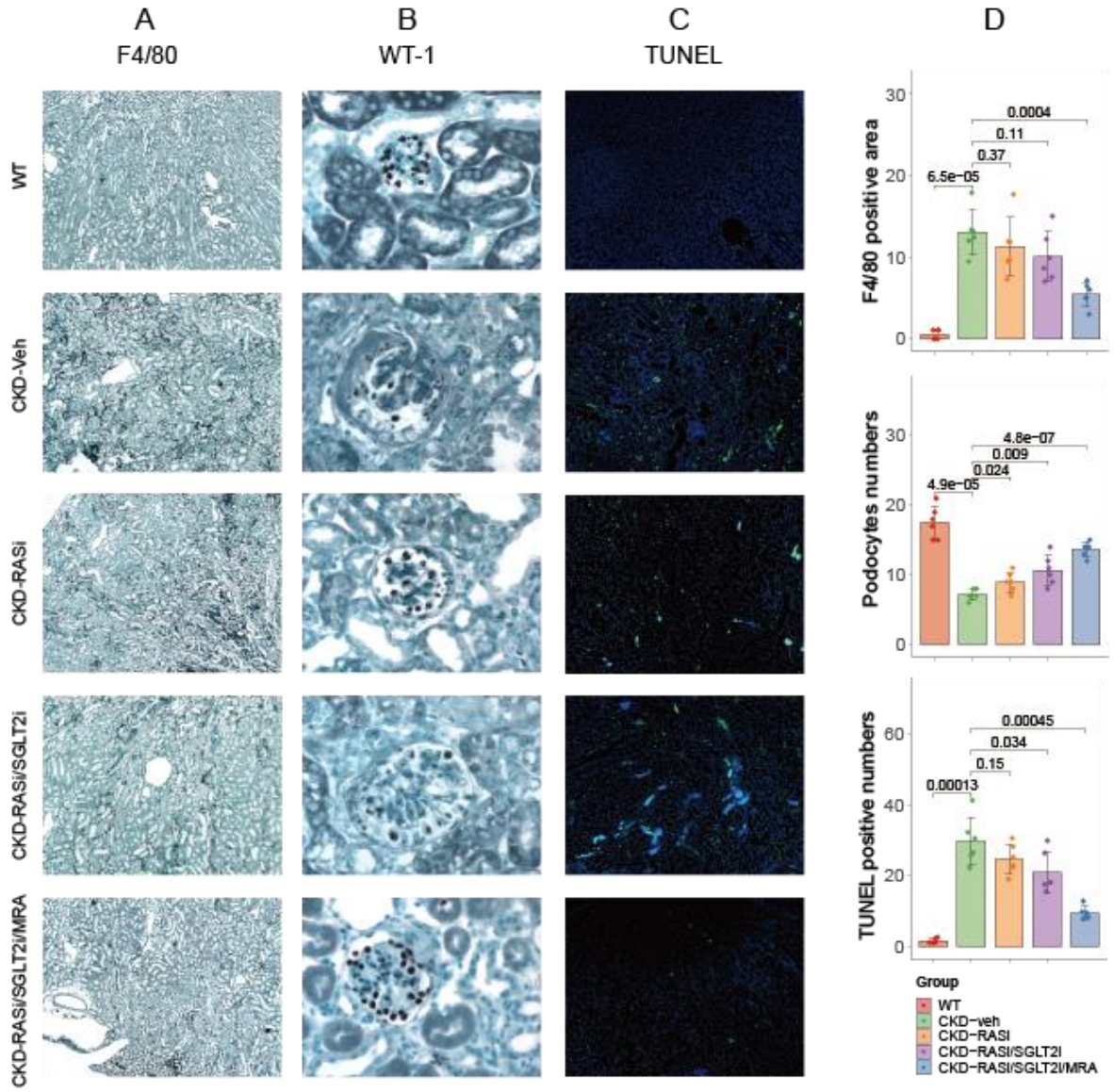

Figure 5.14 Tissue morphology and F4/80, WT-1, and TUNEL staining quantitative assessment of scores from *Col4a3*-/- mice in WT, veh, RASi, RASi/SGLT2i, and RASi/SGLT2i/MRA groups.

(A) Representative F4/80-stained images from junction of kidney cortex and medulla are presented. (B) Representative WT1-stained images from the kidney glomerulus are presented. (C) Representative TUNEL stained images from the kidneys are presented. (D) Kidney sections were independently scored for F4/80 positive percent, podocytes numbers, and the number of TUNEL-positive nuclei per 100 tubules. All quantitative data are means ± SD. Images are shown at the magnification of 200x and 400x.

5.6 Secondary endpoint: kidney mRNA expression

To gain further mechanistic insights into mechanism-of-action of the treatment, we analyzed gene expression in whole kidney lysate samples from 5 groups (WT, CKD-veh, CKD-RASi, CKD-RASi/SGLT2i, and CKD-RASi/SGLT2i/MRA) after 8.5 weeks. This aimed to reveal crucial molecular changes responsible for the observed outcomes and to shed light on the mechanisms behind kidney disease progression or prevention.

The qPCR results confirmed a significant rise in mRNA expression of several fibrosis markers in CKD-veh group compared to WT group ($p < 0.05$). These markers, including *αSMA*, *FN*, *TGFβ*, and *Col1a1*, play a pivotal role in kidney disease progression. However, the CKD-RASi/SGLT2i/MRA group, which received finerenone in addition to dual RAS/SGLT2 inhibition, effectively reduced expression of these markers when compared with CKD-veh group ($p < 0.05$) (Figure 5.15), in agreement with the pathological staining results.

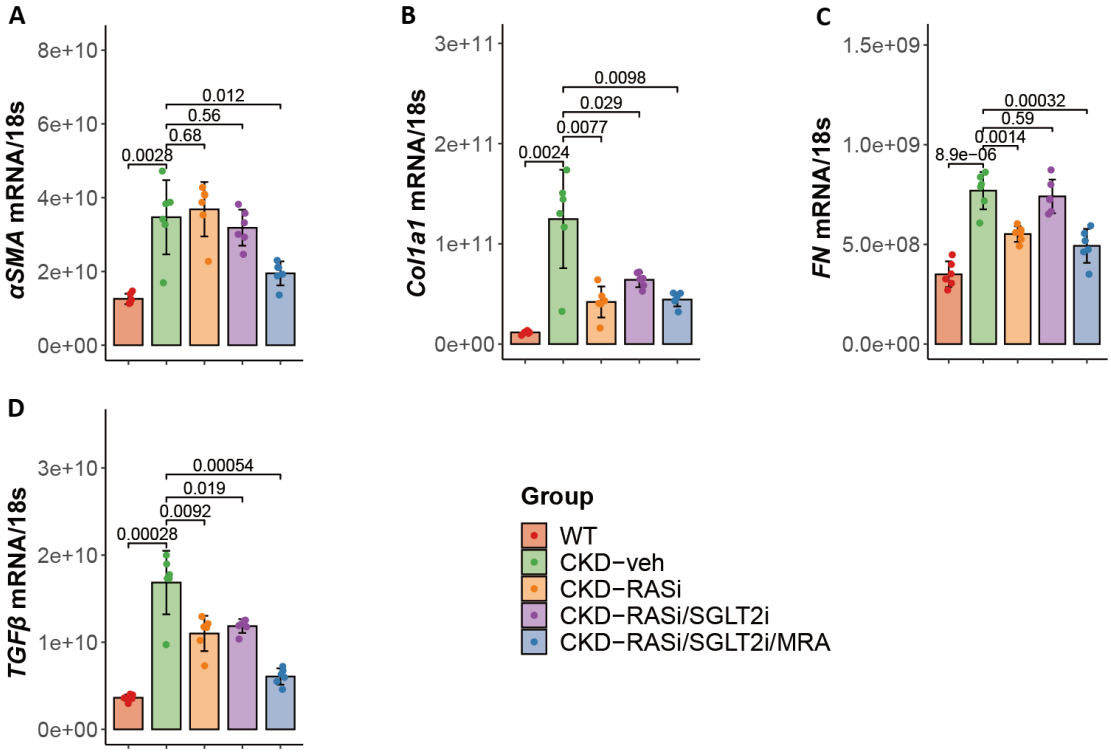

Figure 5.15 Relative kidney mRNA expression of kidney fibrosis markers.
Gene expression was analyzed by RT-qPCR for (A) *αSMA*. (B) *Col1a1*. (C) *FN*. (D) *TGFβ*. All quantitative data are means ± SD.

The qPCR analysis revealed that the mRNA expression levels of various inflammation markers including *CCR5*, *ICAM1*, *VCAM1*, *IL1β*, as well as kidney injury markers including *KIM1*, *NGAL*, *IL6*, *IL18*, *TIMP2*, and *TNFα*, were increased in CKD-veh group when compared with WT group. Our findings

showed a significant difference ($p < 0.05$) between these two groups. However, triple treatment of RASi/SGLT2i/MRA was found to significantly reduce the mRNA expression levels of these markers ($p < 0.05$), as seen in figure 5.16 and 5.17. This finding supports the earlier observations from the PAS, F4/80, and TUNEL staining analyses.

Finally, the qPCR analysis conducted revealed alterations in the mRNA expression levels of two crucial podocyte markers, *nephrin* and *podocin*. These markers are an indicator of the podocyte loss that occurred in the four different treatment groups. The findings indicated that the CKD-veh group experienced a drop in the expression of these markers as compared to the WT group ($p < 0.05$), while the expression of *nephrin* and *podocin* was increased in the CKD-RASi/SGLT2i/MRA group. ($p < 0.05$) (figure 5.18). This result aligns with the results obtained from the WT-1 staining examination.

In summary, the combined results at the mRNA level present a compelling argument for the therapeutic benefits of incorporating finerenone into a dual inhibition approach targeting the RAS and SGLT2 in order to slow down the advancement of various negative outcomes, including tissue fibrosis, inflammation, kidney damage, and podocyte loss in *Col4a3*-/- mice. This evidence highlights the potential for this treatment strategy to be an effective means of mitigating the progression of these negative outcomes.

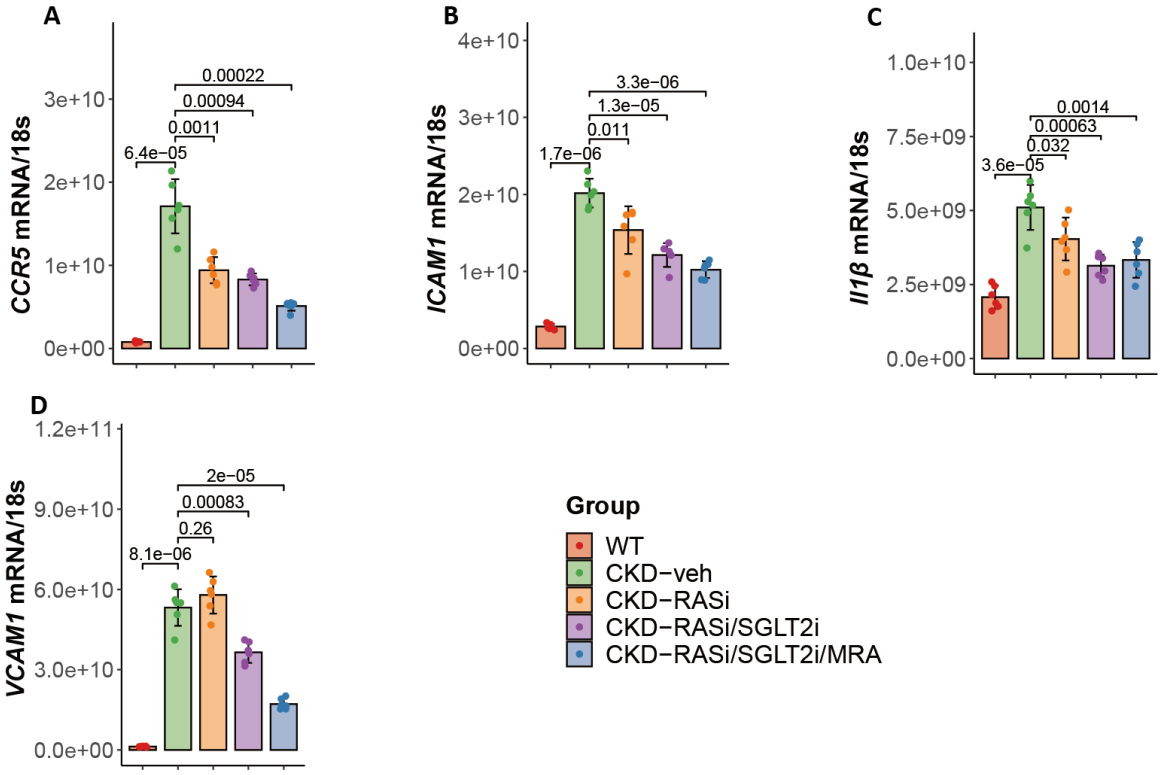

Figure 5.16 Relative kidney mRNA expression of kidney inflammation markers.
Gene expression was analyzed by RT-qPCR for (A) *CCR5*. (B) *ICAM1*. (C) *Il1β*. (D) *VCAM1*. All quantitative data are means ± SD.

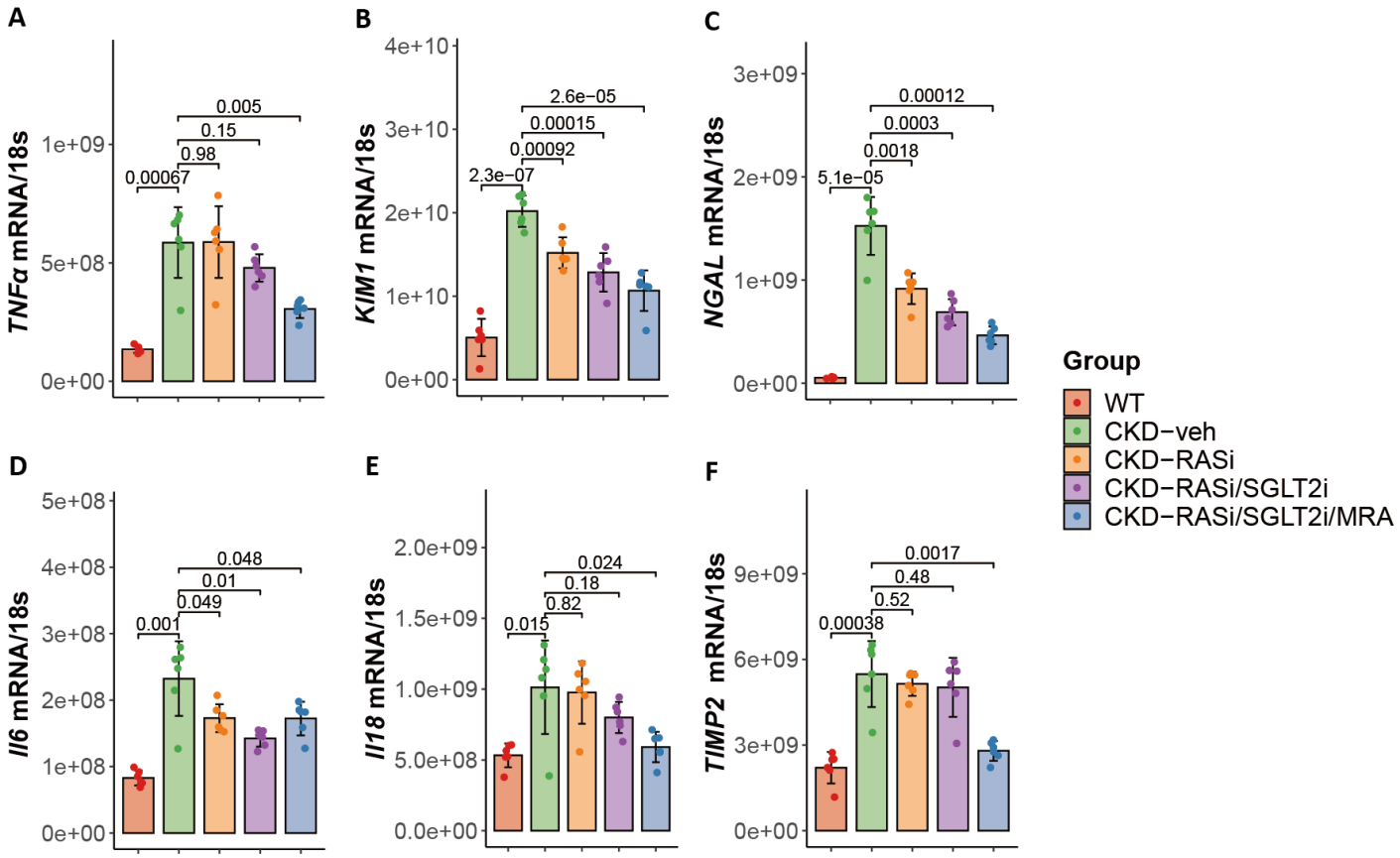

Figure 5.17 Relative kidney mRNA expression of kidney injury markers.

Gene expression was analyzed by RT-qPCR for (A) *TNFα*. (B) *KIM1*. (C) *NGAL*. (D) *Il6*. (E) *Il18*. (F) *TIMP2*. All quantitative data are means ± SD.

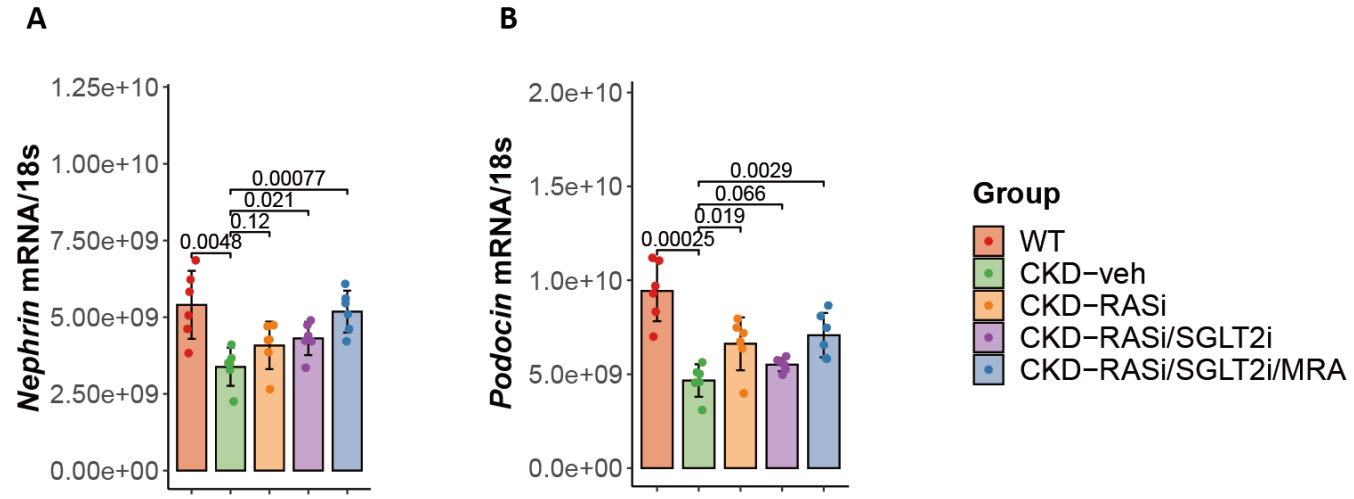

Figure 5.18 Relative kidney mRNA expression of podocyte markers.

Gene expression was analyzed by RT-qPCR for (A) *Nephrin*. (B) *Podocin*. All quantitative data are means ± SD.

5.7 Secondary endpoint: RNA sequencing

To gain a deeper understanding of how finerenone impacts the kidney defect present in *Col4a3*-/- mice, when added to dual RAS/SGLT2 inhibition therapy, we performed next-generation RNA sequencing on

kidney samples obtained from five groups of mice (WT, CKD-veh, CKD-RASi, CKD-RASi/SGLT2i, and CKD-RASi/SGLT2i/MRA) at 8.5 weeks.

A pairwise comparison of group WT and group CKD-veh was conducted using RNA-seq data, which revealed a marked alteration in gene expression within the CKD-veh group. The results of the analysis indicated a substantial alteration in gene expression within the CKD-veh group, with 4,360 genes upregulated and 3,246 genes downregulated. Further examination utilizing Gene Set Enrichment Analysis (GSEA) showed that pathways linked to inflammation and pro-fibrotic responses were notably heightened in the CKD-veh mouse kidneys compared to the WT group. These findings were consistent with previous observations from qPCR and pathological staining experiments. In addition, our analysis uncovered that the CKD-veh group experienced a suppression of mitochondrial function as compared to the WT group, as demonstrated in figure 5.19.

RNA-seq data was then used to conduct a pairwise comparison between the vehicle-treated Alport mouse group and the dual RAS/SGLT2 inhibition plus finerenone (CKD-RASi/SGLT2i/MRA)-treated Alport mouse group, revealing a significant change in gene expression between the two groups. The analysis results showed a substantial change in gene expression within the CKD-veh group, with 2,307 genes upregulated and 1,771 genes downregulated. Further analysis using GSEA showed that pathways linked to inflammation and pro-fibrotic responses were significantly elevated in the CKD-veh mouse kidneys compared to the CKD-RASi/SGLT2i/MRA group. Further, our findings revealed that mitochondrial functions in CKD-veh group were suppressed compared to CKD-RASi/SGLT2i/MRA group. Our analysis indicated that pathways related to fibrosis such as "positive regulation of fibroblast proliferation", "tabula muris senis kidney fibroblast aging", and "fibroblast proliferation" were suppressed in the CKD-RASi/SGLT2i/MRA group. This suggests that the combination of dual RAS/SGLT2 inhibition and finerenone inhibits the progression of kidney fibrosis. Our findings showed that the pathways related to inflammation, such as "regulation of inflammatory response", "inflammatory response to wounding", and "tolerant macrophage upregulation" were suppressed in the CKD-RASi/SGLT2i/MRA group. This finding suggests that the addition of finerenone to dual RAS/SGLT2 inhibition has an inhibitory effect on the processes of inflammation and fibrosis during kidney atrophy in Alport nephropathy. Our findings were in line with the qPCR data focusing on the same pathways (Figure 5.15, 5.16), e.g., pro-inflammatory genes such as *CCR5*, *Il1β*, and *VCAM1*; pro-fibrosis genes such as *αSMA*, *Col1a1*, *FN*, and *TGFβ* were overexpressed in the CKD-veh group compared to the CKD-RASi/SGLT2i/MRA group (Figure 5.20).

Next, we compared the gene expression differences between CKD-RASi/SGLT2i/MRA and CKD-RASi/SGLT2i, as well as CKD-RASi/SGLT2i/MRA and CKD-RASi using RNA-seq data. The results showed that pathways linked to inflammation and pro-fibrotic responses were significantly downregulated in the CKD-RASi/SGLT2i/MRA mouse kidneys compared to the CKD-RASi/SGLT2i and CKD-RASi groups, respectively (Figure 5.21, 5.22). This result indicates that the combination of finerenone with dual RAS/SGLT2 inhibition produces a more potent inhibitory effect on the processes of inflammation and fibrosis, when compared to the outcomes of CKD-RASi/SGLT2i and CKD-RASi treatments. These findings concurred with the results obtained from previous qPCR and pathological staining experiments. Thus, finerenone suppresses these pathogenic pathways beyond the capacity of dual RAS/SGLT2 inhibition, i.e., a synergistic mechanism-of-action.

In all, the analysis of RNA sequencing revealed a strong anti-inflammatory and anti-fibrotic effect of the triple combination. The results demonstrate the synergistic effectiveness of the RASi/SGLT2i/MRA combination in reducing inflammation and fibrosis, which are both key indicators of positive outcomes in related medical conditions.

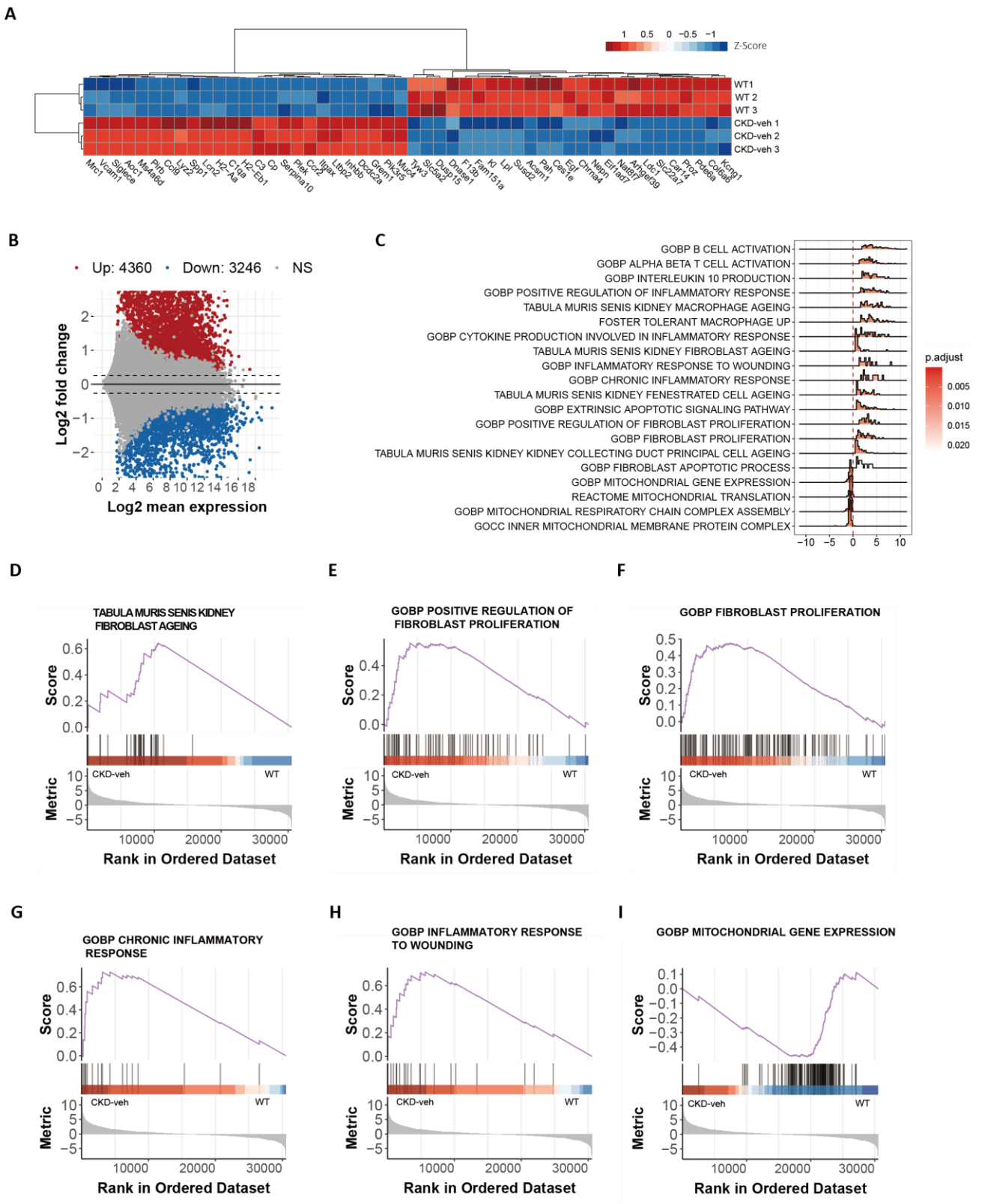

Figure 5.19 Bulk RNA-seq on Veh-treated Alport mouse and wild type mouse kidney.

(A) The heatmap presents the biological replicates of the top genes with differing expression levels between the CKD-veh and WT mouse kidneys. A heatmap and dendrogram were used to display the differentially expressed genes' z-scores of normalized counts. (B) An MA plot was also created to display the shrink log2 fold change between the CKD-veh and WT mouse kidneys. Genes that are found to be significant in differential expression testing, as indicated by an adjusted *p*-value, are labeled either in red or blue. (C) The density ridge plot shows the gene expression distribution of core-enriched genes in enriched gene sets, with gradient color indicating adjusted *p*-values using the Benjamini-Hochberg method. (D-I) The selected enrichment plots from the GSEA analysis based on the gene enrichment profiles of the CKD-veh and WT mouse kidneys. The plots highlight the enrichment for transcriptional signatures related to inflammation, fibrosis, and mitochondrial function.

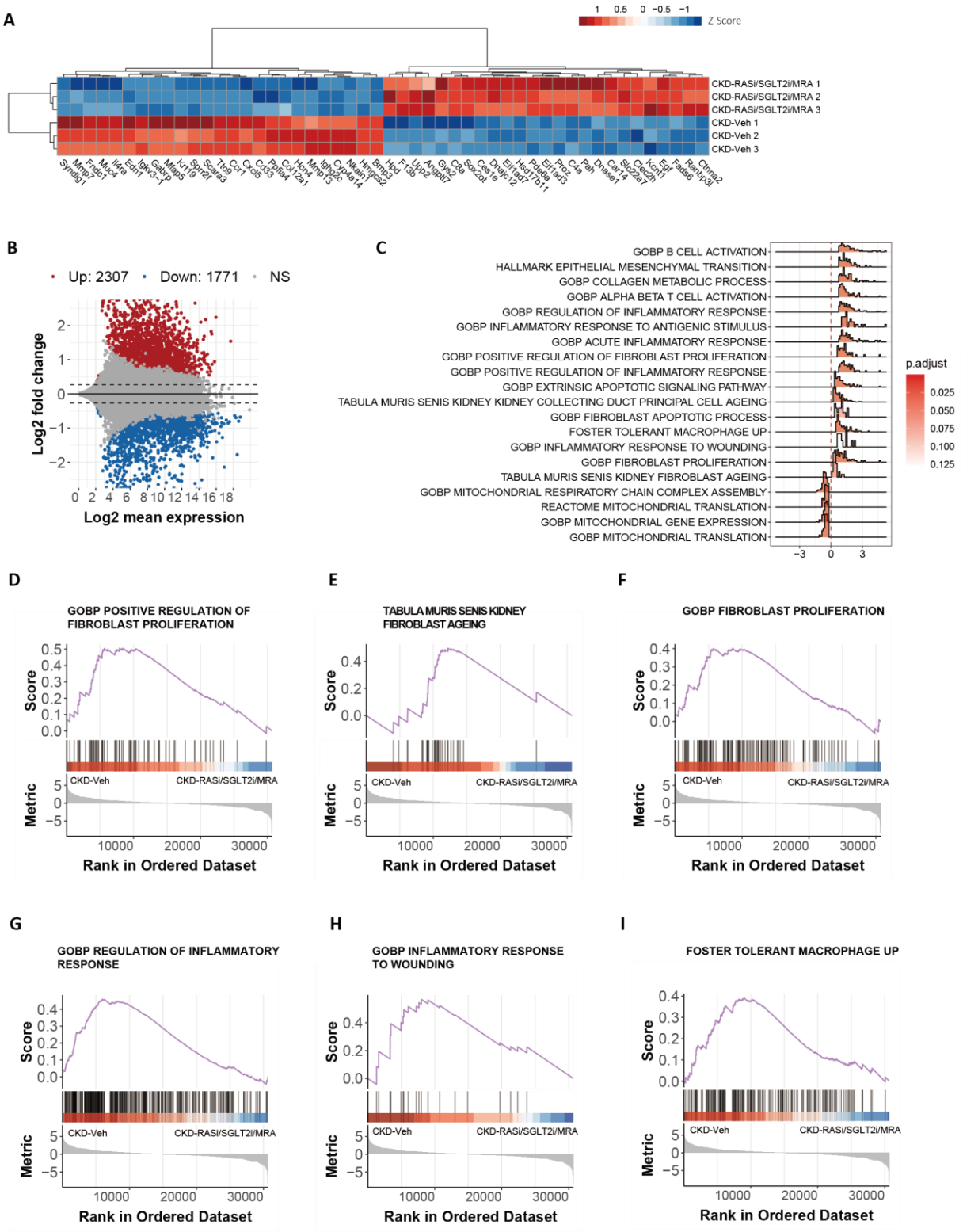

Figure 5.20 Bulk RNA-seq on Veh-treated Alport mouse and RASi/SGLT2i/MRA-treated Alport mouse kidney.

(A) The heatmap presents the biological replicates of the top genes with differing expression levels between the CKD-veh and CKD-RASi/SGLT2i/MRA mouse kidneys. A heatmap and dendrogram were used to display the differentially expressed genes' z-scores of normalized counts. (B) An MA plot was also created to display the shrink log2 fold change between the CKD-veh and CKD-RASi/SGLT2i/MRA mouse kidneys. Genes that are found to be significant in differential expression testing, as indicated by an adjusted *p*-value, are labeled either in red or blue. (C) The density ridge plot shows the gene expression distribution of core-enriched genes in enriched gene sets, with gradient color indicating adjusted *p*-values using the Benjamini-Hochberg method. (D-I) The selected enrichment plots from the GSEA analysis based on the gene enrichment profiles of the CKD-veh and CKD-RASi/SGLT2i/MRA mouse kidneys. The plots highlight the enrichment for transcriptional signatures related to inflammation, fibrosis, and mitochondrial function.

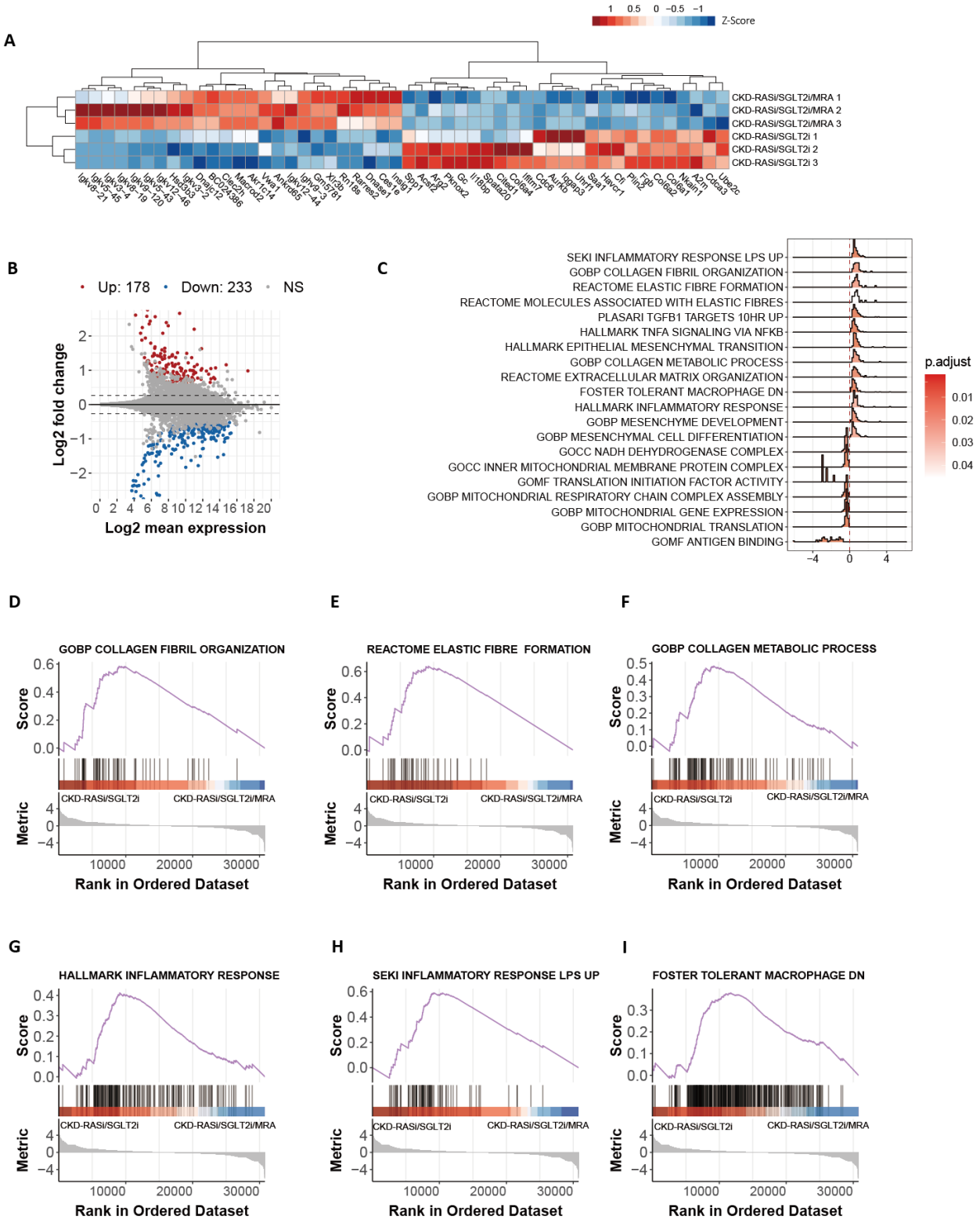

Figure 5.21 Bulk RNA-seq on RASi/SGLT2i-treated Alport mouse and RASi/SGLT2i /MRA-treated Alport mouse kidney. (A) The heatmap presents the biological replicates of the top genes with differing expression levels between the CKD-RASi/SGLT2i and CKD-RASi/SGLT2i/MRA mouse kidneys. A heatmap and dendrogram were used to display the differentially expressed genes' z-scores of normalized counts. (B) An MA plot was also created to display the shrink log2 fold change between the CKD-RASi/SGLT2i and CKD-RASi/SGLT2i/MRA mouse kidneys. Genes that are found to be significant in differential expression testing, as indicated by an adjusted *p*-value, are labeled either in red or blue. (C) The density ridge plot shows the gene expression distribution of core-enriched genes in enriched gene sets, with gradient color indicating adjusted *p*-values using the Benjamini-Hochberg method. (D-I) The selected enrichment plots from the GSEA analysis based on the gene enrichment profiles of the CKD-RASi/SGLT2i and CKD-RASi/SGLT2i/MRA mouse kidneys. The plots highlight the enrichment for transcriptional signatures related to inflammation, fibrosis, and mitochondrial function.

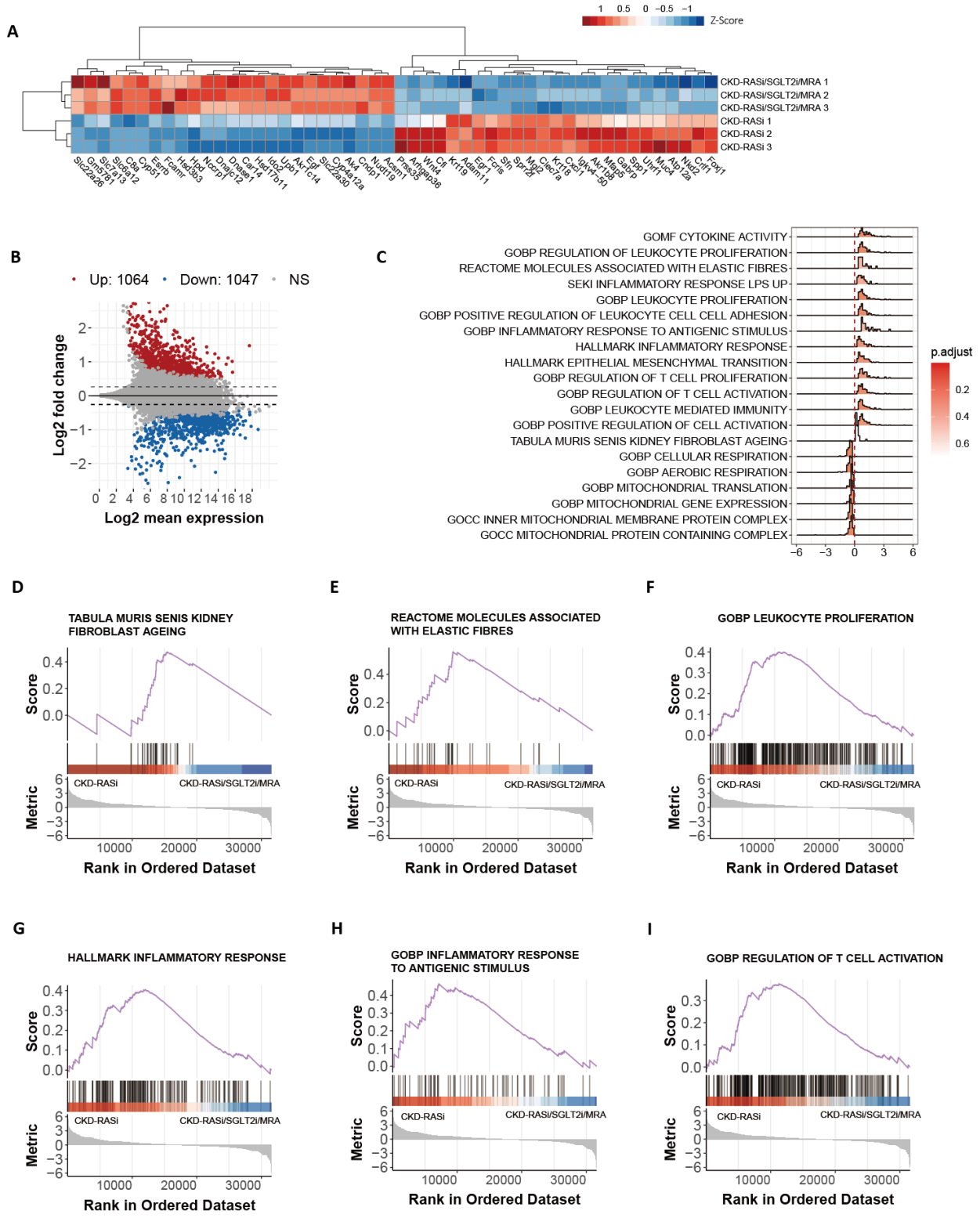

Figure 5.22 Bulk RNA-seq on RASi-treated Alport mouse and RASi/SGLT2i /MRA-treated Alport mouse kidney.
(A) The heatmap presents the biological replicates of the top genes with differing expression levels between the CKD-RASi and CKD-RASi/SGLT2i/MRA mouse kidneys. A heatmap and dendrogram were used to display the differentially expressed genes' z-scores of normalized counts. (B) An MA plot was also created to display the shrink log2 fold change between the CKD-RASi and CKD-RASi/SGLT2i/MRA mouse kidneys. Genes that are found to be significant in differential expression testing, as indicated by an adjusted *p*-value, are labeled either in red or blue. (C) The density ridge plot shows the gene expression distribution of core-enriched genes in enriched gene sets, with gradient color indicating adjusted *p*-values using the Benjamini-Hochberg method. (D-I) The selected enrichment plots from the GSEA analysis based on the gene enrichment profiles of the CKD-RASi and CKD-RASi/SGLT2i/MRA mouse kidneys. The plots highlight the enrichment for transcriptional signatures related to inflammation, fibrosis, and mitochondrial function.

6. Discussion

We had hypothesized that a combination of three drugs, ramipril (RASi), empagliflozin (SGLT2i), and finerenone (MRA), would significantly enhance the longevity of the kidneys compared to the use of dual RAS/SGLT2 inhibition. Our findings confirmed this hypothesis and even revealed an almost exponential increase in kidney lifespan when finerenone is added to dual RAS/SGLT2 inhibition. The experiment was carried out as a double-blinded, randomized controlled trial at a single center with a pre-registered trial protocol. The primary endpoint was total lifespan and most secondary analyses were performed in a blinded and automated manner. The design of the preclinical RCT was carefully considered to minimize potential sources of bias and increase the reliability of the results, particularly for CKD progression in Alport syndrome. pRCTs are innovative experimental tools that can provide reliable predictions on the efficacy of drug interventions. For instance, our previous multi-center pRCT accurately predicted the lack of efficacy of baricitinib in systemic lupus [150], which was later confirmed in human trials (NCT03843125, NCT03616964) and led to the discontinuation of the trial program.

CKD is a growing global health issue, with significant economic implications and affecting the life quality of patients [3]. CKD is associated with significant morbidity and mortality, and it is a major risk factor for cardiovascular disease (CVD) and stroke [162]. CKD also has economic implications, as the cost of treating kidney failure with dialysis or transplantation is high and can be a substantial burden for individuals, families, and healthcare systems [163]. CKD screening may be critical for detecting and managing the disease at an early stage. Early diagnosis and treatment can decelerate CKD progression, diminish the likelihood of complications, and improve outcomes [164]. While high income countries started to consider CKD screening, low- and middle-income countries (LMICs) may lack the resources to provide routine screening for CKD, resulting in late diagnosis and poor outcomes [165]. Patients in these countries who have advanced CKD and do not have access to dialysis have limited treatment options, resulting in significant morbidity and mortality [166]. Addressing this issue requires a concerted effort to improve CKD treatment in LMICs. This can involve increasing access to screening and diagnostic tests, enhancing infrastructure and resources for managing CKD, and implementing community-based interventions and public health campaigns to heighten awareness [167-169]. Moreover, it is essential to investigate alternative treatment options to dialysis to offer greater chances of survival and extend the life of CKD patients [170]. The emergence of finerenone has given hope to the treatment of CKD, and its potential positive effect in combination with SGLT2 inhibitors offers new possibilities for managing CKD [141].

MRs, which are nuclear hormone receptors, have a significant role in regulating electrolyte balance and blood pressure. [117]. MRs are activated by the hormones cortisol and aldosterone, which promote stress adaptation including sodium retention and potassium excretion in the kidneys [171]. Persistent dysregulation of the aldosterone-MR system can lead to hypertension, heart failure, and other cardiovascular and kidney disorders [118]. Steroidal and non-steroidal MR antagonists have been developed as therapeutic agents to counteract the deleterious effects of aldosterone excess. The first generation of MRAs were based on the structure of aldosterone and are therefore classified as steroidal MRAs [171]. Steroidal MRAs have several advantages, including high affinity for MRs and a long half-life, which allows for once-daily dosing. However, they also have some drawbacks, including low specificity for MRs and potential for off-target effects. In recent years, non-steroidal MRAs have been developed as an alternative to steroidal MRAs [172]. Non-steroidal MRAs are designed to bind to the MR in a different way than aldosterone, which allows for greater specificity and fewer off-target effects [173].

Our results suggest that these additive proteinuric effects may translate into a significantly longer kidney lifespan. Indeed, triple therapy exponentially extended lifspan of *Col4a3*-/- mice compared to the effect size of ramipril monotherapy and the ramipril-empagliflozin combination. The distinctive mechanism of action of finerenone involves the selective blocking of aldosterone's effects on MR, potentially resulting in better outcomes for individuals with CKD, heart failure, and other medical conditions. [126]. Studies have utilized mouse models of kidney disease to investigate the potential therapeutic benefits of finerenone. A study discussed the potential benefits of using finerenone over steroidal MR antagonists such as eplerenone in treating chronic heart failure [174]. The study found that finerenone evenly across the cardiac and kidney tissues of rats and prevented heart and kidney injury in a functional and structural manner, without decreasing systemic blood pressure. Additionally, finerenone was observed to be more efficacious than eplerenone in decreasing cardiac hypertrophy, proteinuria, and plasma prohormone of brain natriuretic peptide levels. [174]. A separate study examined how finerenone affects cardiac hypertrophy in mice [175]. The researchers found that treatment with finerenone led to a notable decrease in left ventricular wall thickening induced by transverse aortic constriction and lesser increase in the calculated left ventricular mass in comparison to treatment with vehicle or steroidal MR antagonist, eplerenone. The study suggests that finerenone has positive impacts on left ventricular mass development in pressure overload [175]. A research study investigated how well finerenone can mitigate vascular remodeling and pulmonary hypertension, utilizing two rat models of severe pulmonary hypertension in preclinical settings [176]. The investigators discovered that MR is expressed excessively in both human and experimental pulmonary

arterial hypertension, and that blocking MR inhibits the proliferation of smooth muscle cells in the pulmonary artery, which is sourced from individuals with idiopathic PAH. In addition, administering curative treatments with finerenone led to a partial reversal of established pulmonary hypertension, with total pulmonary vascular resistance and vascular remodeling being reduced. According to the study, finerenone may be a viable treatment option for PAH when used alongside current therapies [176]. A research study examined how the nonsteroidal antagonist of mineralocorticoid receptor, finerenone, affects inflammation and fibrosis in the mouse model of cardiorenal disease that was induced by deoxycorticosterone acetate-salt. [177]. The results showed that finerenone treatment reduced blood pressure and renal damage and ameliorated infiltrating renal RORγt γδ-positive T cells. These findings suggest that finerenone may have potential therapeutic applications for cardiorenal disease [177]. Karoline D et al. investigated the possible direct anti-fibrotic mechanisms and impacts of finerenone and the SGLT2 inhibitor empagliflozin using two appropriate mouse models of kidney fibrosis. [178]. The outcomes revealed that administering finerenone in varying doses led to a decrease in pathological myofibroblast accumulation and collagen deposition. In finerenone-treated mice, the reduction of kidney fibrosis correlated with a decrease in the expression of plasminogen activator inhibitor-1 (PAI-1) and naked cuticle 2 (NKD2) in the kidney. On the other hand, treatment with empagliflozin had no effect on kidney myofibroblasts or collagen deposition. However, it reduced albuminuria induced by ischemia [178]. Jonatan BC et al. reported the effect finerenone on CKD progression following an episode of AKI caused by bilateral kidney ischemia/reperfusion in mice [179]. The study revealed that administering finerenone or selective ablation of myeloid mineralocorticoid receptor safeguarded against chronic dysfunction and fibrosis. Macrophages expressing M2-anti-inflammatory markers increased while the number of inflammatory macrophages decreased, which was associated with the protection against kidney fibrosis. Inhibition of MR promoted macrophage polarization towards an M2 phenotype. These findings provide evidence in favor of utilizing finerenone as a preventive measure against the development of CKD from AKI [179]. A different study examined the impact of finerenone on cardiac complications that arise due to kidney failure using a CKD mouse model [180]. Subtotal nephrectomy was used to induce CKD, and a low dose of finerenone was administered from week 4 to week 10 after the procedure. The results showed that finerenone effectively prevented both systolic and diastolic dysfunctions of the heart, as well as cardiac fibrosis, without causing any adverse effects on renal function or hyperkalemia. [180]. Our discovery bolsters the notion that the renoprotective impact of finereone is especially potent when paired with

RAS/SGLT2 inhibition. Our analysis of the tissue demonstrated a significant antifibrotic effect that aligns with the established mechanism of action for MRA.

CKD is a progressive and irreversible condition that affects the function of the kidneys. Although there is no cure for CKD, there are various treatment options available to slow its progression and manage its symptoms. One such option is drug combination therapy [121]. Drug combination therapy involves the use of two or more medications to achieve a greater therapeutic effect than what could be achieved with a single medication alone [181]. In CKD, drug combination therapy has demonstrated effectiveness in decreasing proteinuria, blood pressure, as well as the likelihood of cardiovascular events [181, 182]. One example of drug combination therapy for CKD is the use of RAAS inhibitors and diuretics [183]. RAAS inhibitors are commonly used to reduce blood pressure and proteinuria in CKD. However, these medications can sometimes cause potassium retention, which can be dangerous in patients with CKD [183]. Diuretics, such as furosemide and spironolactone, can help to remove excess potassium from the body while also reducing blood pressure [184]. By combining these medications, patients with CKD can receive the benefits of both drugs while minimizing the risks. Another example of drug combination therapy for CKD is the use of statins and ezetimibe [185]. Many CKD patients use statins to lower their cholesterol levels. However, in some patients, statins alone may not be enough to achieve optimal cholesterol levels. In these cases, adding ezetimibe, a medication that inhibits cholesterol absorption in the intestines can help to further reduce cholesterol levels[185, 186]. This combination has been proven to be efficacious in decreasing the risk of cardiovascular events in CKD patients.

While drug combination therapy can be effective in managing CKD, it is crucial to consider the possibility of drug interactions and side effects [187]. As an illustration, administering RAAS inhibitors and diuretics simultaneously may heighten the chances of dehydration and electrolyte imbalances, which could necessitate careful monitoring of both kidney function and electrolyte levels [183]. Similarly, statins and ezetimibe can increase the risk of muscle damage and liver problems and may require regular monitoring of liver function and creatine kinase levels [185]. Alongside these factors, tailoring drug therapy according to the unique requirements and medical history of each patient is imperative [188, 189]. Some patients with CKD may have other health conditions that require additional medications or limit the use of certain drugs. For example, patients with diabetes may need medications to manage their blood glucose levels, which can interact with other medications used for CKD [190]. In all, drug combination therapy is an effective treatment option for managing CKD. By combining medications with complementary mechanisms of action, patients with CKD can receive greater therapeutic benefits than what could be

achieved with a single medication alone. However, it is vital to consider potential drug interactions and and customize drug therapy to cater to the specific demands and medical background of each patient. With appropriate monitoring and management, drug combination therapy can help to slow CKD progression and improve patients' life quality with this condition.

The 2022 ADA guidelines recommend SGLT-2 inhibitors together with finerenone for the treatment of CKD associated with T2D [191]. These two medications have different mechanisms of action and combining them could lead to a synergistic impact. A study was conducted using hypertensive renin-transgenic rats with hypertension-induced end-organ damage [136]. The rats were orally administered with a single daily dosage of either a placebo, empagliflozin (3 and 10 mg per kg), finerenone (1 and 3 mg per kg), or a low-dose combination of empagliflozin and finerenone for a maximum duration of 7 weeks. Empagliflozin and finerenone exhibited dose-dependent reduction of albuminuria, however, their low-dose combination had a sustained over-additive effect. Also, both monotherapies regressed cardiac and kidney fibrosis dose-dependently, but the combination of low doses of the drugs proved to be more effective in ameliorating cardiovascular and kidney pathology. All drug therapies improved rats' survival, but the low-dose combination had a greater survival benefit over the 7-week study period [136]. Analyses of subgroup in DAPA-CKD and FIDELIO-DKD studies indicate that concomitant use of single medication did not impact the safety or effectiveness of other drugs in decreasing albuminuria and enhancing long-term clinical outcomes [138, 192]. Additionally, combining the two medications may reduce the incidence of hyperkalemia. It should be noted that the retrospective nature and constrained statistical potency impede the establishment of a conclusive causal relationship regarding the risk association. Nonetheless, the data implies that there might be advantages in combining SGLT-2 inhibitors and MRA therapy, which led to the development of randomized trials comparing combination therapy versus monotherapy. To arrive at a definitive answer to this important research question, we should await a conclusion from ongoing CONFIDENCE trial [140].

Tissue remodeling occurs in organs in response to injury and inflammation. It is a crucial factor in the progression of CKD as well as HF [193]. Similarities in tissue remodeling suggest that treatment strategies for both may be alike. Firstly, both HF and CKD show extracellular matrix (ECM) deposition leading to fibrosis, which stiffens heart and kidney tissues, impairing their function [194, 195]. ECM remodeling is regulated by cytokines, growth factors, and matrix metalloproteinases. Inhibiting these factors reduces ECM deposition and improves tissue function in both conditions [196]. Secondly, both HF and CKD are linked to inflammation, causing tissue remodeling [197]. Inflammatory cells like macrophages and T cells

enter affected tissues and release cytokines and other mediators that promote fibrosis and tissue damage. Corticosteroids and immunomodulatory agents, which are anti-inflammatory therapies, can decrease inflammation and decelerate tissue remodeling in both conditions [198]. Thirdly, both HF and CKD have an imbalance between vasoconstrictor and vasodilator factors, impairing blood flow and causing tissue hypoxia and damage [199]. Targeting the RAAS improves blood flow and reduces tissue remodeling in both conditions [200]. Last, both HF and CKD are associated with oxidative stress, causing tissue damage and remodeling [201, 202]. Excess reactive oxygen species (ROS) production leads to oxidative damage to proteins, lipids, and DNA. Antioxidant therapies like vitamin E and N-acetylcysteine reduce ROS production and slow down tissue remodeling in both conditions [203]. In total, the tissue remodeling process in HF and CKD shares several similarities, including ECM deposition, inflammation, vasoconstriction, and oxidative stress. Therefore, the treatment strategies for both conditions may be similar, targeting common pathways involved in tissue remodeling.

When it comes to combination therapy for CKD and HF, RAAS inhibitors and SGLT2 inhibitors in combination has shown promising results in reducing the risk of kidney failure and cardiovascular events. Various clinical studies have examined the effectiveness of this combination treatment, such as the EMPA-KIDNEY and DAPA-CKD trials [86, 101]. Adding MRA to the dual therapy of RAAS inhibitors and SGLT2 inhibitors has also been studied in HF patients and has been proven to further diminish the risk of cardiovascular mortality. This combination therapy has been tested in the EMPEROR-Reduced trial, which demonstrated a significant reduction in cardiovascular death and hospitalization for HF in patients with reduced ejection fraction [204]. Based on the above information, the combination therapy of RAAS inhibitors, SGLT2 inhibitors, and MRA may also be effective in reducing the risk of kidney failure and cardiovascular events in CKD patients. However, additional research is required to validate this theory and ascertain the most effective combination treatment for individuals with CKD. Our study indicate that adding MR inhibition to RAS/SGLT2 inhibition results in a synergistic and protective effect on the kidneys. This is consistent with prior small-scale studies that showed an additive effect on proteinuria in diabetic CKD patients receiving a triple therapy [138]. Another study, albeit smaller and cross-over in design, reported similar results with eplerenone as a combination partner [141]. In contrast to these preliminary studies, we have demonstrated a robust effect not only on the surrogate marker of proteinuria but also on the critical patient-oriented endpoint of time to kidney failure. This is a crucial and hardly studied efficacy endpoint, even in large clinical trials [205]. Our mechanistic studies provide further insight into the mechanism of action of the triple therapy and show that MR inhibition not only enhances the suppression of proteinuria

but also continues to suppress tubulointerstitial inflammation and fibrosis beyond what is achieved with RAS/SGLT2 inhibition alone [117, 178, 206, 207]. For example, sequential addition of the MRA spironolactone to early ramipril therapy had additive effects on kidney fibrosis in the same *Col4a3*-/- mouse model [208]. Interestingly, this dual blockade approach did not prolong kidney lifespan, probably because spironolactone caused fatal hyperkalemia in *Col4a3*-/- mice [208], not so with the non-steroidal MRA finerenone in our hands.

The interaction between inflammation and fibrosis in causing kidney injury is intricate and involves a sequence of events that can exacerbate the damage [209]. Inflammation can trigger the generation of pro-inflammatory cytokines that activate fibroblasts, resulting in the buildup of collagen and other extracellular matrix proteins. This leads to tissue scarring and fibrosis that hinders kidney function [210]. While therapies such as RAS and SGLT2 inhibitors can be beneficial in decreasing inflammation and fibrosis, they may not be adequate in completely eliminating all aspects of inflammation and fibrosis. One reason why RAS/SGLT2 inhibitors may not completely abrogate all inflammation and fibrosis is that these pathways are not the only drivers of these processes [211, 212]. While RAS is a major regulator of blood pressure and sodium balance, it also has various other functions, including promoting inflammation and fibrosis [213]. Similarly, SGLT2 inhibitors primarily work by reducing glucose reabsorption in the kidneys, but they may also have other effects on metabolic and inflammatory pathways [214]. Therefore, inhibiting these pathways may not be sufficient to completely halt all inflammation and fibrosis. Additional therapies such as MRAs, such as finerenone, may be necessary for optimal treatment. MRAs operate by blocking aldosterone, a hormone that can cause inflammation and fibrosis in the kidneys, and studies have shown that they can reduce inflammation and fibrosis in animal models of kidney disease [215, 216]. Notably, the combination of RAS/SGLT2 inhibitors and MRAs is not only additive but synergistic, resulting in more potent inhibition of inflammatory and fibrotic processes. Our bulk RNA-seq results confirm that the combination of finerenone and dual RAS/SGLT2 inhibition has a more significant inhibitory effect on inflammation and fibrosis than either therapy alone or CKD-RASi/SGLT2i and CKD-RASi treatment. Therefore, the combination of RAS/SGLT2 inhibitors and MRAs can provide better clinical outcomes for patients with kidney disease by significantly reducing inflammation and fibrosis.

The autosomal-recessive Alport syndrome in both humans and mice share many similarities, making the results from studies on RAS inhibition in *Col4a3*-/- mice a strong indicator of the potential treatment effects in human Alport nephropathy [217, 218]. Based on these similarities, we propose conducting clinical trials in patients with Alport syndrome to demonstrate the renal protective advantages of a triple therapy

approach involving RAS/SGLT2/MR inhibition. Starting therapy at an earlier stage is expected to have an even greater impact on prolonging kidney lifespan, providing a bright outlook for patients with Alport nephropathy to live several years without needing dialysis. Alport syndrome can lead to CKD and may present similarly to other forms of CKD, such as AKI-CKD transition, toxic CKD, autoimmune CKD, diabetic kidney disease, and tubulointerstitial disorders, including autosomal dominant polycystic kidney disease (ADPKD). Although the impact of the triple combination therapy on other forms of CKD is uncertain, our team retains a hopeful outlook. This optimism stems from the belief that the suppression of tubulointerstitial inflammation and fibrosis, two common factors involved in all forms of CKD, will result in an additive improvement of kidney lifespan in a majority, if not all, cases of CKD progression. While this possibility may not be entirely clear, it is a positive outlook that we hold onto.

In our study, the effect size of ramipril monotherapy was small, which we attribute to the late onset at 6 weeks in mice that succumb to uremia starting from 8 weeks of life. Our baseline tissue analysis documents glomerulosclerosis, tubular atrophy, and interstitial fibrosis at the time of therapy initiation. Indeed, the renoprotective effect of ramipril in *Col4a3*-/- mice declines with a later onset of treatment [161]. The lack of any additive effect of SGLT2 inhibition with empagliflozin should have the same reason and should not relate to insufficient exposure to empagliflozin because the presence of glucosuria documents sufficient bioactivity.

Our study has several limitations. Although *Col4a3*-/- mice are a reliable model for Alport nephropathy, it is uncertain if the findings can be applied to other forms of progressive CKD. Additionally, our data pertains only to the initiation of triple therapy during advanced stages of CKD. However, previous research suggests that greater renoprotective effects can be achieved if therapy is initiated in the early stages of CKD progression, as demonstrated by a comparison between early and late initiation of RAS inhibition [52, 161]. Moreover, we lack information on the efficacy of triple treatment for X-linked Alport syndrome, which is more prevalent than the autosomal recessive form that only constitutes 15% of cases. Cardiovascular disease was not investigated in our study on Alport syndrome, and we did not explore the synergistic mechanism at the molecular level. Furthermore, empagliflozin and finerenone monotherapy were not included in the initial preclinical RCT because RAS inhibition is the standard-of-care for CKD, including Alport nephropathy. Due to animal welfare restrictions, we evaluated uremic death in our study using a welfare scoring system, which may have resulted in some animals being scored for reasons other than uremic death, such as hyperkalemia. Despite these limitations, our study demonstrated the beneficial impact of finerenone on kidney lifespan.

Together, the combination of triple RAS/SGLT2/MR blockade has been found to significantly improve the uremia-free lifespan of *Col4a3*-/- mice, which is a critical outcome in the treatment of CKD. The "no touch" study design reduced multiple sources of bias, giving us confidence in the generalizability of the results to a comparable human trial. In particular, for human Alport syndrome, the accuracy of these results is expected to be high. Additionally, if the therapy is started earlier, it is believed to be even more effective. While the predictive accuracy may be lower for other forms of progressive CKD, the combination therapy to extend the lifespan of kidneys in CKD is a promising and achievable area of research and treatment.

7. Reference

1. Romagnani P, Remuzzi G, Glassock R, Levin A, Jager KJ, Tonelli M, Massy Z, Wanner C, Anders HJ: **Chronic kidney disease**. *Nat Rev Dis Primers* 2017, **3**:17088.
2. Webster AC, Nagler EV, Morton RL, Masson P: **Chronic Kidney Disease**. *Lancet* 2017, **389**(10075):1238-1252.
3. August P: **Chronic Kidney Disease - Another Step Forward**. *N Engl J Med* 2023, **388**(2):179-180.
4. Jager KJ, Kovesdy C, Langham R, Rosenberg M, Jha V, Zoccali C: **A single number for advocacy and communication-worldwide more than 850 million individuals have kidney diseases**. *Kidney Int* 2019, **96**(5):1048-1050.
5. Bello AK, Johnson DW, Feehally J, Harris D, Jindal K, Lunney M, Okpechi IG, Salako BL, Wiebe N, Ye F *et al*: **Global Kidney Health Atlas (GKHA): design and methods**. *Kidney Int Suppl (2011)* 2017, **7**(2):145-153.
6. **http://www.die-nephrologen.de/nieren-nierenerkrankungen-und-nierenpatienten.html** [http://www.die-nephrologen.de/nieren-nierenerkrankungen-und-nierenpatienten.html]
7. Staples A, Wong C: **Risk factors for progression of chronic kidney disease**. *Curr Opin Pediatr* 2010, **22**(2):161-169.
8. Zoccali C, Ruggenenti P, Perna A, Leonardis D, Tripepi R, Tripepi G, Mallamaci F, Remuzzi G, Group RS: **Phosphate may promote CKD progression and attenuate renoprotective effect of ACE inhibition**. *J Am Soc Nephrol* 2011, **22**(10):1923-1930.
9. Kalantar-Zadeh K, Jafar TH, Nitsch D, Neuen BL, Perkovic V: **Chronic kidney disease**. *Lancet* 2021, **398**(10302):786-802.
10. National Kidney F: **K/DOQI clinical practice guidelines for chronic kidney disease: evaluation, classification, and stratification**. *Am J Kidney Dis* 2002, **39**(2 Suppl 1):S1-266.
11. Stevens PE, Levin A, Kidney Disease: Improving Global Outcomes Chronic Kidney Disease Guideline Development Work Group M: **Evaluation and management of chronic kidney disease: synopsis of the kidney disease: improving global outcomes 2012 clinical practice guideline**. *Ann Intern Med* 2013, **158**(11):825-830.
12. Matsushita K, Ballew SH, Wang AY, Kalyesubula R, Schaeffner E, Agarwal R: **Epidemiology and risk of cardiovascular disease in populations with chronic kidney disease**. *Nat Rev Nephrol* 2022.
13. Levey AS, Eckardt KU, Tsukamoto Y, Levin A, Coresh J, Rossert J, De Zeeuw D, Hostetter TH, Lameire N, Eknoyan G: **Definition and classification of chronic kidney disease: a position statement from Kidney Disease: Improving Global Outcomes (KDIGO)**. *Kidney Int* 2005, **67**(6):2089-2100.
14. Gibson J, Fieldhouse R, Chan MMY, Sadeghi-Alavijeh O, Burnett L, Izzi V, Persikov AV, Gale DP, Storey H, Savige J *et al*: **Prevalence Estimates of Predicted Pathogenic COL4A3-COL4A5 Variants in a Population Sequencing Database and Their Implications for Alport Syndrome**. *J Am Soc Nephrol* 2021, **32**(9):2273-2290.
15. Kashtan CE: **Alport Syndrome: Achieving Early Diagnosis and Treatment**. *Am J Kidney Dis* 2021, **77**(2):272-279.
16. Lagona E, Tsartsali L, Kostaridou S, Skiathitou A, Georgaki E, Sotsiou F: **Skin biopsy for the diagnosis of Alport syndrome**. *Hippokratia* 2008, **12**(2):116-118.
17. Naylor RW, Morais M, Lennon R: **Complexities of the glomerular basement membrane**. *Nat Rev Nephrol* 2021, **17**(2):112-127.
18. Omachi K, Miner JH: **Alport Syndrome Therapeutics: Ready for Prime-Time Players**. *Trends Pharmacol Sci* 2019, **40**(11):803-806.
19. Yamamura T, Horinouchi T, Adachi T, Terakawa M, Takaoka Y, Omachi K, Takasato M, Takaishi K, Shoji T, Onishi Y *et al*: **Development of an exon skipping therapy for X-linked Alport syndrome with truncating variants in COL4A5**. *Nat Commun* 2020, **11**(1):2777.
20. Hertz JM, Thomassen M, Storey H, Flinter F: **Clinical utility gene card for: Alport syndrome - update 2014**. *Eur J Hum Genet* 2015, **23**(9).

21. Yuan X, Su Q, Wang H, Shi S, Liu L, Lv J, Wang S, Zhu L, Zhang H: **Genetic Variants of the COL4A3 , COL4A4 , and COL4A5 Genes Contribute to Thinned Glomerular Basement Membrane Lesions in Sporadic IgA Nephropathy Patients**. *J Am Soc Nephrol* 2023, **34**(1):132-144.
22. Nozu K, Nakanishi K, Abe Y, Udagawa T, Okada S, Okamoto T, Kaito H, Kanemoto K, Kobayashi A, Tanaka E *et al*: **A review of clinical characteristics and genetic backgrounds in Alport syndrome**. *Clin Exp Nephrol* 2019, **23**(2):158-168.
23. Jais JP, Knebelmann B, Giatras I, Marchi M, Rizzoni G, Renieri A, Weber M, Gross O, Netzer KO, Flinter F *et al*: **X-linked Alport syndrome: natural history in 195 families and genotype- phenotype correlations in males**. *J Am Soc Nephrol* 2000, **11**(4):649-657.
24. Jais JP, Knebelmann B, Giatras I, De Marchi M, Rizzoni G, Renieri A, Weber M, Gross O, Netzer KO, Flinter F *et al*: **X-linked Alport syndrome: natural history and genotype-phenotype correlations in girls and women belonging to 195 families: a "European Community Alport Syndrome Concerted Action" study**. *J Am Soc Nephrol* 2003, **14**(10):2603-2610.
25. Vos P, Zietse R, van Geel M, Brooks AS, Cransberg K: **Diagnosing Alport Syndrome: Lessons from the Pediatric Ward**. *Nephron* 2018, **140**(3):203-210.
26. Voskarides K, Pierides A, Deltas C: **On 'Incidence of renal failure and nephroprotection by RAAS inhibition in heterozygous carriers of X-chromosomal and autosomal recessive Alport mutations'**. *Kidney Int* 2013, **83**(2):331.
27. Stock J, Kuenanz J, Glonke N, Sonntag J, Frese J, Tonshoff B, Hocker B, Hoppe B, Feldkotter M, Pape L *et al*: **Prospective study on the potential of RAAS blockade to halt renal disease in Alport syndrome patients with heterozygous mutations**. *Pediatr Nephrol* 2017, **32**(1):131-137.
28. Daga S, Ding J, Deltas C, Savige J, Lipska-Zietkiewicz BS, Hoefele J, Flinter F, Gale DP, Aksenova M, Kai H *et al*: **The 2019 and 2021 International Workshops on Alport Syndrome**. *Eur J Hum Genet* 2022, **30**(5):507-516.
29. Savige J, Lipska-Zietkiewicz BS, Watson E, Hertz JM, Deltas C, Mari F, Hilbert P, Plevova P, Byers P, Cerkauskaite A *et al*: **Guidelines for Genetic Testing and Management of Alport Syndrome**. *Clin J Am Soc Nephrol* 2022, **17**(1):143-154.
30. Oohashi T, Naito I, Ueki Y, Yamatsuji T, Permpoon R, Tanaka N, Naomoto Y, Ninomiya Y: **Clonal overgrowth of esophageal smooth muscle cells in diffuse leiomyomatosis-Alport syndrome caused by partial deletion in COL4A5 and COL4A6 genes**. *Matrix Biol* 2011, **30**(1):3-8.
31. Rost S, Bach E, Neuner C, Nanda I, Dysek S, Bittner RE, Keller A, Bartsch O, Mlynski R, Haaf T *et al*: **Novel form of X-linked nonsyndromic hearing loss with cochlear malformation caused by a mutation in the type IV collagen gene COL4A6**. *Eur J Hum Genet* 2014, **22**(2):208-215.
32. Zhang Y, Bockhaus J, Wang F, Wang S, Rubel D, Gross O, Ding J: **Genotype-phenotype correlations and nephroprotective effects of RAAS inhibition in patients with autosomal recessive Alport syndrome**. *Pediatr Nephrol* 2021, **36**(9):2719-2730.
33. Matthaiou A, Poulli T, Deltas C: **Prevalence of clinical, pathological and molecular features of glomerular basement membrane nephropathy caused by COL4A3 or COL4A4 mutations: a systematic review**. *Clin Kidney J* 2020, **13**(6):1025-1036.
34. Lee JM, Nozu K, Choi DE, Kang HG, Ha IS, Cheong HI: **Features of Autosomal Recessive Alport Syndrome: A Systematic Review**. *J Clin Med* 2019, **8**(2).
35. Kamiyoshi N, Nozu K, Fu XJ, Morisada N, Nozu Y, Ye MJ, Imafuku A, Miura K, Yamamura T, Minamikawa S *et al*: **Genetic, Clinical, and Pathologic Backgrounds of Patients with Autosomal Dominant Alport Syndrome**. *Clin J Am Soc Nephrol* 2016, **11**(8):1441-1449.
36. Sa MJ, Fieremans N, de Brouwer AP, Sousa R, e Costa FT, Brito MJ, Carvalho F, Rodrigues M, de Sousa FT, Felgueiras J *et al*: **Deletion of the 5'exons of COL4A6 is not needed for the development of diffuse leiomyomatosis in patients with Alport syndrome**. *J Med Genet* 2013, **50**(11):745-753.

37. Nozu K, Minamikawa S, Yamada S, Oka M, Yanagita M, Morisada N, Fujinaga S, Nagano C, Gotoh Y, Takahashi E *et al*: **Characterization of contiguous gene deletions in COL4A6 and COL4A5 in Alport syndrome-diffuse leiomyomatosis**. *J Hum Genet* 2017, **62**(7):733-735.
38. Buzza M, Dagher H, Wang YY, Wilson D, Babon JJ, Cotton RG, Savige J: **Mutations in the COL4A4 gene in thin basement membrane disease**. *Kidney Int* 2003, **63**(2):447-453.
39. Hu Y, Li W, Tian L, Fu S, Min Y, Liu J, Xiong F: **Case Report: Identification of a Novel Heterozygous Missense Mutation in COL4A3 Gene Causing Variable Phenotypes in an Autosomal-Dominant Alport Syndrome Family**. *Front Genet* 2022, **13**:839212.
40. Funk SD, Lin MH, Miner JH: **Alport syndrome and Pierson syndrome: Diseases of the glomerular basement membrane**. *Matrix Biol* 2018, **71-72**:250-261.
41. Kruegel J, Rubel D, Gross O: **Alport syndrome--insights from basic and clinical research**. *Nat Rev Nephrol* 2013, **9**(3):170-178.
42. Meehan DT, Delimont D, Cheung L, Zallocchi M, Sansom SC, Holzclaw JD, Rao V, Cosgrove D: **Biomechanical strain causes maladaptive gene regulation, contributing to Alport glomerular disease**. *Kidney Int* 2009, **76**(9):968-976.
43. Cosgrove D: **Glomerular pathology in Alport syndrome: a molecular perspective**. *Pediatr Nephrol* 2012, **27**(6):885-890.
44. Cosgrove D, Liu S: **Collagen IV diseases: A focus on the glomerular basement membrane in Alport syndrome**. *Matrix Biol* 2017, **57-58**:45-54.
45. Bae EH, Fang F, Williams VR, Konvalinka A, Zhou X, Patel VB, Song X, John R, Oudit GY, Pei Y *et al*: **Murine recombinant angiotensin-converting enzyme 2 attenuates kidney injury in experimental Alport syndrome**. *Kidney Int* 2017, **91**(6):1347-1361.
46. Choi HS, Kim IJ, Kim CS, Ma SK, Scholey JW, Kim SW, Bae EH: **Angiotensin-[1-7] attenuates kidney injury in experimental Alport syndrome**. *Sci Rep* 2020, **10**(1):4225.
47. Heidet L, Gubler MC: **The renal lesions of Alport syndrome**. *J Am Soc Nephrol* 2009, **20**(6):1210-1215.
48. Kashtan CE, Ding J, Gregory M, Gross O, Heidet L, Knebelmann B, Rheault M, Licht C, Alport Syndrome Research C: **Clinical practice recommendations for the treatment of Alport syndrome: a statement of the Alport Syndrome Research Collaborative**. *Pediatr Nephrol* 2013, **28**(1):5-11.
49. Bomback AS, Klemmer PJ: **The incidence and implications of aldosterone breakthrough**. *Nat Clin Pract Nephrol* 2007, **3**(9):486-492.
50. Sato A, Saruta T: **Aldosterone breakthrough during angiotensin-converting enzyme inhibitor therapy**. *Am J Hypertens* 2003, **16**(9 Pt 1):781-788.
51. Ku E, Campese VM: **Role of aldosterone in the progression of chronic kidney disease and potential use of aldosterone blockade in children**. *Pediatr Nephrol* 2009, **24**(12):2301-2307.
52. Gross O, Licht C, Anders HJ, Hoppe B, Beck B, Tonshoff B, Hocker B, Wygoda S, Ehrich JH, Pape L *et al*: **Early angiotensin-converting enzyme inhibition in Alport syndrome delays renal failure and improves life expectancy**. *Kidney Int* 2012, **81**(5):494-501.
53. Temme J, Kramer A, Jager KJ, Lange K, Peters F, Muller GA, Kramar R, Heaf JG, Finne P, Palsson R *et al*: **Outcomes of male patients with Alport syndrome undergoing renal replacement therapy**. *Clin J Am Soc Nephrol* 2012, **7**(12):1969-1976.
54. Sarafidis PA, Bakris GL: **Renin-angiotensin blockade and kidney disease**. *Lancet* 2008, **372**(9638):511-512.
55. Wolf G, Ritz E: **Combination therapy with ACE inhibitors and angiotensin II receptor blockers to halt progression of chronic renal disease: pathophysiology and indications**. *Kidney Int* 2005, **67**(3):799-812.
56. Brenner BM, Cooper ME, de Zeeuw D, Keane WF, Mitch WE, Parving HH, Remuzzi G, Snapinn SM, Zhang Z, Shahinfar S *et al*: **Effects of losartan on renal and cardiovascular outcomes in patients with type 2 diabetes and nephropathy**. *N Engl J Med* 2001, **345**(12):861-869.

57. Group TG: **Randomised placebo-controlled trial of effect of ramipril on decline in glomerular filtration rate and risk of terminal renal failure in proteinuric, non-diabetic nephropathy. The GISEN Group (Gruppo Italiano di Studi Epidemiologici in Nefrologia)**. *Lancet* 1997, **349**(9069):1857-1863.
58. Dahlof B, Devereux RB, Kjeldsen SE, Julius S, Beevers G, de Faire U, Fyhrquist F, Ibsen H, Kristiansson K, Lederballe-Pedersen O *et al*: **Cardiovascular morbidity and mortality in the Losartan Intervention For Endpoint reduction in hypertension study (LIFE): a randomised trial against atenolol**. *Lancet* 2002, **359**(9311):995-1003.
59. Lambers Heerspink HJ, de Zeeuw D: **Novel drugs and intervention strategies for the treatment of chronic kidney disease**. *Br J Clin Pharmacol* 2013, **76**(4):536-550.
60. Shabaka A, Cases-Corona C, Fernandez-Juarez G: **Therapeutic Insights in Chronic Kidney Disease Progression**. *Front Med (Lausanne)* 2021, **8**:645187.
61. Kunz R, Friedrich C, Wolbers M, Mann JF: **Meta-analysis: effect of monotherapy and combination therapy with inhibitors of the renin angiotensin system on proteinuria in renal disease**. *Ann Intern Med* 2008, **148**(1):30-48.
62. Investigators O, Yusuf S, Teo KK, Pogue J, Dyal L, Copland I, Schumacher H, Dagenais G, Sleight P, Anderson C: **Telmisartan, ramipril, or both in patients at high risk for vascular events**. *N Engl J Med* 2008, **358**(15):1547-1559.
63. Mann JF, Schmieder RE, McQueen M, Dyal L, Schumacher H, Pogue J, Wang X, Maggioni A, Budaj A, Chaithiraphan S *et al*: **Renal outcomes with telmisartan, ramipril, or both, in people at high vascular risk (the ONTARGET study): a multicentre, randomised, double-blind, controlled trial**. *Lancet* 2008, **372**(9638):547-553.
64. Fried LF, Duckworth W, Zhang JH, O'Connor T, Brophy M, Emanuele N, Huang GD, McCullough PA, Palevsky PM, Seliger S *et al*: **Design of combination angiotensin receptor blocker and angiotensin-converting enzyme inhibitor for treatment of diabetic nephropathy (VA NEPHRON-D)**. *Clin J Am Soc Nephrol* 2009, **4**(2):361-368.
65. Motrapu M, Swiderska MK, Mesas I, Marschner JA, Lei Y, Martinez Valenzuela L, Fu J, Lee K, Angelotti ML, Antonelli G *et al*: **Drug Testing for Residual Progression of Diabetic Kidney Disease in Mice Beyond Therapy with Metformin, Ramipril, and Empagliflozin**. *J Am Soc Nephrol* 2020, **31**(8):1729-1745.
66. Luyckx VA, Rule AD, Tuttle KR, Delanaye P, Liapis H, Gandjour A, Romagnani P, Anders HJ: **Nephron overload as a therapeutic target to maximize kidney lifespan**. *Nat Rev Nephrol* 2022, **18**(3):171-183.
67. Remuzzi G, Benigni A, Remuzzi A: **Mechanisms of progression and regression of renal lesions of chronic nephropathies and diabetes**. *J Clin Invest* 2006, **116**(2):288-296.
68. Zhang Q, Shao B, Tong Z, Ouyang Q, Wang Y, Xu G, Li S, Li H: **A phase Ib study of camrelizumab in combination with apatinib and fuzuloparib in patients with recurrent or metastatic triple-negative breast cancer**. *BMC Med* 2022, **20**(1):321.
69. Liu H, Li Y, Yao Y, Chen K, Gan J: **Meta-Analysis of Efficacy and Safety of Karelizumab Combined with Apatinib in the Treatment of Advanced Gastric Cancer**. *Dis Markers* 2022, **2022**:6971717.
70. Dustan HP, Roccella EJ, Garrison HH: **Controlling hypertension. A research success story**. *Arch Intern Med* 1996, **156**(17):1926-1935.
71. Atkinson MA, Roep BO, Posgai A, Wheeler DCS, Peakman M: **The challenge of modulating beta-cell autoimmunity in type 1 diabetes**. *Lancet Diabetes Endocrinol* 2019, **7**(1):52-64.
72. Qu J, Zhang H, Rao C, Chen S, Zhao Y, Sun H, Song Y, Liu S, Wang L, Feng W *et al*: **Dual Antiplatelet Therapy with Clopidogrel and Aspirin Versus Aspirin Monotherapy in Patients Undergoing Coronary Artery Bypass Graft Surgery**. *J Am Heart Assoc* 2021, **10**(11):e020413.
73. Lewis EJ, Hunsicker LG, Clarke WR, Berl T, Pohl MA, Lewis JB, Ritz E, Atkins RC, Rohde R, Raz I *et al*: **Renoprotective effect of the angiotensin-receptor antagonist irbesartan in patients with nephropathy due**

to type 2 diabetes. *N Engl J Med* 2001, **345**(12):851-860.

74. Parving HH, Lehnert H, Brochner-Mortensen J, Gomis R, Andersen S, Arner P, Irbesartan in Patients with Type D, Microalbuminuria Study G: **The effect of irbesartan on the development of diabetic nephropathy in patients with type 2 diabetes**. *N Engl J Med* 2001, **345**(12):870-878.
75. Wright JT, Jr., Bakris G, Greene T, Agodoa LY, Appel LJ, Charleston J, Cheek D, Douglas-Baltimore JG, Gassman J, Glassock R *et al*: **Effect of blood pressure lowering and antihypertensive drug class on progression of hypertensive kidney disease: results from the AASK trial**. *JAMA* 2002, **288**(19):2421-2431.
76. Fried LF, Emanuele N, Zhang JH, Brophy M, Conner TA, Duckworth W, Leehey DJ, McCullough PA, O'Connor T, Palevsky PM *et al*: **Combined angiotensin inhibition for the treatment of diabetic nephropathy**. *N Engl J Med* 2013, **369**(20):1892-1903.
77. Parving HH, Brenner BM, McMurray JJ, de Zeeuw D, Haffner SM, Solomon SD, Chaturvedi N, Persson F, Desai AS, Nicolaides M *et al*: **Cardiorenal end points in a trial of aliskiren for type 2 diabetes**. *N Engl J Med* 2012, **367**(23):2204-2213.
78. Fernandez Juarez G, Luno J, Barrio V, de Vinuesa SG, Praga M, Goicoechea M, Cachofeiro V, Nieto J, Fernandez Vega F, Tato A *et al*: **Effect of dual blockade of the renin-angiotensin system on the progression of type 2 diabetic nephropathy: a randomized trial**. *Am J Kidney Dis* 2013, **61**(2):211-218.
79. Rahman M, Ford CE, Cutler JA, Davis BR, Piller LB, Whelton PK, Wright JT, Jr., Barzilay JI, Brown CD, Colon PJ, Sr. *et al*: **Long-term renal and cardiovascular outcomes in Antihypertensive and Lipid-Lowering Treatment to Prevent Heart Attack Trial (ALLHAT) participants by baseline estimated GFR**. *Clin J Am Soc Nephrol* 2012, **7**(6):989-1002.
80. Vasilakou D, Karagiannis T, Athanasiadou E, Mainou M, Liakos A, Bekiari E, Sarigianni M, Matthews DR, Tsapas A: **Sodium-glucose cotransporter 2 inhibitors for type 2 diabetes: a systematic review and meta-analysis**. *Ann Intern Med* 2013, **159**(4):262-274.
81. Shubrook JH, Bokaie BB, Adkins SE: **Empagliflozin in the treatment of type 2 diabetes: evidence to date**. *Drug Des Devel Ther* 2015, **9**:5793-5803.
82. Usman MS, Siddiqi TJ, Memon MM, Khan MS, Rawasia WF, Talha Ayub M, Sreenivasan J, Golzar Y: **Sodium-glucose co-transporter 2 inhibitors and cardiovascular outcomes: A systematic review and meta-analysis**. *Eur J Prev Cardiol* 2018, **25**(5):495-502.
83. Bonora BM, Avogaro A, Fadini GP: **Extraglycemic Effects of SGLT2 Inhibitors: A Review of the Evidence**. *Diabetes Metab Syndr Obes* 2020, **13**:161-174.
84. American Diabetes Association Professional Practice C, Draznin B, Aroda VR, Bakris G, Benson G, Brown FM, Freeman R, Green J, Huang E, Isaacs D *et al*: **9. Pharmacologic Approaches to Glycemic Treatment: Standards of Medical Care in Diabetes-2022**. *Diabetes Care* 2022, **45**(Suppl 1):S125-S143.
85. van der Aart-van der Beek AB, de Boer RA, Heerspink HJL: **Kidney and heart failure outcomes associated with SGLT2 inhibitor use**. *Nat Rev Nephrol* 2022, **18**(5):294-306.
86. The E-KCG, Herrington WG, Staplin N, Wanner C, Green JB, Hauske SJ, Emberson JR, Preiss D, Judge P, Mayne KJ *et al*: **Empagliflozin in Patients with Chronic Kidney Disease**. *N Engl J Med* 2023, **388**(2):117-127.
87. DeFronzo RA, Reeves WB, Awad AS: **Pathophysiology of diabetic kidney disease: impact of SGLT2 inhibitors**. *Nat Rev Nephrol* 2021, **17**(5):319-334.
88. Brown E, Heerspink HJL, Cuthbertson DJ, Wilding JPH: **SGLT2 inhibitors and GLP-1 receptor agonists: established and emerging indications**. *Lancet* 2021, **398**(10296):262-276.
89. Liu J, Tian J, Sodhi K, Shapiro JI: **The Na/K-ATPase Signaling and SGLT2 Inhibitor-Mediated Cardiorenal Protection: A Crossed Road?** *J Membr Biol* 2021, **254**(5-6):513-529.
90. Anders HJ, Davis JM, Thurau K: **Nephron Protection in Diabetic Kidney Disease**. *N Engl J Med* 2016, **375**(21):2096-2098.
91. Packer M: **Mechanisms Leading to Differential Hypoxia-Inducible Factor Signaling in the Diabetic Kidney:**

Modulation by SGLT2 Inhibitors and Hypoxia Mimetics. *Am J Kidney Dis* 2021, **77**(2):280-286.

92. Vallon V, Thomson SC: **The tubular hypothesis of nephron filtration and diabetic kidney disease**. *Nat Rev Nephrol* 2020, **16**(6):317-336.
93. Ravindran S, Munusamy S: **Renoprotective mechanisms of sodium-glucose co-transporter 2 (SGLT2) inhibitors against the progression of diabetic kidney disease**. *J Cell Physiol* 2022, **237**(2):1182-1205.
94. Fonseca-Correa JI, Correa-Rotter R: **Sodium-Glucose Cotransporter 2 Inhibitors Mechanisms of Action: A Review**. *Front Med (Lausanne)* 2021, **8**:777861.
95. Wanner C, Inzucchi SE, Lachin JM, Fitchett D, von Eynatten M, Mattheus M, Johansen OE, Woerle HJ, Broedl UC, Zinman B *et al*: **Empagliflozin and Progression of Kidney Disease in Type 2 Diabetes**. *N Engl J Med* 2016, **375**(4):323-334.
96. Neal B, Perkovic V, Mahaffey KW, de Zeeuw D, Fulcher G, Erondu N, Shaw W, Law G, Desai M, Matthews DR *et al*: **Canagliflozin and Cardiovascular and Renal Events in Type 2 Diabetes**. *N Engl J Med* 2017, **377**(7):644-657.
97. Mosenzon O, Wiviott SD, Cahn A, Rozenberg A, Yanuv I, Goodrich EL, Murphy SA, Heerspink HJL, Zelniker TA, Dwyer JP *et al*: **Effects of dapagliflozin on development and progression of kidney disease in patients with type 2 diabetes: an analysis from the DECLARE-TIMI 58 randomised trial**. *Lancet Diabetes Endocrinol* 2019, **7**(8):606-617.
98. Perkovic V, Jardine MJ, Neal B, Bompoint S, Heerspink HJL, Charytan DM, Edwards R, Agarwal R, Bakris G, Bull S *et al*: **Canagliflozin and Renal Outcomes in Type 2 Diabetes and Nephropathy**. *N Engl J Med* 2019, **380**(24):2295-2306.
99. Heerspink HJL, Karasik A, Thuresson M, Melzer-Cohen C, Chodick G, Khunti K, Wilding JPH, Garcia Rodriguez LA, Cea-Soriano L, Kohsaka S *et al*: **Kidney outcomes associated with use of SGLT2 inhibitors in real-world clinical practice (CVD-REAL 3): a multinational observational cohort study**. *Lancet Diabetes Endocrinol* 2020, **8**(1):27-35.
100. Heerspink HJL, Stefansson BV, Correa-Rotter R, Chertow GM, Greene T, Hou FF, Mann JFE, McMurray JJV, Lindberg M, Rossing P *et al*: **Dapagliflozin in Patients with Chronic Kidney Disease**. *N Engl J Med* 2020, **383**(15):1436-1446.
101. Wheeler DC, Stefansson BV, Jongs N, Chertow GM, Greene T, Hou FF, McMurray JJV, Correa-Rotter R, Rossing P, Toto RD *et al*: **Effects of dapagliflozin on major adverse kidney and cardiovascular events in patients with diabetic and non-diabetic chronic kidney disease: a prespecified analysis from the DAPA-CKD trial**. *Lancet Diabetes Endocrinol* 2021, **9**(1):22-31.
102. Zou H, Zhou B, Xu G: **SGLT2 inhibitors: a novel choice for the combination therapy in diabetic kidney disease**. *Cardiovasc Diabetol* 2017, **16**(1):65.
103. Kojima N, Williams JM, Takahashi T, Miyata N, Roman RJ: **Effects of a new SGLT2 inhibitor, luseogliflozin, on diabetic nephropathy in T2DN rats**. *J Pharmacol Exp Ther* 2013, **345**(3):464-472.
104. Kojima N, Williams JM, Slaughter TN, Kato S, Takahashi T, Miyata N, Roman RJ: **Renoprotective effects of combined SGLT2 and ACE inhibitor therapy in diabetic Dahl S rats**. *Physiol Rep* 2015, **3**(7).
105. Heerspink HJ, Johnsson E, Gause-Nilsson I, Cain VA, Sjostrom CD: **Dapagliflozin reduces albuminuria in patients with diabetes and hypertension receiving renin-angiotensin blockers**. *Diabetes Obes Metab* 2016, **18**(6):590-597.
106. Weber MA, Mansfield TA, Alessi F, Iqbal N, Parikh S, Ptaszynska A: **Effects of dapagliflozin on blood pressure in hypertensive diabetic patients on renin-angiotensin system blockade**. *Blood Press* 2016, **25**(2):93-103.
107. Weber MA, Mansfield TA, Cain VA, Iqbal N, Parikh S, Ptaszynska A: **Blood pressure and glycaemic effects of dapagliflozin versus placebo in patients with type 2 diabetes on combination antihypertensive therapy: a randomised, double-blind, placebo-controlled, phase 3 study**. *Lancet Diabetes Endocrinol* 2016, **4**(3):211-220.

108. Sha S, Polidori D, Heise T, Natarajan J, Farrell K, Wang SS, Sica D, Rothenberg P, Plum-Morschel L: **Effect of the sodium glucose co-transporter 2 inhibitor canagliflozin on plasma volume in patients with type 2 diabetes mellitus**. *Diabetes Obes Metab* 2014, **16**(11):1087-1095.
109. Burrell LM, Johnston CI, Tikellis C, Cooper ME: **ACE2, a new regulator of the renin-angiotensin system**. *Trends Endocrinol Metab* 2004, **15**(4):166-169.
110. Tojo A, Hatakeyama S, Kinugasa S, Nangaku M: **Angiotensin receptor blocker telmisartan suppresses renal gluconeogenesis during starvation**. *Diabetes Metab Syndr Obes* 2015, **8**:103-113.
111. Agarwal R, Anker SD, Bakris G, Filippatos G, Pitt B, Rossing P, Ruilope L, Gebel M, Kolkhof P, Nowack C *et al*: **Investigating new treatment opportunities for patients with chronic kidney disease in type 2 diabetes: the role of finerenone**. *Nephrol Dial Transplant* 2022, **37**(6):1014-1023.
112. Bauersachs J, Jaisser F, Toto R: **Mineralocorticoid receptor activation and mineralocorticoid receptor antagonist treatment in cardiac and renal diseases**. *Hypertension* 2015, **65**(2):257-263.
113. Brown NJ: **Contribution of aldosterone to cardiovascular and renal inflammation and fibrosis**. *Nat Rev Nephrol* 2013, **9**(8):459-469.
114. Gomez-Sanchez E, Gomez-Sanchez CE: **The multifaceted mineralocorticoid receptor**. *Compr Physiol* 2014, **4**(3):965-994.
115. Buonafine M, Bonnard B, Jaisser F: **Mineralocorticoid Receptor and Cardiovascular Disease**. *Am J Hypertens* 2018, **31**(11):1165-1174.
116. Barrera-Chimal J, Girerd S, Jaisser F: **Mineralocorticoid receptor antagonists and kidney diseases: pathophysiological basis**. *Kidney Int* 2019, **96**(2):302-319.
117. Agarwal R, Kolkhof P, Bakris G, Bauersachs J, Haller H, Wada T, Zannad F: **Steroidal and non-steroidal mineralocorticoid receptor antagonists in cardiorenal medicine**. *Eur Heart J* 2021, **42**(2):152-161.
118. Pandey AK, Bhatt DL, Cosentino F, Marx N, Rotstein O, Pitt B, Pandey A, Butler J, Verma S: **Non-steroidal mineralocorticoid receptor antagonists in cardiorenal disease**. *Eur Heart J* 2022, **43**(31):2931-2945.
119. Beldhuis IE, Myhre PL, Claggett B, Damman K, Fang JC, Lewis EF, O'Meara E, Pitt B, Shah SJ, Voors AA *et al*: **Efficacy and Safety of Spironolactone in Patients With HFpEF and Chronic Kidney Disease**. *JACC Heart Fail* 2019, **7**(1):25-32.
120. Lerma EV, Wilson DJ: **Finerenone: a mineralocorticoid receptor antagonist for the treatment of chronic kidney disease associated with type 2 diabetes**. *Expert Rev Clin Pharmacol* 2022, **15**(5):501-513.
121. Kolkhof P, Joseph A, Kintscher U: **Nonsteroidal mineralocorticoid receptor antagonism for cardiovascular and renal disorders - New perspectives for combination therapy**. *Pharmacol Res* 2021, **172**:105859.
122. Duggan S: **Esaxerenone: First Global Approval**. *Drugs* 2019, **79**(4):477-481.
123. Frampton JE: **Finerenone: First Approval**. *Drugs* 2021, **81**(15):1787-1794.
124. Gonzalez-Juanatey JR, Gorriz JL, Ortiz A, Valle A, Soler MJ, Facila L: **Cardiorenal benefits of finerenone: protecting kidney and heart**. *Ann Med* 2023, **55**(1):502-513.
125. Rossing P, Agarwal R, Anker SD, Filippatos G, Pitt B, Ruilope LM, Fonseca V, Umpierrez GE, Caramori ML, Joseph A *et al*: **Finerenone in patients across the spectrum of chronic kidney disease and type 2 diabetes by glucagon-like peptide-1 receptor agonist use**. *Diabetes Obes Metab* 2023, **25**(2):407-416.
126. Filippatos G, Anker SD, August P, Coats AJS, Januzzi JL, Mankovsky B, Rossing P, Ruilope LM, Pitt B, Sarafidis P *et al*: **Finerenone and effects on mortality in chronic kidney disease and type 2 diabetes: a FIDELITY analysis**. *Eur Heart J Cardiovasc Pharmacother* 2023, **9**(2):183-191.
127. Filippatos G, Pitt B, Agarwal R, Farmakis D, Ruilope LM, Rossing P, Bauersachs J, Mentz RJ, Kolkhof P, Scott C *et al*: **Finerenone in patients with chronic kidney disease and type 2 diabetes with and without heart failure: a prespecified subgroup analysis of the FIDELIO-DKD trial**. *Eur J Heart Fail* 2022, **24**(6):996-1005.
128. Fu EL, Kutz A, Desai RJ: **Finerenone in chronic kidney disease and type 2 diabetes: the known and the unknown**. *Kidney Int* 2023, **103**(1):30-33.

129. Kolkhof P, Barfacker L: **30 YEARS OF THE MINERALOCORTICOID RECEPTOR: Mineralocorticoid receptor antagonists: 60 years of research and development**. *J Endocrinol* 2017, **234**(1):T125-T140.
130. Le Billan F, Perrot J, Carceller E, Travers S, Viengchareun S, Kolkhof P, Lombes M, Fagart J: **Antagonistic effects of finerenone and spironolactone on the aldosterone-regulated transcriptome of human kidney cells**. *FASEB J* 2021, **35**(2):e21314.
131. Pitt B, Kober L, Ponikowski P, Gheorghiade M, Filippatos G, Krum H, Nowack C, Kolkhof P, Kim SY, Zannad F: **Safety and tolerability of the novel non-steroidal mineralocorticoid receptor antagonist BAY 94-8862 in patients with chronic heart failure and mild or moderate chronic kidney disease: a randomized, double-blind trial**. *Eur Heart J* 2013, **34**(31):2453-2463.
132. Bakris GL, Agarwal R, Chan JC, Cooper ME, Gansevoort RT, Haller H, Remuzzi G, Rossing P, Schmieder RE, Nowack C *et al*: **Effect of Finerenone on Albuminuria in Patients With Diabetic Nephropathy: A Randomized Clinical Trial**. *JAMA* 2015, **314**(9):884-894.
133. Filippatos G, Anker SD, Bohm M, Gheorghiade M, Kober L, Krum H, Maggioni AP, Ponikowski P, Voors AA, Zannad F *et al*: **A randomized controlled study of finerenone vs. eplerenone in patients with worsening chronic heart failure and diabetes mellitus and/or chronic kidney disease**. *Eur Heart J* 2016, **37**(27):2105-2114.
134. Bakris GL, Agarwal R, Anker SD, Pitt B, Ruilope LM, Rossing P, Kolkhof P, Nowack C, Schloemer P, Joseph A *et al*: **Effect of Finerenone on Chronic Kidney Disease Outcomes in Type 2 Diabetes**. *N Engl J Med* 2020, **383**(23):2219-2229.
135. Pitt B, Filippatos G, Agarwal R, Anker SD, Bakris GL, Rossing P, Joseph A, Kolkhof P, Nowack C, Schloemer P *et al*: **Cardiovascular Events with Finerenone in Kidney Disease and Type 2 Diabetes**. *N Engl J Med* 2021, **385**(24):2252-2263.
136. Kolkhof P, Hartmann E, Freyberger A, Pavkovic M, Mathar I, Sandner P, Droebner K, Joseph A, Huser J, Eitner F: **Effects of Finerenone Combined with Empagliflozin in a Model of Hypertension-Induced End-Organ Damage**. *Am J Nephrol* 2021, **52**(8):642-652.
137. Agarwal R, Filippatos G, Pitt B, Anker SD, Rossing P, Joseph A, Kolkhof P, Nowack C, Gebel M, Ruilope LM *et al*: **Cardiovascular and kidney outcomes with finerenone in patients with type 2 diabetes and chronic kidney disease: the FIDELITY pooled analysis**. *Eur Heart J* 2022, **43**(6):474-484.
138. Rossing P, Filippatos G, Agarwal R, Anker SD, Pitt B, Ruilope LM, Chan JCN, Kooy A, McCafferty K, Schernthaner G *et al*: **Finerenone in Predominantly Advanced CKD and Type 2 Diabetes With or Without Sodium-Glucose Cotransporter-2 Inhibitor Therapy**. *Kidney Int Rep* 2022, **7**(1):36-45.
139. Rossing P, Agarwal R, Anker SD, Filippatos G, Pitt B, Ruilope LM, Amod A, Marre M, Joseph A, Lage A *et al*: **Efficacy and safety of finerenone in patients with chronic kidney disease and type 2 diabetes by GLP-1RA treatment: A subgroup analysis from the FIDELIO-DKD trial**. *Diabetes Obes Metab* 2022, **24**(1):125-134.
140. Green JB, Mottl AK, Bakris G, Heerspink HJL, Mann JFE, McGill JB, Nangaku M, Rossing P, Scott C, Gay A *et al*: **Design of the COmbinatioN effect of FInerenone anD EmpagliflozIN in participants with chronic kidney disease and type 2 diabetes using an UACR Endpoint study (CONFIDENCE)**. *Nephrol Dial Transplant* 2022.
141. Provenzano M, Puchades MJ, Garofalo C, Jongs N, D'Marco L, Andreucci M, De Nicola L, Gorriz JL, Heerspink HJL, group R-s *et al*: **Albuminuria-Lowering Effect of Dapagliflozin, Eplerenone, and Their Combination in Patients with Chronic Kidney Disease: A Randomized Crossover Clinical Trial**. *J Am Soc Nephrol* 2022, **33**(8):1569-1580.
142. Nangaku M, Fogo AB: **Does a preclinical randomized controlled trial, pRCT, resolve the gap between animal studies and human trials?** *Kidney Int* 2021, **99**(6):1262-1264.
143. McNutt M: **Journals unite for reproducibility**. *Science* 2014, **346**(6210):679.
144. Llovera G, Liesz A: **The next step in translational research: lessons learned from the first preclinical randomized controlled trial**. *J Neurochem* 2016, **139 Suppl 2**:271-279.

145. Dirnagl U, Fisher M: **International, multicenter randomized preclinical trials in translational stroke research: it's time to act**. *J Cereb Blood Flow Metab* 2012, **32**(6):933-935.
146. Holman C, Piper SK, Grittner U, Diamantaras AA, Kimmelman J, Siegerink B, Dirnagl U: **Where Have All the Rodents Gone? The Effects of Attrition in Experimental Research on Cancer and Stroke**. *PLoS Biol* 2016, **14**(1):e1002331.
147. Iqbal SA, Wallach JD, Khoury MJ, Schully SD, Ioannidis JP: **Reproducible Research Practices and Transparency across the Biomedical Literature**. *PLoS Biol* 2016, **14**(1):e1002333.
148. Macleod MR, Lawson McLean A, Kyriakopoulou A, Serghiou S, de Wilde A, Sherratt N, Hirst T, Hemblade R, Bahor Z, Nunes-Fonseca C *et al*: **Risk of Bias in Reports of In Vivo Research: A Focus for Improvement**. *PLoS Biol* 2015, **13**(10):e1002273.
149. Kimmelman J, Mogil JS, Dirnagl U: **Distinguishing between exploratory and confirmatory preclinical research will improve translation**. *PLoS Biol* 2014, **12**(5):e1001863.
150. Lei Y, Sehnert B, Voll RE, Jacobs-Cacha C, Soler MJ, Sanchez-Nino MD, Ortiz A, Bulow RD, Boor P, Anders HJ: **A multicenter blinded preclinical randomized controlled trial on Jak1/2 inhibition in MRL/MpJ-Fas(lpr) mice with proliferative lupus nephritis predicts low effect size**. *Kidney Int* 2021, **99**(6):1331-1341.
151. https://www.lupus.org/news/lilly-discontinues-development-of-olumiant-for-lupus.
152. Schreiber A, Shulhevich Y, Geraci S, Hesser J, Stsepankou D, Neudecker S, Koenig S, Heinrich R, Hoecklin F, Pill J *et al*: **Transcutaneous measurement of renal function in conscious mice**. *Am J Physiol Renal Physiol* 2012, **303**(5):F783-788.
153. Marschner JA, Mulay SR, Steiger S, Anguiano L, Zhao Z, Boor P, Rahimi K, Inforzato A, Garlanda C, Mantovani A *et al*: **The Long Pentraxin PTX3 Is an Endogenous Inhibitor of Hyperoxaluria-Related Nephrocalcinosis and Chronic Kidney Disease**. *Front Immunol* 2018, **9**:2173.
154. Kim D, Paggi JM, Park C, Bennett C, Salzberg SL: **Graph-based genome alignment and genotyping with HISAT2 and HISAT-genotype**. *Nat Biotechnol* 2019, **37**(8):907-915.
155. Li H, Handsaker B, Wysoker A, Fennell T, Ruan J, Homer N, Marth G, Abecasis G, Durbin R, Genome Project Data Processing S: **The Sequence Alignment/Map format and SAMtools**. *Bioinformatics* 2009, **25**(16):2078-2079.
156. Liao Y, Smyth GK, Shi W: **featureCounts: an efficient general purpose program for assigning sequence reads to genomic features**. *Bioinformatics* 2014, **30**(7):923-930.
157. Gaidatzis D, Burger L, Florescu M, Stadler MB: **Analysis of intronic and exonic reads in RNA-seq data characterizes transcriptional and post-transcriptional regulation**. *Nat Biotechnol* 2015, **33**(7):722-729.
158. Yu G, Wang LG, Han Y, He QY: **clusterProfiler: an R package for comparing biological themes among gene clusters**. *OMICS* 2012, **16**(5):284-287.
159. Ninichuk V, Gross O, Reichel C, Khandoga A, Pawar RD, Ciubar R, Segerer S, Belemezova E, Radomska E, Luckow B *et al*: **Delayed chemokine receptor 1 blockade prolongs survival in collagen 4A3-deficient mice with Alport disease**. *J Am Soc Nephrol* 2005, **16**(4):977-985.
160. Cosgrove D, Kalluri R, Miner JH, Segal Y, Borza DB: **Choosing a mouse model to study the molecular pathobiology of Alport glomerulonephritis**. *Kidney Int* 2007, **71**(7):615-618.
161. Gross O, Beirowski B, Koepke ML, Kuck J, Reiner M, Addicks K, Smyth N, Schulze-Lohoff E, Weber M: **Preemptive ramipril therapy delays renal failure and reduces renal fibrosis in COL4A3-knockout mice with Alport syndrome**. *Kidney Int* 2003, **63**(2):438-446.
162. Jankowski J, Floege J, Fliser D, Bohm M, Marx N: **Cardiovascular Disease in Chronic Kidney Disease: Pathophysiological Insights and Therapeutic Options**. *Circulation* 2021, **143**(11):1157-1172.
163. Glassock RJ, Warnock DG, Delanaye P: **The global burden of chronic kidney disease: estimates, variability and pitfalls**. *Nat Rev Nephrol* 2017, **13**(2):104-114.
164. Gaitonde DY, Cook DL, Rivera IM: **Chronic Kidney Disease: Detection and Evaluation**. *Am Fam Physician* 2017, **96**(12):776-783.

165. George C, Echouffo-Tcheugui JB, Jaar BG, Okpechi IG, Kengne AP: **The need for screening, early diagnosis, and prediction of chronic kidney disease in people with diabetes in low- and middle-income countries-a review of the current literature**. *BMC Med* 2022, **20**(1):247.
166. Ke C, Liang J, Liu M, Liu S, Wang C: **Burden of chronic kidney disease and its risk-attributable burden in 137 low-and middle-income countries, 1990-2019: results from the global burden of disease study 2019**. *BMC Nephrol* 2022, **23**(1):17.
167. Ene-Iordache B, Perico N, Bikbov B, Carminati S, Remuzzi A, Perna A, Islam N, Bravo RF, Aleckovic-Halilovic M, Zou H *et al*: **Chronic kidney disease and cardiovascular risk in six regions of the world (ISN-KDDC): a cross-sectional study**. *Lancet Glob Health* 2016, **4**(5):e307-319.
168. Xie Y, Bowe B, Mokdad AH, Xian H, Yan Y, Li T, Maddukuri G, Tsai CY, Floyd T, Al-Aly Z: **Analysis of the Global Burden of Disease study highlights the global, regional, and national trends of chronic kidney disease epidemiology from 1990 to 2016**. *Kidney Int* 2018, **94**(3):567-581.
169. Stanifer JW, Muiru A, Jafar TH, Patel UD: **Chronic kidney disease in low- and middle-income countries**. *Nephrol Dial Transplant* 2016, **31**(6):868-874.
170. Voorend CGN, van Oevelen M, Verberne WR, van den Wittenboer ID, Dekkers OM, Dekker F, Abrahams AC, van Buren M, Mooijaart SP, Bos WJW: **Survival of patients who opt for dialysis versus conservative care: a systematic review and meta-analysis**. *Nephrol Dial Transplant* 2022, **37**(8):1529-1544.
171. Kintscher U, Bakris GL, Kolkhof P: **Novel non-steroidal mineralocorticoid receptor antagonists in cardiorenal disease**. *Br J Pharmacol* 2022, **179**(13):3220-3234.
172. Rahman A, Jahan N, Rahman MT, Nishiyama A: **Potential Impact of Non-Steroidal Mineralocorticoid Receptor Antagonists in Cardiovascular Disease**. *Int J Mol Sci* 2023, **24**(3).
173. Chen Q, Liang Y, Yan J, Du Y, Li M, Chen Z, Zhou J: **Efficacy and safety of non-steroidal mineralocorticoid receptor antagonists for renal outcomes: A systematic review and meta-analysis**. *Diabetes Res Clin Pract* 2023, **195**:110210.
174. Kolkhof P, Delbeck M, Kretschmer A, Steinke W, Hartmann E, Barfacker L, Eitner F, Albrecht-Kupper B, Schafer S: **Finerenone, a novel selective nonsteroidal mineralocorticoid receptor antagonist protects from rat cardiorenal injury**. *J Cardiovasc Pharmacol* 2014, **64**(1):69-78.
175. Grune J, Benz V, Brix S, Salatzki J, Blumrich A, Hoft B, Klopfleisch R, Foryst-Ludwig A, Kolkhof P, Kintscher U: **Steroidal and Nonsteroidal Mineralocorticoid Receptor Antagonists Cause Differential Cardiac Gene Expression in Pressure Overload-induced Cardiac Hypertrophy**. *J Cardiovasc Pharmacol* 2016, **67**(5):402-411.
176. Tu L, Thuillet R, Perrot J, Ottaviani M, Ponsardin E, Kolkhof P, Humbert M, Viengchareun S, Lombes M, Guignabert C: **Mineralocorticoid Receptor Antagonism by Finerenone Attenuates Established Pulmonary Hypertension in Rats**. *Hypertension* 2022, **79**(10):2262-2273.
177. Luettges K, Bode M, Diemer JN, Schwanbeck J, Wirth EK, Klopfleisch R, Kappert K, Thiele A, Ritter D, Foryst-Ludwig A *et al*: **Finerenone Reduces Renal RORgammat gammadelta T Cells and Protects against Cardiorenal Damage**. *Am J Nephrol* 2022, **53**(7):552-564.
178. Droebner K, Pavkovic M, Grundmann M, Hartmann E, Goea L, Nordlohne J, Klar J, Eitner F, Kolkhof P: **Direct Blood Pressure-Independent Anti-Fibrotic Effects by the Selective Nonsteroidal Mineralocorticoid Receptor Antagonist Finerenone in Progressive Models of Kidney Fibrosis**. *Am J Nephrol* 2021, **52**(7):588-601.
179. Barrera-Chimal J, Estrela GR, Lechner SM, Giraud S, El Moghrabi S, Kaaki S, Kolkhof P, Hauet T, Jaisser F: **The myeloid mineralocorticoid receptor controls inflammatory and fibrotic responses after renal injury via macrophage interleukin-4 receptor signaling**. *Kidney Int* 2018, **93**(6):1344-1355.
180. Bonnard B, Pieronne-Deperrois M, Djerada Z, Elmoghrabi S, Kolkhof P, Ouvrard-Pascaud A, Mulder P, Jaisser F, Messaoudi S: **Mineralocorticoid receptor antagonism improves diastolic dysfunction in chronic kidney disease in mice**. *J Mol Cell Cardiol* 2018, **121**:124-133.

181. Vart P, Vaduganathan M, Jongs N, Remuzzi G, Wheeler DC, Hou FF, McCausland F, Chertow GM, Heerspink HJL: **Estimated Lifetime Benefit of Combined RAAS and SGLT2 Inhibitor Therapy in Patients with Albuminuric CKD without Diabetes**. *Clin J Am Soc Nephrol* 2022, **17**(12):1754-1762.
182. Tsukamoto S, Morita R, Yamada T, Urate S, Azushima K, Uneda K, Kobayashi R, Kanaoka T, Wakui H, Tamura K: **Cardiovascular and kidney outcomes of combination therapy with sodium-glucose cotransporter-2 inhibitors and mineralocorticoid receptor antagonists in patients with type 2 diabetes and chronic kidney disease: A systematic review and network meta-analysis**. *Diabetes Res Clin Pract* 2022, **194**:110161.
183. Georgianos PI, Agarwal R: **Revisiting RAAS blockade in CKD with newer potassium-binding drugs**. *Kidney Int* 2018, **93**(2):325-334.
184. Ku E, McCulloch CE, Vittinghoff E, Lin F, Johansen KL: **Use of Antihypertensive Agents and Association With Risk of Adverse Outcomes in Chronic Kidney Disease: Focus on Angiotensin-Converting Enzyme Inhibitors and Angiotensin Receptor Blockers**. *J Am Heart Assoc* 2018, **7**(19):e009992.
185. Baigent C, Landray MJ, Reith C, Emberson J, Wheeler DC, Tomson C, Wanner C, Krane V, Cass A, Craig J *et al*: **The effects of lowering LDL cholesterol with simvastatin plus ezetimibe in patients with chronic kidney disease (Study of Heart and Renal Protection): a randomised placebo-controlled trial**. *Lancet* 2011, **377**(9784):2181-2192.
186. Suzuki H, Watanabe Y, Kumagai H, Shuto H: **Comparative efficacy and adverse effects of the addition of ezetimibe to statin versus statin titration in chronic kidney disease patients**. *Ther Adv Cardiovasc Dis* 2013, **7**(6):306-315.
187. Drew DA, Weiner DE, Sarnak MJ: **Cognitive Impairment in CKD: Pathophysiology, Management, and Prevention**. *Am J Kidney Dis* 2019, **74**(6):782-790.
188. Vellanki K, Hou S: **Menopause in CKD**. *Am J Kidney Dis* 2018, **71**(5):710-719.
189. Laville SM, Metzger M, Stengel B, Jacquelinet C, Combe C, Fouque D, Laville M, Frimat L, Ayav C, Speyer E *et al*: **Evaluation of the adequacy of drug prescriptions in patients with chronic kidney disease: results from the CKD-REIN cohort**. *Br J Clin Pharmacol* 2018, **84**(12):2811-2823.
190. Hahr AJ, Molitch ME: **Management of diabetes mellitus in patients with chronic kidney disease**. *Clin Diabetes Endocrinol* 2015, **1**:2.
191. American Diabetes Association Professional Practice C: **11. Chronic Kidney Disease and Risk Management: Standards of Medical Care in Diabetes-2022**. *Diabetes Care* 2022, **45**(Suppl 1):S175-S184.
192. Provenzano M, Jongs N, Vart P, Stefansson BV, Chertow GM, Langkilde AM, McMurray JJV, Correa-Rotter R, Rossing P, Sjostrom CD *et al*: **The Kidney Protective Effects of the Sodium-Glucose Cotransporter-2 Inhibitor, Dapagliflozin, Are Present in Patients With CKD Treated With Mineralocorticoid Receptor Antagonists**. *Kidney Int Rep* 2022, **7**(3):436-443.
193. Kaesler N, Babler A, Floege J, Kramann R: **Cardiac Remodeling in Chronic Kidney Disease**. *Toxins (Basel)* 2020, **12**(3).
194. Kruszewska J, Cudnoch-Jedrzejewska A, Czarzasta K: **Remodeling and Fibrosis of the Cardiac Muscle in the Course of Obesity-Pathogenesis and Involvement of the Extracellular Matrix**. *Int J Mol Sci* 2022, **23**(8).
195. Bulow RD, Boor P: **Extracellular Matrix in Kidney Fibrosis: More Than Just a Scaffold**. *J Histochem Cytochem* 2019, **67**(9):643-661.
196. Bonnans C, Chou J, Werb Z: **Remodelling the extracellular matrix in development and disease**. *Nat Rev Mol Cell Biol* 2014, **15**(12):786-801.
197. Schefold JC, Filippatos G, Hasenfuss G, Anker SD, von Haehling S: **Heart failure and kidney dysfunction: epidemiology, mechanisms and management**. *Nat Rev Nephrol* 2016, **12**(10):610-623.
198. Colombo PC, Ganda A, Lin J, Onat D, Harxhi A, Iyasere JE, Uriel N, Cotter G: **Inflammatory activation: cardiac, renal, and cardio-renal interactions in patients with the cardiorenal syndrome**. *Heart Fail Rev* 2012, **17**(2):177-190.

199. Franssen CF, Navis G: **Chronic kidney disease: RAAS blockade and diastolic heart failure in chronic kidney disease**. *Nat Rev Nephrol* 2013, **9**(4):190-192.
200. Ferreira JP, Rossignol P, Zannad F: **Renin-angiotensin-aldosterone system and kidney interactions in heart failure**. *J Renin Angiotensin Aldosterone Syst* 2019, **20**(4):1470320319889415.
201. Irazabal MV, Torres VE: **Reactive Oxygen Species and Redox Signaling in Chronic Kidney Disease**. *Cells* 2020, **9**(6).
202. Mongirdiene A, Skrodenis L, Varoneckaite L, Mierkyte G, Gerulis J: **Reactive Oxygen Species Induced Pathways in Heart Failure Pathogenesis and Potential Therapeutic Strategies**. *Biomedicines* 2022, **10**(3).
203. Tsutsui H, Kinugawa S, Matsushima S: **Oxidative stress and heart failure**. *Am J Physiol Heart Circ Physiol* 2011, **301**(6):H2181-2190.
204. Ferreira JP, Zannad F, Pocock SJ, Anker SD, Butler J, Filippatos G, Brueckmann M, Jamal W, Steubl D, Schueler E *et al*: **Interplay of Mineralocorticoid Receptor Antagonists and Empagliflozin in Heart Failure: EMPEROR-Reduced**. *J Am Coll Cardiol* 2021, **77**(11):1397-1407.
205. Weldegiorgis M, de Zeeuw D, Heerspink HJ: **Renal end points in clinical trials of kidney disease**. *Curr Opin Nephrol Hypertens* 2015, **24**(3):284-289.
206. Barrera-Chimal J, Jaisser F, Anders HJ: **The mineralocorticoid receptor in chronic kidney disease**. *Br J Pharmacol* 2022, **179**(13):3152-3164.
207. Grune J, Beyhoff N, Smeir E, Chudek R, Blumrich A, Ban Z, Brix S, Betz IR, Schupp M, Foryst-Ludwig A *et al*: **Selective Mineralocorticoid Receptor Cofactor Modulation as Molecular Basis for Finerenone's Antifibrotic Activity**. *Hypertension* 2018, **71**(4):599-608.
208. Rubel D, Zhang Y, Sowa N, Girgert R, Gross O: **Organoprotective Effects of Spironolactone on Top of Ramipril Therapy in a Mouse Model for Alport Syndrome**. *J Clin Med* 2021, **10**(13).
209. Lv W, Booz GW, Wang Y, Fan F, Roman RJ: **Inflammation and renal fibrosis: Recent developments on key signaling molecules as potential therapeutic targets**. *Eur J Pharmacol* 2018, **820**:65-76.
210. Black LM, Lever JM, Agarwal A: **Renal Inflammation and Fibrosis: A Double-edged Sword**. *J Histochem Cytochem* 2019, **67**(9):663-681.
211. Vallon V, Thomson SC: **Targeting renal glucose reabsorption to treat hyperglycaemia: the pleiotropic effects of SGLT2 inhibition**. *Diabetologia* 2017, **60**(2):215-225.
212. Ruiz-Ortega M, Rayego-Mateos S, Lamas S, Ortiz A, Rodrigues-Diez RR: **Targeting the progression of chronic kidney disease**. *Nat Rev Nephrol* 2020, **16**(5):269-288.
213. Coffman TM: **The inextricable role of the kidney in hypertension**. *J Clin Invest* 2014, **124**(6):2341-2347.
214. Bailey CJ, Day C, Bellary S: **Renal Protection with SGLT2 Inhibitors: Effects in Acute and Chronic Kidney Disease**. *Curr Diab Rep* 2022, **22**(1):39-52.
215. Palacios-Ramirez R, Lima-Posada I, Bonnard B, Genty M, Fernandez-Celis A, Hartleib-Geschwindner J, Foufelle F, Lopez-Andres N, Bamberg K, Jaisser F: **Mineralocorticoid Receptor Antagonism Prevents the Synergistic Effect of Metabolic Challenge and Chronic Kidney Disease on Renal Fibrosis and Inflammation in Mice**. *Front Physiol* 2022, **13**:859812.
216. Fletcher EK, Morgan J, Kennaway DR, Bienvenu LA, Rickard AJ, Delbridge LMD, Fuller PJ, Clyne CD, Young MJ: **Deoxycorticosterone/Salt-Mediated Cardiac Inflammation and Fibrosis Are Dependent on Functional CLOCK Signaling in Male Mice**. *Endocrinology* 2017, **158**(9):2906-2917.
217. Savige J, Harraka P: **Pathogenic Variants in the Genes Affected in Alport Syndrome (COL4A3-COL4A5) and Their Association With Other Kidney Conditions: A Review**. *Am J Kidney Dis* 2021, **78**(6):857-864.
218. Widjaja AA, Shekeran SG, Adami E, Ting JGW, Tan J, Viswanathan S, Lim SY, Tan PH, Hubner N, Coffman T *et al*: **A Neutralizing IL-11 Antibody Improves Renal Function and Increases Lifespan in a Mouse Model of Alport Syndrome**. *J Am Soc Nephrol* 2022, **33**(4):718-730.

Appendix 1 pRCT Study calendar

Daily duties	Weekly duties	Upon sacrifice
1.Check and add foods mixed with special drugs. 2. Observe and record the general state and behavior of the mice. 3. Record date of death or adverse event (if present) 4. Measure and record weight 5. Fill out the score sheet and sign.	1. Urine collection 2. GFR testing on 6,7,10 weeks 3. pRCT Research group members regular meeting.	1. Take pictures of kidney 2. Blood draw (≈1mL) 3. Cardiac perfusion 4. Take organs (Kidney, Heart, Liver, Spleen, Lung, Brain)

Appendix 2 Chemicals and reagents

PRECLINICAL PROTOCOL LMU

Date: 20 October 2021

TITLE OF STUDY:

A Preclinical, Randomized, Double-Blind, Placebo-Controlled Study to Evaluate the Efficacy and Safety of Combination Therapy to target CKD Progression in Adult Mice

STUDY COORDINATOR:

Zhihui Zhu & Hans-Joachim Anders

Medizinische Klinik und Poliklinik IV

LMU Klinikum der Universität Muenchen

Nephrologisches Zentrum

Goethestraße 31

D-80336 Munich, Germany

Study Synopsis

Study Number: 2021-COMB-CKD-001

Preclinical Development Phase: Academic research, single centre study.

Coordinating center:

Department of Internal Medicine IV, Hospital of the Ludwig Maximilians University, Kidney Division, Munich, Germany.

Participating centers:

Department of Internal Medicine IV, Hospital of the Ludwig Maximilians University, Kidney Division, Munich, Germany.

Objectives:

A triple combination of ramipril (RASi), empagliflozin (SGLT2i), and finerenone (MRA) significantly prolongs kidney lifespan over dual RAS/SGLT2 inhibition.

Inclusion Criteria

Male and female *Col4a3*^{tm1Dec}-/- mice, six weeks of age.

Exclusion Criteria:

Mice will be excluded from participating in the study if they meet any of the following exclusion criteria:

1.A score four or score $\geqslant$ 2 for more than 6h during animal welfare surveillance.

2.Exposure to any other drug during the study period, e.g., treatment requested by the veterinarian for skin wounds.

3.Any sign of infection.

4.Pregnancy.

5.Signs of ramipril, empagliflozin, finerenone intolerance (anaphylactic reactions).

Study Design and Schedule:

This is a preclinical, randomized, double-blind, placebo-controlled study to evaluate the efficacy and safety of combination therapy to target CKD progression in adult mice. The randomization of all eligible mice will be stratified by their induction regimen. Alport mice will be dosed with a vehicle, ramipril, ramipril-empagliflozin, or ramipril-empagliflozin-finerenone once daily with the study agent by gastric tube administration for eight weeks.

The primary efficacy endpoint will be the kidney lifespan.

Secondary endpoints will be kidney function, proteinuria, histomorphological parameters of kidney atrophy. Kidney function assessments will be based on measured glomerular filtration rate (mGFR) at study sites where the necessary experience and hardware are available. In addition, serum markers of kidney excretory function (serum creatinine/SCr and blood urea nitrogen/BUN levels) will be measured.

A safety analysis will include animal welfare scoring in all animals and a histomorphological analysis of non-kidney tissues in a subset of animals.

Experimental animals, housing, and husbandry

Col4a3^{tm1Dec}-/- mice with spontaneous CKD (Alport nephropathy) will be used in this study and bred in an in-house colony. All mice will be kept under pathogen-free conditions in a 12-hour light and dark cycle with free access to food and water. Enrichment will be provided as per local regulatory requirements. Health status, cleaning, beddings, water, and food supply with standard chow will be according to our center's local standard operating procedures.

The primary efficacy endpoint

Time to lethal uremia (kidney lifespan).

Major Secondary Endpoints:

Markers of kidney excretory function (mGFR, SCr, BUN).

Histomorphological parameters of the kidney in a subgroup of animals.

Safety analysis: Animal welfare scoring (all animals), histomorphological analysis of non-kidney tissues (subset of animals).

Sample Size Calculation:

Group comparisons are determined about the (kidney) survival time, defined as achieving a stress score greater than 2 for more than 6 hours. A comparison is made with vehicle-treated animals. A minimum survival time of 60 days is assumed here. The expected median duration in the control group is 70 days. An extension to 85 days is clinically relevant. It can be assumed that there will be no failures up today 60. The log-rank test is used as a statistical test. This corresponds to a clinically relevant hazard coefficient of (85-60) / (70-60) = 2.5. With an error of the first type of $\alpha = 0.05$ and an error of the second type $\beta = 0.2$, the sample size is n = 20 per group. The use of a two-sided test is necessary because it cannot be ruled out that individual therapy groups also lead to a shortening of the (kidney) survival time, which would be significant since all test substances are already in clinical use elsewhere.

Randomized and Double-Blind Strategy:

We use the idea of "Stratified randomization" to achieve randomization. We use the function to create random assignments for clinical trials (or any experiment where the subjects come one at a time). The randomization is done within blocks so that the balance between treatments stays close to equal throughout the trial.

Safety Endpoints and Analysis:

Descriptive statistics will be used to summarize adverse events (AEs). The frequency and rate of laboratory abnormalities will be tabulated by treatment group. The frequency and rate of AEs will be tabulated by MedDRA system organ class (SOC) and preferred term and compared between placebo and the treatment group.

No Data Monitoring Committee (DMC) will be installed.

Appendix 3 Animal welfare surveillance

No alterations	**Mildly altered (1 point)**	**Moderately altered (2 points)**	**Severely altered (4 points)**
Shiny, clean fur Builds nest Social interactions Reacting to stimulus Normal motions Exploratory behavior GFR＞150 ul/min	Weight loss <10% Partially pilo erection Dampened but reactive Transient bent back Transients tremor Transient abnormal respiration Transient wet wound GFR 50-150ul/min	Weight loss <15% Permanent piloerection Dampened on provocation Intermittent bent back Repeated abnormal breathing Intermittent tremor Transient exhaustion· Redness, swelling at the injection site GFR＜50 µl/min	Weight loss >15% Moderate-severe dehydration Not reactive to stimuli Persistent back bending Persistent abnormal breathing Persistent tremor Convulsions Persistent exhaustion Self-destructive injuries Self-isolation

1. “transient”: only one time detected in two subsequent checks

2. “intermittent”: in three subsequent checks 1. Timepoint: yes; 2. Timepoint: no; 3. Timepoint: yes.

3. “repeated”: at two-time points.

4. “persistent”: > 2-time points.

5. “moderate dehydration”: piloerection and possible cause of mild weight loss. Give volume (s.c. NaCl 0.9 % 0.2 - 0.4 mL at max. volume 10 mL/kg in single injection site).

6. Termination (cervical dislocation) once 4 points have been reached in summation or at the one-time point.

7. A sum score of 2 or 3 points: repeat assessment after 6 and 12 h. Worsening should lead to consultation with a veterinarian.

Appendix 4 The R code of ‘Package blockrand’

```
library(blockrand)
male<-blockrand(n=40,num.levels=4,levels=c("A","B","C","D"),id.prefix='M',
block.prefix='M',stratum='Male')
female<-blockrand(n=40,num.levels=4,levels=c("A","B","C","D"),id.prefix='F',
block.prefix='F',stratum='Female')
my.study <- rbind(male,female)

p=plotblockrand(my.study,'mystudy.pdf',
top=list(text=c('Combination therapy in Mice with Alport Syndrome',
'Mouse ID: %ID%','Treatment: %TREAT%',
'from Cage: ',"Ear mark:","DOB:","Experiment date:","","Signature:"),
col=c('black','black','black','red','black','black','black','black','black','black'),
font=c(1,1,1,4,1,1,1,1,1,1)),

middle=list(text=c("Combination therapy in Mice with Alport Syndrome",
"Sex: %STRAT%","Mouse ID: %ID%"),
col=c('#80afd2','#6594c4','#4575b4'),font=c(1,2,3)),

bottom="Demo",
cut.marks=TRUE)
```

https://cran.r-project.org/web/packages/blockrand/index.html

Appendix 5 Abbreviation

Abbreviation	Full name	Abbreviation	Full name
CKD	Chronic kidney disease	TGF	Transforming growth factor
KDIGO	Kidney Disease: Improving Global Outcomes	eNOS	Endothelial nitric oxide synthase
GFR	Glomerular filtration rate	ICAM	Intercellular protein
GBM	Glomerular basement membrane	NADPH	Nicotinamide adenine dinucleotide phosphate
AD	Autosomal dominant	AR	Autosomal recessive
NGAL	Neutrophil gelatinase-associated lipocalin	PAL	Plasminogen activator inhibitor
HbA1c	Glycated haemoglobin	CNI	Connective tissue growth factor
MMPs	Matrix metalloproteinases	AKI	Acute kidney injury
RAS	Renin-angiotensin system	TNF	Tumor necrosis factor
ACEi	Angiotensin-converting enzyme inhibitors	FDA	Food and Drug Administration
NF-κB	Nuclear factor kappa B	RCT	Randomized controlled trial
ARB	Angiotensin receptor blockers	HFrEF	Heart Failure with Reduced Ejection Fraction
DM	Diabetes mellitus	MI	Myocardial infarction
SCr	Serum Creatinine	ESKD	End-stage kidney disease
LMICs	Low- and middle-income countries	pRCTs	Preclinical randomized controlled trials
CVD	Cardiovascular disease	SLE	Systemic lupus erythematosus
HR	Hazard ratio	BUN	Blood urea nitrogen
SGLT2	Inhibitors of the sodium-glucose cotransporter 2	ADA	American Diabetes Association
T2DM	Type 2 diabetes	SOC	System organ class
AEs	Adverse events	DMC	Data Monitoring Committee
DKD	Diabetic kidney disease	FPG	Fasting plasma glucose
CI	Confidence interval	BGI	Beijing Genomics Institute
RT-qPCR	Real-time quantitative polymerase chain reaction	GSEA	Gene Set Enrichment Analysis
UACR	Urinary albumin creatinine ratio	MR	Mineralocorticoid receptor
DNPA	Dapagliflozin	MET	Metformin
PBO	Placebo	CANA	Canagliflozin
ECM	Extracellular matrix	ADPKD	Autosomal dominant polycystic kidney disease

Acknowledgement

As I reflect back, I am filled with emotions, realizing that a decade has already passed since I embarked on my journey in the field of medicine. The thought that my student career is coming to a close is both bittersweet and humbling. I still vividly recall the excitement and anticipation I felt when I first entered medical school and the awe-inspiring sensation that washed over me as I read the medical student oath, "Health belongs to, life relies on." The long nights spent studying during my undergraduate years are indelibly etched in my memory. During those moments, I often pondered, how far must I journey as a medical student to become a physician of exceptional caliber? How much effort must I put forth to enter the august halls of the medical community? My academic journey at Munich University was a brilliant chapter in my life, where I gained countless enriching experiences and spent some of the most youthful years of my existence. Although it is with a heavy heart that I bid farewell, I am forever grateful for the time I spent here.

To have such a mentor is a blessing beyond measure. I am eternally grateful to my advisor, Prof. Dr. med. Hans-Joachim Anders, for his kindness and generosity. I still remember the first time I met Achim, when he asked me, "What are your dreams and how can I help you achieve them?" For me, Achim is not just a professor but also a friend and a family member. His rigorous and meticulous academic style has shone a light on my path of scientific research. His modest, elegant, and warm personality has elevated my personal standards. The process of writing my thesis was no easy feat, but every step of the way, from selecting the topic, to collecting and organizing data, to conducting experiments and finalizing the manuscript, I was guided and taught by my professor. In the early stages of my research, he provided me with a novel topic that gave direction to my aimless pursuit. In the mid-stages, every time I encountered a roadblock, my professor's insightful guidance and patient demeanor always restored my hope and strength. In my life, every time I was discouraged or confused, my professor's wealth of experience lifted me up. I will always cherish the kindness of my teacher and remember his compassion. I wish for my teacher to be happy, healthy, and successful in his work!

I am filled with gratitude towards my two guiding instructors: Prof. Dr. med. Volker Vielhauer and Prof. Dr. med. Bärbel Lange-Sperandio, for their guidance and invaluable advice on my project. I am thankful to Prof. Dr. Maciej Lech and PD Dr. Stefanie Steiger for their exceptional organization and management of our lab, providing me with the opportunity to carry out this research project. I express my appreciation to Dr. Angela Lutterbach, Janina Mandelbaum, Anna Anfimiadou, Uschi Kögelperger, Thi Dolidze, and Yvonne Minor for their technical support. I am grateful to Professor Martha Merrow and Dr.

Francesca Sartor for generously granting me access to the Nikon Eclipse Ti2 microscope system. Additionally, I would like to thank our collaborating partners in Aachen, Prof. Dr. med. Peter Boor and Dr. med. Roman D. Bülow, as well as our collaborating partners in Florence, Prof. Dr. med. Paola Romagnani and Dr. med. Maria-Lucia Angelotti, for their technical support. I am also thankful to Dr. med. Martin Klaus for his help in pathology.

I also extend my thanks to the Alport team, Dr. Yoshihiro Kusunoki and Karoline Rosenkranz, for their excellent teamwork and help in improving my skills and knowledge in a collaborative environment. I am grateful to Dr. Julian Marschner, Dr. Yutian Lei, Dr. Zhibo Zhao, Dr. Min Liu, and Khuram Shehzad for their valuable feedback and suggestions on my work. Their insights helped me better understand the research process, and I am deeply thankful for their support. With heartfelt gratitude, I want to express my appreciation for Li Chenyu's unwavering support and assistance in both my research and life. Thank you for being there for me through the moments of experimental failure, rejected papers, long nights of work, and feelings of uncertainty about the future. Your encouragement and companionship has given me the determination to weather any storm and reach for the stars. Without you, my journey of doctor would have been much more challenging and arduous.

I pay my respects to the animals who have sacrificed themselves for the betterment of humanity. Their contributions and sacrifices have led to great strides in fields such as medical research, biotechnology, and others, greatly improving the lives of many. I hope that as a society, we can continue to use their contributions responsibly and ethically. Additionally, I am grateful to all those who contributed financially to this project. I thank the funding agencies CSC and Deutsche Forschungsgemeinschaft for their generous support, without which none of this work would have been possible.

Finally, I want to express my gratitude towards my family, colleagues, teachers, and friends who have consistently and silently supported me throughout my studies in Germany. I am grateful for my family who has been my warmest harbor and solid rock with their love and care. Their understanding and support have given me the courage and confidence to keep moving forward. I also want to thank Professor Zhang Haibo from Anzhen Hospital in Beijing who opened the door of research for me. I am thankful for Professor Yang Qiu, Professor Yang Shiwei, and Professor Hao Yongchen from Anzhen Hospital in Beijing who have helped me both in my research and life.

The distant flute sings a farewell tune, as the sound of departure echoes. This is a form envied by many but hard to return to. I just lingered in the sunset, and before I knew it, it was time to say goodbye. I fear I'll never see the captivating sunset again, nor will I forget Goethestraße 31.

Declaration of academic honesty

Hereby I declare that all of the present work embodied in this thesis was carried out by myself from 06/2021 until 03/2023 under the supervision of Prof. Dr. Hans Joachim Anders, Nephrologisches Zentrum, Medizinische Klinik und Poliklinik IV, Innenstadt Klinikum der Universität München. This work has not been submitted in part or full to any other university or institute for any degree or diploma.

Part of the work has been submitted as an abstract at ESAC and the ADMIRE Network meeting 2023.
Part of the work has been submitted as an abstract at the ERA Congress 2023.

Date: 26.08.2023 Signature Zhihui Zhu

Place: Munich, Germany

Affidavit

LMU LUDWIG-MAXIMILIANS-UNIVERSITÄT MÜNCHEN | Promotionsbüro Medizinische Fakultät | MMRS

Affidavit

Zhu, Zhihui
Surname, first name

I hereby declare, that the submitted thesis entitled:

The effects of triple blockade of the mineralocorticoid receptor, the renin-angiotensin system, and sodium glucose transporter 2 on kidney lifespan in mice with Alport nephropathy. A preclinical double-blinded randomized controlled trial.
is my own work. I have only used the sources indicated and have not made unauthorized use of services of a third party. Where the work of others has been quoted or reproduced, the source is always given.

I further declare that the dissertation presented here has not been submitted in the same or similar form to any other institution for the purpose of obtaining an academic degree.

Munich, 26.08.2023
Place, date

Zhihui Zhu
Signature doctoral candidate